Characterization of mesopic vision for luminance photometry

zur Erlangung des akademischen Grades eines

DOKTORS DER INGENIEURWISSENSCHAFTEN (Dr.-Ing.)

der Fakultät für Maschinenbau

der Universität Paderborn

Dissertation

vorgelegt von

Dipl.-Ing. Sabine Raphael

Januar 2010

Danksagung

Abstract

The need for a reliable photometric system in the mesopic range results from discrepancies between current photometry, which is solely based on daylight vision, and visual perception under dim light conditions. A luminance based mesopic photometric system to evaluate light distributions is particularly relevant for safety related applications like automotive, street, and emergency lighting.

In order to describe rod and cone contributions to mesopic vision and to determine a measure of mesopic luminance several methods were used: minimally distinct border settings, minimum motion settings, threshold contrasts for the detection of flashes, motion discrimination thresholds, and the detection of a counterphasing stimulus. While minimally distinct borders and minimum motion settings were expected to favor the achromatic luminance channel, detection threshold contrasts and detection thresholds for a counterphasing stimulus incorporate both the achromatic and the chromatic pathways of the visual system. In all studies the emphasis lies on extrafoveal perception under adaptation conditions ranging from photopic to scotopic.

Results show a decrease of cone contribution with decreasing adaptation luminance which can be described with a sigmoid function. Foveal and near foveal vision is dominated by cones also at mesopic light levels, whereas far peripheral vision is rod dominated at high mesopic and low photopic adaptation conditions. An increase in S/P ratio of the adaptation background and spatial frequency of the object leads to a decreased effectiveness of rods relative to cone stimulation at mesopic levels. Mechanistically inspired models are suggested to provide an account of these trends.

Zusammenfassung

Für sicherheitsrelevante Beleuchtungssysteme wie Automobilscheinwerfer, Straßen- und Notfallbeleuchtung ist eine wahrnehmungsangepasste Bewertung der Lichtverteilung im mesopischen Helligkeitsbereich (Dämmerungsbereich) von großer Bedeutung. Hierdurch ergibt sich die Notwendigkeit die Wahrnehmung im Dämmerungsbereich auf Basis der Leuchtdichte zu charakterisieren und ein photometrisches Modell zu entwickeln.

Um den relativen Einfluss der Zapfen und Stäbchen zu untersuchen, wurden in der vorliegenden Arbeit mehrere experimentelle Methoden zur Bestimmung der Leuchtdichte im mesopischen Bereich angewandt: Minimale Wahrnehmung der Grenze („minimally distinct border"), Minimale Bewegung („minimum motion"), Schwellenkontrast zur Erkennung der Rotationsrichtung („motion discrimination threshold"), Schwellenkontrast für die Wahrnehmung peripherer Objekte und gegenphasig schwingender Stimuli. Während die Methoden der Minimalen Wahrnehmung der Grenze und der Minimalen Bewegung den achromatischen Kanal ansprechen, basieren Schwellenkontraste sowohl auf achromatischen als auch auf chromatischen Informationen. Der Schwerpunkt der durchgeführten Studien liegt auf der peripheren Wahrnehmung unter photopischen, mesopischen und skotopischen Adaptationsbedingungen.

Die Ergebnisse zeigen, dass sich der Einfluss der Zapfen mit abnehmender Adaptationsleuchtdichte gemäß einer Sigmoid-Funktion verringert. Allerdings basiert die foveale Wahrnehmung auch im mesopischen Bereich ausschließlich auf den Zapfenrezeptoren, wohingegen die Wahrnehmung in der Peripherie auch bei einem hohen mesopischen Leuchtdichteniveau von den Stäbchen dominiert wird. Zudem verschiebt sich die relative Gewichtung der Rezeptorbeiträge zugunsten der Zapfen mit ansteigendem S/P-Verhältnis des Adaptationsfeldes und der Objektgröße (Raumfrequenz).

Content

Symbols and Abbreviations

k	Photopic luminous efficacy in Watt/lumen
k'	Scotopic luminous efficacy in Watt/lumen
(x, y)	Chromaticity coordinates
eew	Equal energy white
f_S	Spatial frequency in cycles per degree (cpd)
f_T	Temporal frequency in Hz
HBM	Heterochromatic brightness matching
k	Slope of threshold vs. intensity curves (TVI-curves)
L, M, S	Long, middle, short wavelength cones and their excitations
$L_e(\lambda)$	Spectral radiance in W/(m²·nm·sr)
m	Modulation amplitude
MDB	Minimally distinctness of borders
MinMot	Minimum motion
P	Photopic luminance based on $V_{10}(\lambda)$
P'	Individual photopic luminance
P_2	Photopic luminance based on $V(\lambda)$
P_{Ref} / S_{Ref}	Photopic / scotopic luminance of the reference field
P_{cf} / S_{cf}	Photopic / scotopic luminance of the comparison field
P_{adapt} /S_{adapt}	Photopic / scotopic adaptation luminance
P_S	Photopic luminance of the stimulus
P_R, P_B, P_G	Photopic luminance based on $V_{10}(\lambda)$ of the red/blue/green phosphor of the CRT monitor
R, G, B	Red, Green, Blue phosphors of the monitor
RMSE	Root mean square error
S	Scotopic luminance based on $V'(\lambda)$
S'	Individual scotopic luminance
td	Troland
$V(\lambda)$	Photopic luminous efficiency function of a 2° standard observer
$V'(\lambda)$	Scotopic luminous efficiency function of a 10° standard observer
$V_{10}(\lambda)$	Photopic luminous efficiency function of a 10° standard observer
W'_P	Independent photopic weight
W'_S	Independent scotopic weight
W_P	Relative photopic weight
W_S	Relative scotopic weight

$X_{2°}$, $Y_{2°}$, $Z_{2°}$	Tristimulus values based on the 2° CIE Color matching functions
ΔM	Mesopic incremental luminance
$\Delta^* S$	Scotopic incremental threshold luminance
$\Delta^* P$	Photopic incremental threshold luminance
ω_R, ω_B	Phosphor weights for the red and blue phosphor
θ	Radius of the annulus / eccentricity

Chapter 1

Introduction

No other human sense organ incorporates as much information about our environment as the eyes. The human visual system possesses the amazing ability to cover more than eleven decades of luminance. To perform under this immense range of illumination the visual system incorporates a dual receptor system – the rods and the cones. While the cones are active under bright light the rods come into play at dim light levels. This receptor dualism together with other mechanisms of adaptation allows us to get along on bright sunny days as well as under moonlight conditions. A particularly interesting light level under physiological aspects is the twilight range, the so called mesopic adaptation range. The word 'mesopic' is derived from the greek word 'meso' or 'mesos', which means 'middle', 'in between'. In the context of light and vision, mesopic means in between day vision and night vision. This range which extends over more than four decades of luminance is characterized by the joint stimulation of rods and cones. The mutual activity and interactions between the two different kinds of receptors make twilight vision highly complex and the perception based evaluation and measurement of light particularly challenging.

A good understanding of the processes incorporated in vision is necessary for an appropriate photometric system. In the last years the demand of a perception based system to measure photometric quantities under mesopic conditions grew more urgent. Two developments caused this increased interest. Firstly, new illuminants with different photometric nature like high power light emitting diodes (LEDs) were developed, and furthermore awareness grew of the need for illumination related improvements of safety in e. g. emergency lighting, aviation signal lighting, street and automotive lighting. These safety related lighting systems are most important under dim brightness conditions, when both rod and cone receptors are involved in perception. Due to the multiple receptor response a photometric evaluation under these brightness conditions is particularly difficult to accomplish. So far, when measuring photometric units only the photopic spectral sensitivity of the eye is considered. The mesopic state of adaptation of the eye is disregarded which leads to an underestimation of short wavelengths compared to the sensitivity of the eye at dim light conditions. These differences between photometry and the visual impression were not regarded as problematic automotive lighting since most car headlamps were tungsten halogen lamps whose spectra have little energy in the short wavelength range where sensitivity is highest. However, with the raise and improvement of new light sources like gas discharge lamps and LEDs for automotive headlights or metal halide lamps for street lighting installations the discrepancies between photometry and perception became more obvious. Discrepancies arise from the high blue spectral energy of these lamp types compared to tungsten lamps. A spectral power distribution with a lot of energy in the short wavelengths will address the rod photoreceptors and let the light subjectively appear brighter than photopic luminance would suggest. Since there is no

unified way of measuring subjective visibility, luminance or other photometric quantities in the mesopic range, the inaccuracies are difficult to grasp and to rectify. Consequently, for the design and dimensioning of safety related lighting systems manufacturers rely solely on the well established and standardized photopic photometry. However, the need for an objective rating system has become urgent with the demand to objectively evaluate the performance of e. g. headlights, emergency lighting and street lighting systems. As a basis for such an evaluation a practical mesopic photometric system is crucial.

For the description of visual impressions by photometry the sensitivity of the human visual system to spectral radiation is of special interest. The transformation of radiometric into photometric units is based on the photopic standard observer which is characterized by the luminous efficiency function for photopic vision. In 1924 the CIE (Commission Internationale de l'Eclairage) recommended a luminous efficiency function as a photopic standard observer $V(\lambda)$ to provide a unified photometric approach. The $V(\lambda)$ function is a bell shaped curve with a maximum at 555 nm. Similarly, in 1951 a scotopic luminous efficiency curve for rod vision was recommended by the CIE as 10°-scotopic standard observer $V'(\lambda)$. In contrast to $V(\lambda)$, $V'(\lambda)$ peaks at 505 nm, which means under very dim light conditions the human eye is more sensitive to bluish light than under bright daylight. This effect was first noticed by Jan Evangelista Purkinje in 1825 (Purkinje, 1825) and is therefore now called Purkinje effect. The Purkinje effect, which represents the transition from cone vision to rod vision during dark adaptation, is the main but not the only reason for the lack of a reliable perception based photometry in the mesopic domain. The Purkinje effect suggests that a light source with a high blue spectral content will promote rod vision under dim light conditions and therefore might lead to an improved visual performance. Especially for safety related lighting systems like in automotive and street lighting an improved visual performance is indispensable. Studies that compared visual performance in terms of reaction times to detect peripheral targets under several lamp types that are used in automotive and street lighting showed that illumination with a high spectral energy in the short wavelength range lead to improved reaction times and fewer missed targets (He, Rea, Bierman, Bullough, 1997; Van Derlofske, Bullough, 2003). Differences increase even more for tasks that involve identification of an object (Lewis, 1999).

These examples reveal that photopic luminance is inadequate as a descriptor for peripheral vision at dim light conditions and emphasize the need for an appropriate photometric approach for the mesopic range. The goal of this thesis is to describe luminance at mesopic light levels for a range of peripheral positions in the visual field. A simple definition of a mesopic standardized luminosity function is not applicable since the spectral sensitivity in the mesopic adaptation range varies with eccentricity in a manner roughly consistent with the distribution of rods and cones across the retina. Moreover, the method of flicker photometry that was mainly used to determine $V(\lambda)$ and $V'(\lambda)$ is not applicable in the mesopic range due to phase lags between rod-cone pathways and rod-rod pathways (Vienot & Chiron, 1992). Therefore other methods have to be considered to determine luminance under twilight conditions. It was found that the method of minimizing the distinctness of a border, first extensively employed by Boynton and Kaiser (1968) leads to luminous efficiency curves similar to $V(\lambda)$ under photopic conditions. This technique aims at minimizing the distinctness of a border between two adjacent fields, whereas one of the fields serves as constant reference and the second field is the

test field modified by the observer. Chapter 3 describes a minimum border experiment to assess luminance under a variety of adaptation conditions.

Also the minimum motion technique from Cavanagh, Anstis and MacLeod was found to address the luminance channel only and to produce results in close proximity to flicker photometry (Anstis & Cavanagh, 1983; Cavanagh, MacLeod, Anstis, 1987). This method employs a colored grating that seems to move either to the right or left depending on the relative luminance of the two colored sinusoids. If the luminance of the colored gratings are equal (isoluminance condition) no movement of the grating is visible. So far, both methods were only used under photopic adaptation conditions for foveal vision. Chapter 4 introduces a minimum motion technique for measuring isoluminance ratios between red and blue under adaptation conditions ranging from photopic to scotopic.

Vision is based on the perception of luminance differences between an object and its background rather than on the absolute luminance of the object. Therefore contrast thresholds were measured with three methods: the discrimination of the motion direction, the detection of flashes and the detection of a counterphasing grating. Also here the focus is put on peripheral vision under a variety of adaptation levels. In contrast to minimum border matches and minimum motion the detection of colored objects is regarded to incorporate besides the luminance channel also the color channels of the visual system. The results of these experiments are discussed in chapter 5.

Since a detailed examination of the extra-foveal regions of the human retina is of great interest, the emphasis of all studies lies on the eccentricity of objects to evaluate perceptual differences for several positions in the visual field. Present visual models focus on foveal vision or on one specific eccentric stimulus position. How sensitivity changes in the periphery is not sufficiently considered. The work presented will provide experimental results that contribute to these questions.

The results of all applied methods allow calculating the relative contribution of the rod and cone system to luminance and contrast threshold and therefore provide a basis for mesopic photometry.

Chapter 2

On mesopic vision and mesopic photometry

Purkinje discovered already in 1825 that blue lights appear to be brighter under dim illumination compared to red lights, whereas at high light levels the red lights seem to be brighter than the blue lights (Purkinje, 1825). This shift in sensitivity, called Purkinje effect can be explained with the transition between cone receptors and rod receptors during dark adaptation. The complexity of twilight vision due to the Purkinje shift makes mesopic photometry particularly difficult and is the reason for the lack of any unified photometric approach (CIE, 1994; CIE, 1989). This chapter will give an overview about luminance, the characteristics of mesopic vision and some earlier approaches on mesopic photometry. In addition, the complexities and challenges of understanding mesopic vision and some consequences in practical photometry are outlined.

2.1   Luminance in photometry

To describe visual impressions by photometry the sensitivity of the human visual system to spectral radiation is of special interest. The transformation of radiometric units into photometric units is based on the photopic standard observer which is characterized by the luminous efficiency function for photopic vision. In 1924 the CIE (Commission Internationale de l'Eclairage) recommended a luminous efficiency function as a photopic standard observer $V(\lambda)$ to provide a unified photometric approach. The $V(\lambda)$ function is composed of several datasets collected mostly by flicker photometry from a 2°-3° visual field (LeGrand, 1957; Coblentz & Emerson, 1918; Gibson & Tyndall, 1923; Ives, 1919; Nutting, 1914; CIE, 1983; CIE, 2004). The method of flicker photometry asks observers to minimize flicker by adjusting the luminance of a monochromatic test light at different wavelengths that alternates rapidly with a constant reference light. For the spectral extremes below 490 nm direct brightness matching data from Hartman (1918) and at the red end of the spectrum also brightness matching and step by step matching data were included (Gibson & Tyndall, 1923; Coblentz & Emerson, 1918; Hyde, Forsythe, Cady, 1918), because minimizing flicker under these conditions is difficult to accomplish (LeGrand, 1957). Since most of the data were collected by flicker photometry the character of the $V(\lambda)$ luminous efficiency curve mainly represents sensitivity to rapid changing stimuli. The $V(\lambda)$ function was measured at low photopic luminance levels around 0.5 cd/m² up to a couple of cd/m² and is presently defined between 360 nm and 830 nm. Table 1 shows an overview of the parameters from three studies that were included in the definition of the photopic luminous efficiency function $V(\lambda)$.

Photopic luminous efficiency function V(λ)

	Gibson & Tyndall, 1923	Coblentz & Emerson, 1918	Hyde, Forsythe, Cady, 1918
Method	step-by-step bright. matching	flicker photometry	step-by-step bright. matching
Adaptation-luminance	7-43 td (0.5-3 cd/m²)	22 td (~1.5 cd/m²)	6 td (500nm) – 30 td (560nm), 18td (650 nm)
Fieldsize, Ø	3°	2°	7°
No of Subjects	50	125	21
Refernce light		magnesium oxide illuminated by an incandescent filament lamp, 22 td (1.5 cd/m²)	

Table 1: Parameters used to determine the V(λ) function.

A scotopic luminous efficiency curve analogous to V(λ) for rod vision was recommended by the CIE in 1951 as 10° scotopic standard observer V'(λ). Most of the data were collected by Wald (Wald, 1945) via absolute threshold measurements for a 1° target and Crawford (Crawford, 1949) with direct brightness matches with a 20° field at 0.00003 cd/m².

The photopic (V(λ)) and scotopic (V'(λ)) luminosity curves are both bell shaped and peak at around 555 nm and 505 nm, respectively. V(λ) and V'(λ) are the basis for the CIE definition of luminance, they build the link between radiometric and photometric units. Luminance as the photometric equivalent to radiance is formally defined as the radiance of a light source weighted with the luminous efficiency function V(λ):

$$P_2 = k \cdot \int L_e(\lambda) \cdot V(\lambda) \, d\lambda \, . \qquad \text{Equation 1}$$

Here, P_2 is the photopic luminance for a 2° field according to the CIE (CIE, 1926), $L_e(\lambda)$ in W/(m²·nm·sr) the spectral radiance and V(λ) the CIE luminous efficiency curve defined between 360 and 830 nm. The factor k is the photopic maximum luminous efficacy and takes the value 683 lm/W (LeGrand, 1957). The unit of luminance is cd/m².

In analogy to photopic luminance the scotopic luminance is defined as the integral over the spectral energy of the light source weighted with V'(λ):

$$S = k' \cdot \int L_e(\lambda) \cdot V'(\lambda) \, d\lambda \, , \qquad \text{Equation 2}$$

with V'(λ) being the CIE 10° scotopic standard observer (CIE, 1951) and k' the photopic maximum luminous efficacy which is 1699 lm/W.

Due to measurement uncertainty and the lack of sensitivity values at the spectral ends, the low wavelengths of the V(λ) curve for the 2° field are underestimated. A corrected curve from Judd, which was modified by Vos was later adopted as $V_M(\lambda)$ for a 2° field by the CIE (Vos, 1978).

Since 2005 the CIE color matching function $y_{10}(\lambda)$ suggested by Stiles & Burch (1959) (CIE, 1964) was recommended as a 10° photopic observer $V_{10}(\lambda)$ for para-foveal vision (CIE, 2005). Consequently the luminance based on a 10° field is defined by

$$P = k \cdot \int L_e(\lambda) \cdot V_{10}(\lambda) \, d\lambda \, .$$

By defining luminance as integral over the spectral energy additivity is assumed. Additivity and linearity are essential to almost any metrological system. In photometry additivity is fulfilled if two pairs of stimuli, e. g. A & B and C & D are matched by some criterion e. g. brightness or minimum flicker, and if also the stimuli A & C and B & D obey this matching criterion. Since

the procedure of flicker photometry does produce nearly additive results (Ives, 1912; Wagner & Boynton, 1972; Ikeda, 1983) according to Abney's laws (Abney & Festing, 1886; Abney, 1913), photometry based on V(λ) and V'(λ) fulfill this requirement in most practical cases. Other basic prerequisites for a photometric system are proportionality, which states that if A matches B than also αA matches αB and transitivity, which states that if A matches B and B matches C also A matches C (Grassman, 1853).

Limitations of luminance in photometry

And yet the luminosity functions are not constants, they rather depend on the conditions they were measured under. Luminous efficiency curves change e. g. with field size (Adrian & Kokoschka, 1985; Kinney, 1964), retinal eccentricity, age of the observer, luminance of the adapting field, and chromatic adaptation. Flicker photometry with decreasing field size leads to decreased sensitivity for short wavelength (Hough, 1968; Ikeda, Yaguchi, Yoshimatsu, Ohmi 1982; Hartge, 1991) which can at least partly be assigned to changes in macular pigment optical density. Also with increasing age the sensitivity between 420 and 560 nm decreases, which is consistent with age-related increases in the density of the ocular media (Kraft & Werner, 1994). Pokorny and colleagues made flicker photometric matches at photopic light levels varying over more than 2 log units. They found a narrowing of luminous efficiency curves that they attributed to chromatic adaptation (Pokorny, Jin, Smith, 1993; Marks & Bornstein, 1974). Another influencing parameter is the color of the adaptation background. It has been shown that adaptation to chromatic backgrounds alters the relative contribution of cone receptors and thus sensitivity is changed (Eisner & MacLeod, 1981).

Despite the multiple factors that influence luminous efficiency measured with flicker matches, in photometry V(λ) and V(λ)' are treated as if they are constant under all conditions. This assumption leads under certain conditions to misleading photometric results. This affects in particular e. g. the assessment of saturated colors and spectral lights with a lot of energy in the extreme wavelengths, also assessment of brightness and in general perception under dimmer light levels when rods and cones are active. In addition, differences among observers e. g. in the density of the lens and the amount of macular pigment, can change luminous efficiency functions significantly. Furthermore flicker photometric measurements under high luminance levels show large additivity failures (Dresler, 1953; Ingling et al., 1978). Strictly speaking the standardized luminous efficiency curves obey the linearity laws and represent luminance only in the restricted conditions in which the curves were measured. For practical photometry, the fact that luminance by flicker matches does not represent the brightness of a light (Sperling & Lewis 1959; Boynton & Kaiser 1970) has also been formulated as a concern (CIE, 1989). Saturated lights appear brighter than less saturated lights of the same luminance. This failure in additivity, also called the Helmholtz-Kohlrausch effect is said to be mainly due to cone-cone interactions.

Despite these constrains, the concept of luminance as described above is sufficient for most applications. Especially when observer's task involves high temporal and spatial frequencies, luminance can be regarded as appropriate (Lennie, Pokorny, Smith, 1993). Nevertheless, despite the improved sensitivities at the short spectral range of $V_{10}(\lambda)$ and $V_M(\lambda)$, and despite the significance of V'(λ) in night time vision, only V(λ) is used in photometry.

The ratio between the effectiveness under dark conditions and the effectiveness under daylight is used in form of the S/P ratio to characterize light sources. Here the S/P ratio is defined and used in the following chapters as the ratio of the scotopic luminance to the photopic luminance based on V'(λ) and V_{10}(λ) respectively:

$$S/P = \frac{k' \cdot \int E_e(\lambda) \cdot V'(\lambda)\, d\lambda}{k \cdot \int E_e(\lambda) \cdot V_{10}(\lambda)\, d\lambda}$$

For illumination purposes the S/P ratio is besides the absolute light level, the only parameter that can be influenced by the design of the lighting installation.

2.2 Physiological basis of luminance

The detection of flicker as used in flicker photometry under photopic intensities is accomplished by the middle- (M cones) and long-wavelength sensitive cones (L cones) only. The linear sum of the signals from L and M cones forms the achromatic luminance channel. The achromatic luminance channel can be regarded as a univariant or colorblind system. Univariance here means that the response varies only with the number of photons absorbed, independent of the wavelength of the absorbed photons. Only the chance of eliciting a response by the receptor changes with the receptors sensitivity towards the wavelength of the arriving photon.

In flicker photometry two lights that differ in color and luminance are alternated rapidly. Subjectively, the color variation is not perceived by the subject for high alternation frequencies. It is for this reason that the intensity adjustment made during flicker photometry can produce a well-defined minimum flicker setting, which defines the isoluminant point (Ives, 1919). This phenomenology supports the conception of a color-blind achromatic system which alone is fast enough to respond to rapid flicker. It is not certain what the physiological basis of this achromatic system is, but it can plausibly be identified with the 'non-opponent' or magno-cellular neurons found in the optic nerve and in the lateral geniculate nucleus (LGN) of the brain where the optic nerve fibers terminate (e. g. Livingstone & Hubel, 1987; Lee, Martin, Valberg, 1988; Kaiser, Lee, Martin, Valberg, 1990; Smith, Pokorny, Lennie 1993) (see Figure 1).

The contribution of S cones to the achromatic luminance channel and the magnocellular pathway was discussed for a long time. It was shown that S cone contribution to the magnocellular pathway in macaque monkeys is small (Callaway & Chatterjee, 2002) or negligible (Sun et al., 2006). Also a lot of psychophysical studies with humans found no measureable contribution (Eisner & MacLeod, 1980; Tansley & Boynton 1976 and 1978; Boynton & Kaiser, 1978). However, today evidence exist that S cones can make a small contribution to luminance, but only under specific conditions involving very high intensities (Stockman, MacLeod, DePriest, 1987; Ripamonti, Woo, Crowther, Stockman, 2008).

Although the physiological basis of luminance may be the activation of the achromatic pathway that receives information mainly from the L and M cones, in reality isoluminance settings obtained for a particular subject and condition may diverge from the photometric standardized

luminance. It was noted by Stockman and Sharpe that 'It should be recognized, however, that V(λ) is more of a photometric convention than a physiological reality' (Stockman & Sharpe, 2001). To differentiate between the photometric luminance defined by the CIE and the individual luminance based on an individual spectral sensitivity, Kaiser uses the term 'sensation luminance' for the latter (Kaiser, 1988). This allows for the possibility that a subject's photometric settings reflect the excitation of their own achromatic system, differing slightly from the sensitivity conventionally assumed.

How the visual information reaching the eye is encoded by the retina is a question that has long concerned scientists. The Young-Helmholtz three-component theory (Helmholtz, 1896) assumes the existence of three independent cone types with different spectral sensitivities. The signals of the three cones are transmitted separately to the brain and lead directly to a color sensation. The main drawback of this theory is that it can not explain color appearance of mixed colors. The color-opponent theory proposed by Hering (Hering, 1878) assumes opponent channels made up by neural signals of opposite signs that can account for perception of hues intermediate to e. g. red-blue and red-yellow. With this Hering's theory can explain perception of a variety of colors. Today it is widely acknowledged that a combined theory can explain many visual phenomena to a satisfactory degree.
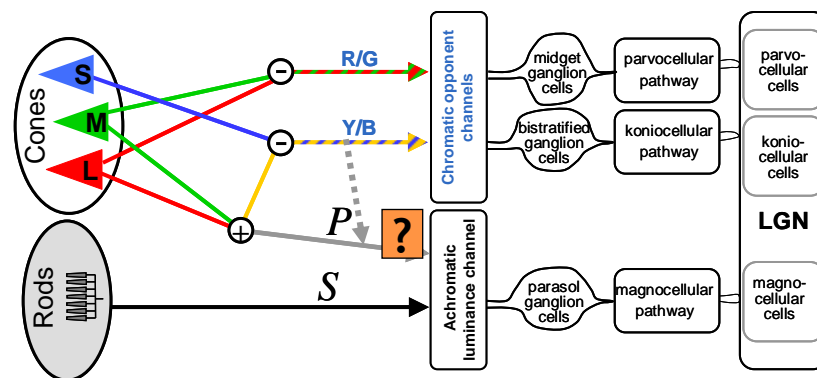
Figure 1: Schematics of the luminance and color pathways and their composition. The achromatic luminance information is transmitted in the magnocellular pathway via the parasol ganglion cells, whereas the opponent color information is mediated by the midget and bistratified ganglion cells that feed into the parvocellular and koniocellular pathways, respectively. The information of these channels is preserved in separate retinotopic layers in the lateral geniculate nucleus (LGN).

Figure 1 shows the composition of the neuro-visual channels of the eye. This simplified sketch indicates that the luminance information as a sum of L and M cone signals is mediated by the parasol ganglion cells and feeds into the magnocellular pathway (Lee, Martin, Valberg, 1988). Hence the sensitivity of the achromatic pathway builds the basis for the photometric system. This pathway is colorblind but highly sensitive and optimized for rapid changing stimuli. And furthermore it reacts according to the additivity law. The achromatic pathway mainly excludes the S cones and color information. The color information is carried by the parvocellular and koniocellular channels in form of opponent cone signals like the red-green and the yellow-blue difference signals. Signals incorporating the opponent channels do not show additive behavior. The description of one luminance channel and two color channels might even be a very simplified view on the circuitry of the visual system. The findings of several more classes of

ganglion cells suggest that there are more pathways involved with different spatio-temporal properties than is currently known (Field, Chichilnisky, 2007).

Polyak (1941) first described and named the parasol and midget ganglion cells. The receptive fields mediated by these cells possess characteristic temporal and spatial properties (Polyak, 1941; Gouras, 1968; Ingling & Drum, 1973). The parasol and midget ganglion cell (also named phasic and tonic after their temporal properties by Gouras (1969)) receptive fields have both an excitatory center and an inhibitory surround. A parasol ganglion cell receptive field feeding in the **magnocellular pathway** responds to the same receptor classes, which can be either L or M cones. (It is assumed that S-cones do not contribute to the achromatic channel besides other evidence there was no S-cone input into the phasic cells found.) This non-opponent organization allows the mangocellular system to enhance edges and contours and to stay relatively unaffected by large uniform fields. The system has a shorter latency than chromatic fibers and is optimized to fast changing stimuli. It is generally assumed from the high agreement in temporal and spatial properties that the parasol cells feed the magnocellular pathway, which in turn makes up the achromatic luminance system (Ingling & Drum, 1973). Moreover, the sensitivity of the parasol ganglion cells shows good agreement with the 10° V(λ) function (Kaiser, Lee, Martin, Valberg, 1990). With darker adaptation levels the achromatic system undergoes a Purkinje shift to a rod spectral sensitivity (Ingling & Drum, 1973). The **parvocellular pathways** mediated by the midget ganglion cells are optimized for color vision and have a longer latency than the achromatic system. The parvocellular receptive fields are characterized by having a center that is spectrally different from the surround e. g. an only L cone center with an only M cone surround, hence they form the red-green opponent pathway. With this, the response of a parvocellular cell to an achromatic contrast is wavelength dependent, which allows to differentiate between colors. The parvocellular system responds only to a luminance edge with enhancement, a chromatic edge (e. g. a red-green edge) leads to a smooth change of the response. In contrast to the center surround organization, the koniocellular receptive fields, feeding the **koniocellular pathway** have only one sensitive area which is a blue-ON and yellow-OFF center.

Whether a visual mechanism leads to a V(λ)-like luminous efficiency curve or not depends not only on various parameters of the stimuli and the adaptation state of the eye, it is also a result of the neuro-visual channels that are involved in different visual tasks. Since the color opponent channels are too slow to follow rapid changing stimuli, methods like flicker photometry, critical flicker frequency and threshold measurements involving very short and small stimuli do not address the chromatic information from the opponent channels. Also methods in conjunction with edges and very small stimuli like border adjustments and visual acuity tap only the luminance system (Lennie, Pokorny, Smith, 1993), since the color channels lack high spatial resolution. In contrast, the detection of objects and brightness perception are visual functions that are known to incorporate achromatic and chromatic information. Sensitivity curves for detection of a flash and recognition of the opening of a Landolt-C ring measured on-axis and 10° off-axis show several peaks at photopic and mesopic adaptation levels (Váradi & Bodrogi, 2006). Sensitivity curves based on brightness matches are wider than the V(λ) curve and show an increased sensitivity in the short wavelength range (Wagner & Boynton, 1972).

As already stated, only the magnocellular pathway exhibits additivity. When both the phasic and tonic systems contribute to e. g. the detection of a target, additivity fails. The opponency of the

two color systems can lead to intriguing effects. When two colored stimuli each of half threshold luminance are mixed, the tonic component can be reduced and the target might not be visible anymore, although the colored targets were visible separately at the full amount of luminance (Ingling & Drum, 1973).

The following section summarizes some methods to measure sensitivity or visual performance and their underlying mechanisms.

2.3 Methods to assess sensitivity and luminous efficiency

Direct heterochromatic brightness matches (HBM)

Comparing the brightness of two adjacent fields was extensively used under various adaptation levels to assess visual perception (Ives, 1912; Kinney, 1955; Wagner & Boynton, 1972; Comerford & Kaiser, 1975; Nakano, Ikeda, Kaiser, 1988). Luminous efficiency functions obtained by direct brightness matching measurements are broader than $V(\lambda)$ and typically show increased sensitivity to short-wavelength (Wagner & Boynton, 1972). However, for stimuli smaller than 10' the differences diminish (Ikeda et al., 1982). The differences are due to the chromatic contribution that brightness matches inherit whereas luminance does not. Brightness matches were also widely used to measure luminous efficiency functions for the mesopic range (Palmer, 1968; Kokoschka, 1972; Ikeda & Shimozono, 1981; Trezona, 1987; Sagawa & Takeichi, 1992).

Brightness matches reveal substantial variations in sensitivity between subjects, which are highest at the spectral ends (Bedford & Wyszecki, 1958; Ikeda, Ikeda, Ayama, 1992). Among others, Sagawa and Takeichi (Sagawa & Takeichi, 1983, 1986) found that individual differences in brightness matchings are more evident in the middle of the mesopic range. Particularly large differences were found when a large field of 10° is used. Palmer determined the luminous efficiency curve of 24 subjects by heterochromatic brightness matching under photopic conditions (Palmer, 1985). Twelve of the sensitivity curves were similar to the $y_{10}(\lambda)$ color matching function and showed additivity. Eight of the curves were double peaked curves with large additivity failures and four more additive curves were found which were similar to $y_{10}(\lambda)$ but broader.

What's more critical for photometry are the additivity failures of this method (Boynton & Kaiser, 1968; Guth, Donley, Marrocco, 1969). Ikeda and Nakano (1986) measured sensitivity curves in the mesopic brightness range and found that some subjects' curves show additivity and some not.

Flicker photometry

The physiological basis of flicker photometry is the mangocellular pathway with input from the parasol ganglion cells (Lee, Martin, Valberg, 1988). Parasol cells can resolve flicker to higher frequencies than do midget cells. That explains the persisting brightness flicker after the fusion of hue at lower frequencies.

Minimally distinct borders (MDB)

Minimally distinct border (MDB) is a matching method where not the brightness is matched to a reference; rather the border between two adjacent areas is adjusted to be minimally visible. Border assessments are mediated by the edge enhancing phasic system. The chromatic system produces no enhanced signal at the matched border. But chromatic information causes the more saturated side to appear brighter (Ingling & Tsou 1988). Kaiser (Kaiser, 1971), Wagner & Boynton (1972), and Boynton (1973) compared the spectral sensitivity measured with the psychophysical criteria of minimal distinct border, minimum flicker and heterochromatic brightness matching (HBM). Results show strong similarities between flicker photometry and MDB. Differences between HBM and the two other methods were comparatively more pronounced. To adjust for equal brightness more luminance is needed for the reference field to match the colored test lights compared to a minimum flicker or minimum border match. The differences between the MDB and HBM matches can be explained with the characteristics of the chromatic and achromatic pathways and parvocellular and magnocellular receptive fields (Ingling & Drum, 1973).

In sum, the basis of MDB matches is the magnocellular pathway with the parasol ganglion cells (Kaiser, Lee, Martin, Valberg, 1990). The univariance of the luminance system leads to MDB matches that are highly linear and additive (Ingling et al, 1978; Kaiser, Lee, Martin, Valberg, 1990; Kaiser & Boynton, 1968; Kaiser, Boynton, Herzberg 1971; Boynton & Greensporn 1972; Boynton & Kaiser, 1968).

One might ask whether MDB is equivalent to flicker photometry with a frequency of 0 Hz. Ingling and colleagues found that MDB and flicker matches require the same amount of light to find a match at 100 td. At higher light levels more light is required for the flicker match than for the MDB match. Also the level of additivity depends on the adaptation level: near 100 td MDB and flicker are additive. Flicker photometry shows additivity failures with changing adaptation level whereas MDB maintains additivity to a high degree (Ingling, et al., 1978).

Furthermore, with MDB a greater reliability is obtained than with other methods like brightness matches because the criterion of minimally distinct border is more unambiguous (Kaiser, 1971).

Motion discrimination & minimum motion (MinMot)

It has been suggested that motion perception is mediated by the luminance pathway and that color does not or only marginally contribute to motion (Anstis, 1970; Ramachandran & Gregory, 1978). However, other research shows that the red-green color opponent channel makes a contribution to or even inhibits motion perception (e. g. Derrington & Badcock, 1985; Cavanagh & Favreau, 1985; Cavanagh & Anstis, 1991). It seems that different mechanisms are involved to detect the moving stimuli and to detect the direction of motion (Stromeyer et al., 1995). The method of nulling the apparent motion is comparable in its response to flicker matches (Cavanagh & Anstis, 1983; Anstis, 1980) suggesting that the two methods address the same channel. The minimum motion method uses a stimulus composed of homochromatic and heterochromatic counterphasing sinusoids and has been used to determine individual isoluminance ratios between two colors under photopic conditions (Anstis & Cavanagh, 1983; Cavanagh, MacLeod, Anstis, 1987; Kaiser, Vimal, Cowan, Hibino, 1989). Kaiser and colleagues

found that minimum motion showed small additivity failures, which can be disregarded for practical purposes (Kaiser, Vimal, Cowan, Hibino, 1989.

Detection

Possible criteria to assess visibility or performance can be among others detection contrast or recognition contrast. Luminous efficiency functions measured addressing these criteria do generally not agree well with luminous efficiency measured with flicker photometry (Lennie, Pokorny, Smith, 1993). The visual information for these mechanisms is mediated by different neurovisual channels. In addition to the achromatic luminance pathway information from the opponent–chromatic channels are involved. This leads to luminous efficiency curves that are higher in the spectral extremes and show several peaks. E. g. the sensitivity curves derived from detection of monochromatic objects are wider (King-Smith & Carden, 1976; Freiding, et al., 2007). Also the off-axis as well as the on-axis sensitivity curves measured by Freiding et al. (2007) with detection threshold show an increased sensitivity at the short wavelength and several peaks at photopic and mesopic adaptation levels. It seems evident that the color-opponent pathways are contributing also at low levels in the far periphery at 10°-30° (Kuyk, 1982; Bodrogi, 2006; Freiding et al., 2007) with decreasing influence from the fovea to the periphery (Mullen & Kingdom, 2002). The shift of sensitivity for detecting targets leads to distinctly different contrast thresholds for colored targets, with blue stimuli showing a lower threshold (Ketomäki, 2006). Also luminous efficiency curves based on recognition of targets are double peaked and show an increased sensitivity in the lower wavelength range below 520 nm (Varady et al., 2007).

A way to assess the contribution of several receptors and pathways to contrast thresholds is to measure threshold contours in contrast space e. g. M-L cone contrast space or photopic vs. scotopic luminance contrast. Detection threshold contours in the L-M cone contrast plane have been measured earlier with the detection of flashes and motion (e. g. Chaparro et al., 1993, 1994; Stromeyer et al., 1995; Giulianini & Eskew, 1998) under photopic conditions. Kremer and Meierkord (1999) measured threshold contours in Rod-L-cone contrast space under photopic and high mesopic adaptation conditions at several eccentricities. They found that the relative influence of rod signals to the L-cone signals increased with increasing retinal eccentriccity and decreasing retinal illuminance. At 20° eccentricity, rod and cone signals were of about equal magnitude at a photopic adaptation luminance. Temporal frequency between 2 Hz and 10 Hz showed no large effect on the contributions of both receptors.

Reaction time

Earlier studies showed that reaction times lead to V(λ)-like luminous efficiency curves (Pollack, 1968; Lit, Young, Shaffer, 1971). However, more recent research found that reaction times are subject to opponent–chromatic information and lead to wide and multi-peaked sensitivity curves (Walkey et al., 2007). Also Szalmas and colleagues (2006) measured reaction times to detect peripheral targets of different colors during a driving task and they could not exclude that chromatic information influences the reaction time results. Hence, whether reaction times for detecting peripheral objects involve only the luminance channel is not conclusive from literature.

2.4   Characterization of rod and cone vision and mesopic vision

The dualism of the human visual system allows us to act confidently over a wide range of light levels. The cones are specialized for the perception of fine details and fast movement under bright conditions. The cone system consists of three cone types sensitive to slightly different wavelength ranges. Unlike the cone system the rod system is univariant; there is only one kind of receptor involved. The rod response varies only by the number of photons that are absorbed. Whether a photon gets absorbed or not depends only on its energy. Therefore the rods can not differentiate between captured photons from short wavelength light and long wavelength light, the rod system is colorblind. As a further consequence of the univariance, the rod spectral sensitivity is additive; the luminous efficiency function does not change with adaptation as long as only rods are involved. In contrast, the cone system is not univariant since more than one receptor is involved. Additivity holds only for the achromatic luminance channel and only under certain conditions, like minimum flicker photometry and minimally distinct borders.

At which luminance does rod vision end and cone vision start? What is the luminance range of mesopic vision? On a physiological level, the answer seems straight forward: always when cones and rods are active. However, the border between mesopic and photopic vision is not clearly defined. The rods remain capable of differentiating light up to a very high saturating luminance of at least 1000 scotopic trolands (sc td) (~150 cd/m^2) (Aguilar & Stiles, 1954). But at which level does rod contribution make a noticeable difference in perception? The CIE gives as guideline 'at least several cd/m^2' (CIE, 1983). Kokoschka sets the luminance limit for pure cone vision to 30 td (~2 cd/m^2).

Contrast thresholds and TVI curves

Some of the earliest extensive studies on threshold contrasts were done by König & Brodhun (1903), Blackwell (1946), Bouman (1950), Aguilar & Stiles (1954), and Barlow (1957). The derived threshold versus intensity curves (TVI-curves) show the log of the incremental threshold intensity ΔI to detect a flash on the ordinate and the log intensity of the background I on the abscissa. Such a curve can be measured for rods and cones to describe the mechanism of dark adaptation as schematically shown in Figure 2.
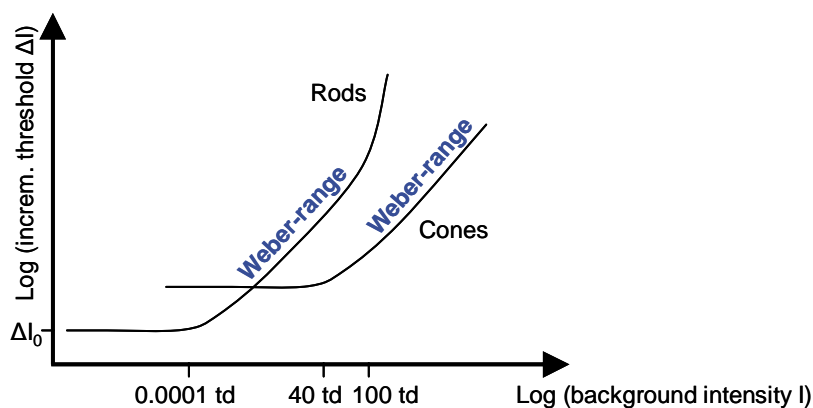
Figure 2: Schematics of TVI-curves for rods and cones. The units of both axes are photopic trolands.

A TVI-curve consists of three distinct sections. At low light levels the incremental threshold levels off (in logarithmic coordinates) to the absolute threshold ΔI_0. The background intensity for rods below which the threshold remains approximately constant (the 'knee' in the rod curve in Figure 2) is between I = 0.01 and 0.001 sc td (Aguilar & Stiles, 1954; Alpern, Rushton, Torii, 1970; Stiles & Wyszecki, 1982). At brighter light levels the incremental threshold raises linearly with adaptation luminance. Under these conditions the receptors work in the Weber range. Saturation occurs when the intensity exceeds the operation range of the receptor. Rods begin to saturate around 200 sc td and saturation is finished at (2000 sc td - 5000 sc td) $120 - 300$ cd/m^2 (Aguilar & Stiles, 1954; Hayhoe, MacLeod, Bruch, 1976). Above 200 sc td rod sensitivity rapidly decreases and linearity between threshold and intensity is lost.

The TVI-curve in the Weber-range can be described by

$$\log \Delta I = k \cdot \log(I + \Delta I_0) + const..$$

Here, k is a parameter that describes the slope of the TVI-curve. The slope characterizes the rapidity of dark adaptation of the receptor system. A k of 1 is in agreement with Weber's law. Weber's law states that the incremental threshold varies in direct proportion to the intensity of the background. From the equation above the following relation can be inferred:

$$\Delta I \sim I^k$$

This relation will be used later to estimate the TVI-slope k from the relative rod and cone weights. For rods the TVI-exponent was found to depend on the duration and the size of the test flash (Barlow, 1957). For long and large stimuli Weber's law is a good approximation at high intensities. Thresholds determined with a tiny and brief flashes rise less quickly with adaptation resulting in considerably lower TVI-slopes of $0.5 - 0.7$ (Blackwell, 1946; Barlow, 1957; Sharpe & Stockman, 1993). Sharpe et al. (1989) found that rods alone do not conform closely to Weber's law, it is only in conjunction with cones that the TVI-slope increases to nearly unity. A red long wavelength background excites cones and inhibits rod adaptation, which results in a steeper increase of the TVI-curve (Sharpe, Fach, Stockman, 1992).

Vision in the periphery

Foveal and peripheral perception differs to a high degree. Mainly the distinctly different distribution of the two kinds of receptors over the retina and the associated change in temporal and spatial behavior with eccentricity lead to differences in sensitivity and other visual tasks. The number of cones per unit area peaks in the fovea with 200,000 cones per sq mm and decreases sharply radially in all directions; beyond 10° off-axis the reduction is slight (Curcio et al., 1990). The peak density of rods on the other hand is at around 15° in the periphery. The inner 0.5° field of the fovea is completely rod free. As a consequence of the change in rod density the sensitivity at very dim lighting conditions increases with eccentricity. Anstis found that this increase occurs linearly at mesopic and scotopic light levels (Anstis, 2002). Also luminous efficiency functions are substantially differed at different retinal locations. Flicker photometry, brightness matches and threshold methods done off-axis reveal sensitivity curves that show a large sensitivity enhancement at short wavelength (Weale, 1952; Abramov & Gordon, 1977; Stabell & Stabell, 1980). The shift of the peak sensitivity to shorter wavelength

and the relative enhancement of sensitivity to shorter wavelength resemble more closely the scotopic than the photopic luminous efficiency function.

With increasing eccentricity the spatial resolution decreases, due to the stronger pooling of signals. The receptive field organization is essential in the rod system and allows detecting as little as a couple of photons under dark adaptation. The photopic receptive fields are limited in size due to lateral inhibition. Barlow (1957) assigned the increased summation at dark adaptation levels to the disappearance of lateral inhibition. Inhibition is less for short flash durations resulting in larger receptive fields.

Temporal aspects and spatial sensitivity of rod and cone vision

The graph in Figure 1, presenting the rod contribution as a single line, is a simplification that does not allow for the duality of the rod visual system. Critical flicker frequency experiments (the luminance of a flickering stimulus is adjusted to a just noticeable flicker) revealed that rod signals travel to the ganglion cells in at least two pathways with different temporal properties (Connor & MacLeod, 1977; Sharpe, Stockman, MacLeod, 1989). The sluggish, but sensitive π_0 pathway gains sensitivity by integrating signals over space and time to an extent that allows single photon absorptions. These slow signals are most probably derived from the ON-rod bipolar pathway and are predominantly at scotopic luminance levels. The faster and less sensitive π_0' pathway is likely derived from the rod-cone gap junction and cone bipolar pathways and predominant in the mesopic range. The temporal differences between the slow π_0 pathway and the fast π_0' pathway can result in a complete cancellation of rod signals at 15 Hz (Conner, 1982; Sharpe, Stockman, MacLeod, 1989).

The rod flicker threshold can be increased by the desensitization of the cones by steady backgrounds. L and M cones can reduce the sensitivity of π_0, but have only a slight, but measureable effect on π'_0 (Sharpe, Stockman, MacLeod, 1989; Sharpe, Fach, Stockman, 1993). In addition to the phase differences within the rod system the rods and cones poses different temporal behavior. The rod system is in general more sluggish; simplified, the rod response of the slow π_0 pathway is delayed by roughly 67 ms in comparison to the cone signals. Hence, a stimulus that flickers at 7.5 Hz and that is detectable by the rods and the cones can lead to complete cancellation of the flicker, whereas the same stimulus at lower and higher frequencies produces an enhanced amplified output signal (MacLeod, 1972). At mesopic levels the rods speed up considerably which results in changes of the phase delay between rods and cones (Stockman & Sharpe, 2006). In summary, the rod system integrates signals over space and time to gain sensitivity by loosing high acuity. Integration over space and time is less pronounced for the photopic system which provides a high spatial and temporal acuity.

The temporal and spatial sensitivity curves of the visual system, that is, the sensitivity as a function of temporal and spatial frequency of the stimulus, exhibit similar shapes. At high light levels these curves show a band-pass characteristic which turns into a low-pass curve at decreased luminance. Due to the slower response times of the rods the peak of the temporal sensitivity function shifts towards lower temporal frequencies for darker adaptation levels (Kelly, 1961). Also for increasing eccentricity sensitivity increases for low temporal frequencies (Kelly, 1984). The rod temporal sensitivity curves drop-off at frequencies higher than 6-7 Hz at scotopic light levels (Sharpe, Stockman, MacLeod, 1989) while the cones are highly sensitive up to 15-20 Hz (Kelly, 1961).

16

The spatial sensitivity for photopic foveal cone vision shows a broad peak between 5 and 10 cpd opposed to around 0.9 cpd for peripheral rod vision (Kelly, 1961; D'Zmura & Lennie, 1986), though the peak varies in its position strongly with parameters. Results from Kelly (1984) show a shift of peak sensitivity from 3 cpd to 1 cpd with increasing eccentricity from 0° to 12°. However, it is not conclusively clear from former results how different rod and cone spatial sensitivities are at the same retinal position. Results from D'Zmura and Lennie (1986) suggest considerable differences though not as substantial as the differences between spatial sensitivity of peripheral rods and foveal cones.

Choice of methods

As described above flicker photometric matches that were used to define the photopic and scotopic standard luminous efficiency functions are due to phase lags between rod-cone pathways and rod-rod pathways not applicable in the mesopic range (Vienot & Chiron, 1992). Therefore other methods have to be considered to examine the mesopic visual response. Among the main consideration in finding a mesopic equivalent to luminance is the question which visual pathways the applied method addresses: which receptors are involved; and what are the temporal and spatial characteristics of the addressed system. It was found that not only flicker photometry but also methods like minimally distinct border, critical flicker fusion, and - with some reservations - reaction time address the achromatic channel and lead to sensitivity functions like $V(\lambda)$. Other methods, such as brightness matches, detection threshold, and absolute threshold measures produce luminous efficiency curves that deviate from $V(\lambda)$, e. g. are broader (heterochromatic brightness matching) and have multiple peaks (chromatic detection threshold). Because of the involvement of the color opponent system the results of these techniques do not obey the linearity laws and show additivity failures. Because of the lack of additivity and the uncertain criterion of brightness assessment brightness matches were not used here.

For a mesopic equivalent to luminance it seems straightforward to find a way to record the response of the magnocellular pathway in the mesopic range as well. Therefore the present work adopts the methods of minimum motion and minimally distinct border for the investigation of the luminance channel. Both techniques show an additive character and have clear matching criteria that lead to smaller deviations in the results. In addition, contrast thresholds were measured for the detection of flashes in the periphery, the detection of a counterphasing annulus, and the discrimination of the direction of motion. One of the questions to be considered in these investigations will be to what extent these methods and results can be transferred to mesopic and scotopic adaptation conditions. Furthermore, due to the importance and peculiar qualities of peripheral vision a strong emphasis is put on measuring sensitivity under various eccentricities. Other central questions arise from the duality of the visual system. How do the responses of the photopic system and the responses of the scotopic system contribute to the mesopic response? Do rods and cones cooperate fully and their responses add up linearly to a sum signal? Or is it rather that the rod response and the cone response have to exceed a threshold to perceive a target?

The next sections will discuss possible ways to address these questions and describe earlier approaches to mesopic photometry.

2.5   Defining and modeling mesopic luminance

In the mesopic brightness range, by definition neither the scotopic luminous efficiency function nor the photopic luminous efficiency function represents the sensitivity of the eye. There is no standardized mesopic luminous efficiency curve comparable with the standard observers that define a standardized sensitivity function for the photopic and scotopic brightness range. The multiple differences between the two receptor classes and their interactions make it questionable whether one unified description or even a set of curves can adequately describe mesopic vision.

Recall that the differences in the rod and cone receptor systems include, but are not limited to the distinct spectral sensitivities and contrast sensitivities, different temporal and spatial characteristics and different spatial distribution over the retina. In addition, rod and cones have no separate neural pathways, e. g. there are no ganglion cells carrying only rod signals. As a consequence complex combination effects like supra-additivity, and sub-additivity occur. Supra-additivity which is mainly evident in the low mesopic region is due to cone-rod interaction, whereas sub-additivity (Helmholtz-Kohlrausch effect) occurs at high mesopic light levels and is caused by cone-cone interactions and the opponent color information. Hence, any mesopic curve of sensitivity or performance will strongly depend on temporal and spatial characteristics of the stimuli; therefore targets with temporal and spatial characteristics might produce mesopic luminous efficiency function with different rod and cone weights (Stockman, Sharpe, 2006).

Some approaches to define a mesopic equivalent to luminance calculate a weighted sum of $V(\lambda)$ and $V'(\lambda)$ to define a mesopic luminous efficiency curve (Orreveteläinen, 2005). The continuous change in sensitivity in the mesopic range ensures that no mesopic function can follow Abney's law of additivity (Berman & Clear, 2001). He et al. (1997), however, state that within a certain luminance level additivity can be achieved for mesopic systems based on reaction time.

By nature, the mathematical definition of luminance for the photopic and scotopic range given in Equation 1 and Equation 2 does not allow for a similar characterization of a mesopic equivalent of luminance: e. g. additivity is not given; multiple receptors contribute to a different extent to luminance depending on the light level, rods contribute nonlinearly in the region of rod saturation (Stockman, 2004, Stockman & Sharpe, 2006). This and other characteristics of mesopic vision make a definition of a luminous efficiency function and luminance in a similar way for this range intricate, if not impossible. To do so, one has to depart from the current concept of photometric luminance. A photometric system for the mesopic adaptation range can be defined in different ways. A model based on achromatic luminance information is desired to maintain consistency with the photopic standard observer. Also at high spatial and temporal frequencies it is only the color blind luminance signal that determines visual perception. Therefore, and for simplicity it seems appropriate to initially only take achromatic information into account.

The following paragraphs outline two theoretical approaches to define luminance; i: as incremental luminance describing a measure of effective contrast and ii: as absolute luminance that characterizes the state of adaptation.

Incremental luminance

For predictions about visibility of objects under mesopic conditions the luminance difference between object and its background is crucial. A model would use incremental rod and cone responses. This approach can be used to aim for conclusions about the visibility of objects under mesopic conditions. The luminance contrast between a target and its background can be defined with the help of a mesopic luminous efficiency function that serves as a spectral weighting function for computing 'mesopic contrasts'. Though applicable under the given conditions, such a function necessarily varies with light level and parameters like object size and presentation time. The computed luminance contrast should be helpful for predicting how well the object is seen. Possible criteria to assess visibility or performance include detection contrast, recognition contrast, or reaction time. However, to predict detection and recognition with precision it may be necessary to depart form a pure luminance model and take achromatic information into account.

A mesopic incremental luminance ΔM would be defined relative to the adapting stimulus by weighting photopic and scotopic quantities with rod and cone weights W_S and W_P. These receptor weights can be relative and normalized weights so that the sum of W_S and W_P equals 1. In a general notion, the weighted quantities can be either incremental luminances defined as the difference between background and target ΔS and ΔP, or contrasts e. g. $\Delta S/S$ and $\Delta P/P$. The former choice leads to a definition of mesopic incremental luminance as shown in Equation 3:

$$\Delta M = W_S \cdot \Delta S + W_P \cdot \Delta P .$$

<div align="right">Equation 3</div>

The incremental luminance difference ΔM as defined here is additive; although as noted above additivity can not hold generally, it may hold approximately for a limited range of increments in a relatively fixed state of adaptation.

Absolute luminance

An absolute luminance as measure for mesopic vision would describe the light level or state of adaptation in a way that it predicts visual performance measured by criteria such as achromatic contrast sensitivity. Equality of adaptation luminance should lead to equal visual performance. Such an approach is natural if rod and cone signals travel in a common pathway and form a 'mesopic' signal. According to D'Zmura and Lennie (D'Zmura, Lennie, 1986) the visual system can not differentiate between a stimulus seen by only rods and a stimulus seen by only cones. They concluded that rod and cone signals travel in common pathways. In this case one can regard mesopic luminance as the combined signals from rods, L- and M-cones. Hence, this univariant channel must be colorblind and is also likely to obey Abbney's law of additivity. This suggests the possibility of defining a mesopic value, a nonlinear function m(S, P) where S and P are absolute rod and photopic values, not differences. The definition of m(S, P) is such that differences in the mesopic value m(S, P) around an adapting level represented by S and P represent the effective increment or decrement in luminance as given by Equation 3. The function m(S, P) would need to be nonlinear in order to generate the observed variation in rod and cone weights with S and P: for example, if cone incremental sensitivity is constant in the mesopic range (see Figure 2), while rod sensitivity conforms to Weber's Law, m(S, P) could be linear with P, and with log(S). Development of such a theoretical approach remains a task for the future.

Picturing and modeling mesopic luminance

A diagram that shows the difference between adaptation luminance and stimulus luminance ΔP (photopic luminance difference) and ΔS (scotopic luminance difference) facilitates drawing conclusions about the relation of rod and cone responses. As an example, Figure 3a shows two ellipses as threshold contours plotted in ΔP-ΔS space. The closed elliptic shape of the contour arises when the color opponent mechanism is involved. In this case a stimulus can still be detected even if it doesn't differ in luminance from the background. With this in mind, one can think of a very elongated contour or two parallel lines as threshold contours for a pure luminance mechanism. A wider ellipse will be measured for mechanisms that involve the color opponent information (Chaparro et al. 1994).

A stimulus with photopic and scotopic luminance increments within the contour is below threshold and would not be seen, though a target is visible when its incremental luminance is beyond the contour. The orientation of such a contour is in the direction of constant luminance (isoluminance). Under photopic adaptation levels it would be oriented along the ordinate in ΔP-ΔS space as depicted with the gray dashed contour in Figure 3a. In this example, a small difference in photopic luminance is sufficient to perceive the stimulus. However, by keeping the photopic luminance of the stimulus at the adaptation luminance and changing the scotopic luminance only, a high scotopic contrast between background and target is necessary for perception. Under the assumption that it is only the luminance channel in form of the sum signal of L and M cones that is responsible for perception, such a stimulus will hardly be seen on the line of constant photopic luminance (with $P_{stim} = P_{adapt}$). In other words, the threshold contours are oriented along the axis of least sensitivity in ΔP-ΔS space, which under photopic conditions will be the vertical line at $\Delta P = 0$ and for scotopic perception it will be a horizontal line at zero scotopic incremental luminance ($\Delta S = 0$).
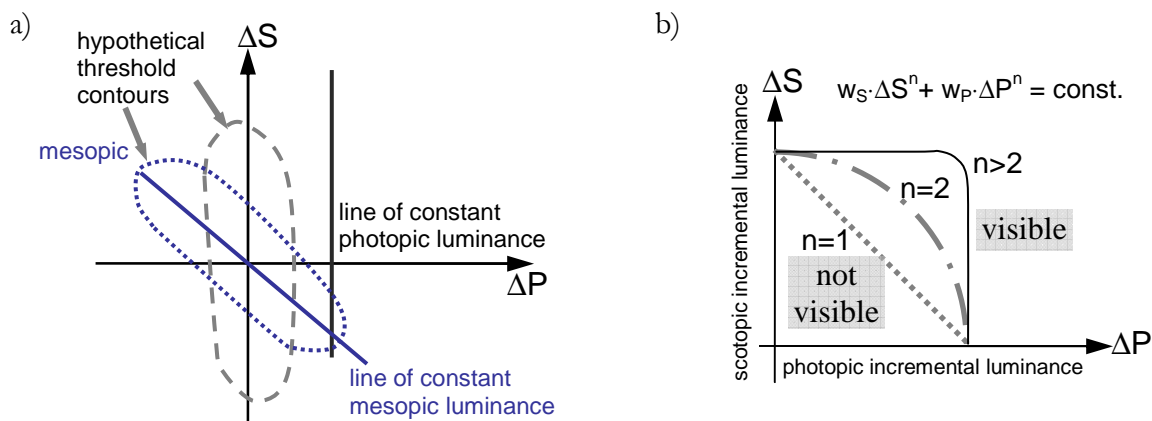
Figure 3: a) Hypothetical threshold contours or contours of equal visibility for a photopic (gray dashed) and mesopic (blue dotted) adaptation state. The long axis of the ellipses are lines of constant luminance. The orientation of the contours depend on the relative contribution of rods and cones to lumiannce, hence on the adaptation state. b) The graph shows the first quadrant of the same diagram with curves for several values of n, determining the degree of cooperation.

While the elongation of the contour depends on the visual channels used for perception, the orientation of the contour is a measure of the relative contribution of the rod and the cone

system to perception. A pure cone response will result in a contour oriented vertically, as described above. Scotopic vision that only taps the rods will lead to horizontally oriented contours. A stimulus that differs only in photopic luminance from the background level will hardly be visible under scotopic adaptation conditions, but a difference in scotopic luminance greater than the scotopic incremental threshold will make the target visible. Under conditions where both, rods and cones contribute to perception a threshold contour will have a negative orientation in the direction of isoluminance in the second and fourth quadrant in ΔP-ΔS space (blue dotted ellipse in Figure 3). Hence the orientation can be used to calculate weights that express the relative contribution of the rod and cone system. If we assume a linear summation of rod and cone luminance information weights can be found for which the weighted sum of photopic and scotopic luminance is constant:

$$c = W'_S \cdot S + W'_P \cdot P \qquad\qquad \text{Equation 4}$$

This equation expresses the dotted line in Figure 3b. Here, W'_P and W'_S are the not normalized cone and rod weights that will be called here independent weights and c is a constant that can be chosen arbitrarily. The iteratively calculated weights can be regarded as the fraction of luminance (or if contrasts are regarded they represent threshold contrasts) seen by the scotopic system and the fraction of luminance (or threshold contrast) seen by the photopic system.

In the above description, rod and cone inputs combine additively to generate a single mesopic luminance signal, or a resultant luminance contrast from the added differences between a target and background as seen by rods and cones. More generally different photoreceptor inputs might be nonlinearly processed in separate pathways (e.g. luminance and color signals) instead of being simply linearly combined. Nonlinear combination can be analyzed graphically as shown in Figure 3b. Equation 4 would turn into:

$$c^n = \left(W'_S \cdot S\right)^n + \left(W'_P \cdot P\right)^n$$

With several photopic and scotopic isoluminant points given in P-S space, one can iteratively determine the optimal parameters W_P, W_S and n at a certain adaptation condition. The parameter n describes the degree of cooperation between rods and cones. A maximum degree of cooperation is reached for a linear addition as in Equation 4, in that case n = 1. A value of n >> 1 shows a low degree of cooperation; rods and cones act independently, meaning that each receptor system has to produce a signal above an individual threshold to generate a visual effect (see solid line in Figure 3b). Here again the weighted combination predicts the relative contribution of the scotopic system and the photopic system. The criterion for finding the optimal parameters can be the least squared deviation between the predicted and observed threshold contrast.

Like many response functions the decrease of cone contribution is likely to follow an s-shaped psychometric function (sigmoid function). Naka and Rushton (1966) introduced an equation to describe cell responses, which has been found to also describe the responses of retinal cells like rods, cones and bipolar cells (Adelson, 1982). A general notion of the Naka-Rushton equation is shown in Equation 5:

$$\frac{V}{V_{max}} = \frac{I^\alpha}{I^\alpha + \sigma^\alpha}, \qquad\qquad \text{Equation 5}$$

where α is an exponent between 0.7 and 1 (Boynton & Whitten, 1970; Norman & Werblin, 1974), I is the intensity of the light, V the cell response (voltage or current of the cells response), and σ the semi-saturation constant of the cell. To fit the cone weights vs. adaptation luminance curves one can rewrite Equation 5 slightly to Equation 6:

$$W_P = \frac{P^\alpha}{P^\alpha + P_\sigma{}^\alpha} \cdot \hspace{4cm} \text{Equation 6}$$

Here, P is the adaptation luminance in cd/m^2, P_σ the adaptation luminance at which rods and cones contribute equally and their weights are therefore 0.5, V would be replaced by the relative cone weight W_P between 0 and 1, with $W_{P,max}$ being 1. An equation of this form can be used to describe the change of rod and cone weights by fitting the parameters n and P_σ. With this the rod and cone contribution can formally be described at several adaptation levels, which makes it possible to quantify a measure of mesopic luminance, as was illustrated above.

2.6 Photometric approaches for the mesopic range

Because of the differences in spectral sensitivity between the two receptor systems the current practice to use photopic photometers under mesopic light levels leads to an under-evaluation of bluish lights compared to their brightness, whereas yellowish and reddish lights appear dimmer than the measured luminance would suggest. The discrepancies between appearance and measured value vary greatly with the spectral energy distribution of the light source (CIE, 1978). Although several approaches of defining an equivalent mesopic luminance were undertaken and published, there is no official recommended system for mesopic photometry.

This section shows some available approaches of mesopic photometry that calculate an equivalent mesopic luminance. The concept of equivalent luminance is as follows: if two different light sources produce the same visual response they are said to have the same equivalent luminance. The equivalent luminance will depend on many parameters like the type of the visual task, the task parameters and the light level. More generally, the basis of this concept is the assumption that for equal visual impression or performance the parameters for example threshold contrast or reaction time should be equalized.

Approaches based upon heterochromatic brightness matching

Most of the earlier approaches that address the mesopic domain are based on brightness matches between two fields. The derived photometric number is the measured luminance of the test field when it appears equally bright than the reference field. Though it is usually termed equivalent luminance or mesopic luminance it has to be emphasized that it is rather an equivalent to brightness than to the luminance information of the visual system.

Palmer's models (Palmer 1966, 1967, 1968; CIE, 1989; CIE, 2001) are based upon data gathered with heterochromatic brightness matching experiments with circular fields of 5°, 15°, and 45° diameter with nearly monochromatic test lights and non-monochromatic test lights. The derived first model uses a linear combination of the photopic luminance based on $V_{10}(\lambda)$ and the scotopic luminance. The later model uses a non-linear combination of scotopic and

photopic luminance (CIE, 1989; CIE, 2001). Calculation involves one mesopic parameter with the dimension of luminance that depends on field size.

Ikeda and Shimozono (1981) suggested a system based on a log-linear combination of photopic and scotopic luminous efficiency functions determined by the heterochromatic brightness matching. They claim as well that there are two factors which determine the mesopic luminous efficiency curves – rod and cone brightness sensitivity curves. They compute a theoretical mesopic luminous efficiency function as the weighted sum of the log sensitivities for rods and cones, though the weights seem to differ strongly between observers.

The approach of **Sagawa and Takeichi** (1986) is based upon the CIE brightness-luminous efficiency functions. The mesopic luminous efficiency function is calculate as a weighted sum of log photopic and log scotopic brightness functions measured with the heterochromatic brightness matching method. They calculate a 'brightness equivalent luminance' as photometric quantity.

Kokoschka proposes a four-component model as a linear weighted combination of the CIE 10° tristimulus values X_{10}, Y_{10}, Z_{10}, and the scotopic luminance (Kokoschka, 1972; Kokoschka & Bodmann, 1975; Kokoschka, 1980). This approach is based on the contribution of three cone components and one rod component to brightness perception. The weights are a function of adaptation luminance and determine the degree of receptor contribution. The basis for the weighting functions are heterochromatic brightness matches with a bipartite 10° field at various adaptation levels and field sizes. A similar approach than Kokoschka was followed by **Trezona** (Trezona, 1973; Trezona, 1991).

Approaches based on performance measures

Two models were proposed that are based on visual performance like reaction times, threshold contrast for detection and recognition. These models aim for a mathematical description of performance based on the adaptation level, rather than psychophysical or neurophysiologic insides. Specifically, they intend to provide a measure to assess driving performance under several street lighting and car headlamp systems.

The model of **He et al**. (He, Rea, Bierman, Bullough, 1997) is based upon reaction times under illuminations used in street lighting like Metal-Halide (MH) and High-Pressure Sodium lamps (HPS). The reaction time results for the on-axis detection show no differences between the two light sources at any adaptation level. For the 15° off-axis target an increased reaction time was measured for the HPS lamps at adaptation levels below 1 cd/m^2. A unified version of the He et al. model for the detection of monochromatic and broadband stimuli was proposed by **Rea et al**. as the X-model (Rea, Bullough, Freyssinier, Bierman, 2004).

The **MOVE–model** (Mesopic Optimization of Visual Efficiency) was developed from data of different visual tasks in night time driving (Goodman et al., 2007). A practical model and a chromatic model were implemented on the basis of measurements of reaction times, chromatic and achromatic contrast thresholds, and the recognition of objects shown on-axis and 10° off-axis. The practical approach of MOVE assumes a linear combination of V(λ) and V'(λ) to form a mesopic luminous efficiency function.

Table 2 gives an overview of the parameters used to define mesopic spectral luminosities and mesopic luminance.

Reference	Experimental method	Target size / angle of visual field	Reference light sources	Nr of subjects	
Palmer, 1966	HBM	Circular field 10° horizontally bisected	tungsten light at 2042 K 0.00062 td …620 td	3	$V_{10}(\lambda)$, sum of the weighted 10° photopic and scotopic luminance
Palmer, 1968	HBM	Circular field 5°, 15° and 45°, horizontally bisected	tungsten light at 2042 K	16	$V_{10}(\lambda)$, sum of the weighted 10° photopic and scotopic luminance
Kokoschka, 1980	HBM	Bisected field of 3, 9.5 and 64° size	0.003…30 td $\lambda = 530$ nm	3	Based on the 10° CIE tristimulus values and scotop. luminance
Trezona, 1991	HBM	10° bipartite field	$\lambda = 588$ nm	9	Based on the 10° CIE tristimulus values and scotop. luminance
Ikeda, Shimozono, 1981; Ikeda, Nakano, 1986	HBM	10° bipartite field	0.01 td … 100 td xenon arc lamp (x=0.327, y=0.345)	2	Log-linear combination of phot. and scot. brightness functions
Sagawa, Takeichi, 1986	HBM	10° bipartite field	0.01 td … 100 td xenon arc lamp	12	Log-linear combination of phot. and scot. brightness functions
X-Model He et al. 1998 / (Rea et al. 2004)	RT / binocular simultaneity method	2° flashing target at 0° and 15°	0.003 … 10 cd/m² HPS and MH	3	x-Model: $V_{10}(\lambda)$ and $V'(\lambda)$ (X-Model: $V_2(\lambda)$ and $V'(\lambda)$, (Rea et al. 2004))
MOVE-Model (Goodman et al., 2007)	RT, chrom. & achromatic detection & recognition thresholds	Objects at 0°, 10°, size 2° & 0.3° quasi-monochromatic, and narrow band light and broad-band spectra	Adapt. luminance: 0.01 / 0.1 / 1 / 10 cd/m²	Total 109	Mesopic luminous efficiency function is calculated as a linear combination of $V(\lambda)$ and $V'(\lambda)$

Table 2: Overview of models of mesopic photometry

2.7 Considerations for photometry in lighting applications

The need to understand mesopic perception and to derive a photometric description is of huge practical interest. The Purkinje-shift at low light levels suggests that a light source with a high S/P ratio (the ratio of scotopic to photopic luminance) enhances the rods under dim light conditions. Hence, by switching from a halogen headlight to high intensity discharge (HID) lamps or LED headlights the visual impression and visual performance might change due to different spectral power distribution. While tungsten halogen lamps have a continuous spectral power distribution with most of the energy in the high and middle wavelength range and very little energy in the low wavelength range, the spectra of gas discharge lamps are discontinuous, show several peaks and provide proportionally more energy in the short wavelength range. This leads to S/P ratios of 1.6 and 1.7 for halogen and high discharge lamps respectively (Van Derlofske, Bullough, Watkinson, 2005). Phosphor based white LEDs show a double humped spectrum with maxima around 450 nm and 550 nm producing S/P ratios between 1.7 and 2.3 (Van Derlofske, Bullough, Watkinson, 2005).

Since photopic photometers are used for the measurement of light at twilight levels, the different spectral natures of the light source and visual impressions are neglected in photo-metric regulations for automotive headlights. This practice results in a misleading evaluation of certain lights, primarily due to the shift in the spectral sensitivity of the eye toward the short wavelengths during dark adaptation. Studies found a consistent but small decrease in reaction

times to peripheral targets and less targets were missed under a HID headlamp and a blue coated halogen bulb compared to a normal tungsten halogen lamp (Van Derlofske, Bullough, 2003; Van Derlofske, Dyer, Bullough 2003). A theoretical approach by Van Derlofske and colleagues showed that the calculated mesopic luminance based on reaction times increases for LED light sources by 10%-30% and for HID light sources up to 10% compared to the tungsten halogen lamp at a luminance level of 0.1 cd/m^2 (Van Derlofske et al., 2005).

Furthermore, the light distribution of the car headlights interacts with the installed street lighting. Typical light levels of street illumination during night time are between 0.3 and 2 cd/m^2 measured on the street with much lower luminances in the surrounding (Eloholma, Ketomäki, Halonen, 2004). Two commonly used lamp types for street lighting are high pressure sodium (HPS) and metal halide lamps (MH). The spectrum of a high pressure sodium lamp is characterized by several peaks around 600 nm with a S/P ratio about 0.6, while the spectrum of a metal halide lamp shows also peaks in the short wavelength range and provides a S/P ratio of 1.6. Several studies compared these two lamp types according to the visual performance. In terms of reaction times to peripheral targets a street luminance of 0.1 cd/m^2 produced by a MH lamp is 60% more efficacious than a HPS illumination at the same photopic luminance level. This discrepancy is more pronounced at lower light levels, but was only found for the detection of peripheral targets (He, Rea, Bierman, Bullough, 1997). Reaction time differences between a MH and a HPS street illumination increase further with increasing eccentricity of the target (Akashi, Rea, 2002). Also a study by Lingard and Rea (2002) including a driving task showed small differences in reaction time between MH and HPS illumination. The differences in reaction time to detect peripheral targets between several light sources of different S/P ratios were significant but small. However, an identification task as used by Lewis (1999) reveals larger benefits for light sources with higher short wavelength content at and below 1 cd/m^2. The reasoning of increased visual performance with lighting that contains increased short wavelength energy leads to speculations whether the use of rod optimized lamps allows to increase energy savings and economic benefits at maintained safety.

Chapter 3

Minimally distinct border perception under photopic, mesopic, and scotopic adaptation levels

3.1   Introduction and Background

The criterion of border distinctness as a photometric method was described by Frauenhofer (Frauenhofer, 1824) as early as 1824. Not until the late sixties the method was extensively used by other scientists (e. g. Boynton & Kaiser, 1968). In this method two adjacent fields are equated by minimizing the visibility of the border between them rather than by a comparative brightness judgment. For lights of the same chromaticity the border between the two fields will completely disappear at equal luminance. However when judging the border between a white reference and a colored test field the patches will not merge to one field but the border will at some point be minimally visible. At this minimum distinct border (MDB) the achromatic luminance of the two test fields will be equal.

Since the MDB method produces luminous efficiency functions that resemble closely Judd's modified CIE photopic sensitivity function obtained by flicker photometry, it was concluded that border matches are accomplished with the same visual information as flicker matches, namely the achromatic luminance information only (Kaiser, 1971; Wagner & Boynton, 1972). In contrast to heterochromatic brightness matches, border settings do not incorporate information from the opponent color channels. Hence, two fields of equal luminance with strong chromatic differences will not necessarily appear equally bright; the more saturated test color will look brighter. This phenomenon is known as 'Farbenglut' or Helmholtz-Kohlrausch effect (Wyszecki & Stiles, 1982; Guth, Donley, Marrocco, 1969).

To explain the differences between border and brightness matches Boynton and colleagues proposed the element theory (Kaiser, Herzberger, Boynton, 1971; Wagner & Boynton, 1972; Boynton, 1973). This theory states that light absorbed by photoreceptors leads to the activation of 'elements' in the higher visual system. They defined two main classes of elements: the chromatic and the achromatic elements. There are four types of chromatic elements (red, yellow, green, and blue), whereas the achromatic elements signal 'white'. The color percept depends on the relative activation of these elements. The activation of each element produces one unit of brightness and one unit of 'chromaticness' or 'whiteness' depending whether a chromatic or achromatic element is activated. Psychophysical evidence suggests that a minimally distinct border is present when the achromatic elements of both fields are equal. When comparing a white field with a chromatic field, the chromatic field will appear brighter by an amount that depends on the difference in chromaticity between the two fields. According to the element theory the increased brightness can be explained by the activation of chromatic

elements in the colored field. Also the transitivity and additivity of the MDB method can be accounted for by that theory.

This type of explanatory scheme can also be formulated in neurophysiological terms by appealing to the response of the parvocellular ganglion cells and their receptive fields (Kaiser et al., 1990; Ingling & Drum, 1973). Kaiser and colleagues (Kaiser et al., 1990) showed that the parasol (phasic) ganglion cells that feed into the magnocellular pathway build the physiological basis for border perception. The parasol ganglion cells gave transient responses to borders depending on luminance contrast, whereas the response of the midget (tonic) ganglion cells that feed into the parvocellular channels were relatively insensitive to luminance changes at the border. They also showed that the response of parasol ganglion cells to borders is additive, proportional and transitive.

Once the achromatic luminance between two fields with different chromaticity is equalized, the remaining distinctness of the border is accounted for by the chromatic information of the opponent red-green color channel (Valberg & Tansley, 1977). This residual border distinctness is made up by the difference signal of the L and the M cones and mediated by the midget ganglion cells. According to Frome and colleagues (Frome, Buck, Boynton, 1981) the opponent signal depends on the tritanopic purity difference (the difference in the relative stimulation of L and M cone excitations across the two fields) and on the adaptation level.

The notion of an exclusive L and M cone involvement is also supported by several studies that showed none or a negligible S cone contribution. Tansley and Boynton found no differences in border assessments between settings made normally and under temporary artificial tritanopia (S-cone deficiency) (Tansley & Boynton, 1978). This was confirmed by other studies that could not detect any S cone contribution (Tansley & Valberg, 1979; Kaiser et al., 1990). A small S cones response to border distinctness was found by Boynton et al. (Boynton, Eskew, Olson, 1985; Kaiser & Boynton, 1985). It can be concluded that border perception is accomplished by the sum of L- and M-cone signals only, agreeing in this respect with luminance as assessed by flicker photometry (Eisner & MacLeod, 1980). The poor response of the S cone system to edges and borders is a consequence of the sparse distribution of the S cones on the retina (Curcio et al., 1991; Ahnelt, Kolb, Pflug, 1987; Williams, MacLeod, Hayhoe, 1981).

MDB shares with flicker photometry several properties that seem to make it an applicable photometric criterion to assess luminance in the mesopic domain. It meets all the requirements of a photometric system i.e. additivity, transitivity, and proportionality (Boynton & Kaiser, 1968; Kaiser, 1971; Wagner & Boynton, 1972; Ingling, et al. 1978; Kaiser et al., 1990).

In contrast to flicker photometry, which was mainly used to determine the CIE luminous efficiency function $V(\lambda)$, border matches do not involve rapidly changing stimuli that can lead to inhibition and enhancements between rod and cone signals and between slow and fast rod signals. In mesopic photometry this is an advantage, since rod-cone phase lags prevent simple addition of flicker signal amplitudes and can lead to complete nulling by opposite-phase rod and cone stimuli (MacLeod, 1972). However, border matching involves edge detection which might reduce the contribution of the rod system due to its larger receptive fields (Barlow, Fitzhugh, Kuffler, 1957; Hallett, 1969; Troy, Bohnsack, Diller, 1999). Border matches also seem to provide a more reliable and less variable measure compared to heterochromatic brightness matches (Boynton & Kaiser, 1968; Kaiser 1971; Wagner & Boynton, 1972).

Because of the mentioned characteristics of the MDB method, the criterion of border distinctness might be a reliable and suitable measure of luminance also under dim conditions and thus a basis for mesopic photometry. However, the MDB method has not yet been investigated as a measure of peripheral luminance under dim conditions. In this chapter the criterion of border distinctness is used with the goal of determining the relative contribution of the cone and rod system to luminance under several states of adaptation ranging from scotopic to photopic. Furthermore, it is tested how luminance changes at several peripheral retinal locations.

3.2   Experimental Design

If mesopic luminance depends on a weighted sum of scotopic and photopic luminances, then contours of constant mesopic luminance are approximately straight lines in scotopic and photopic luminance space (S-P space) and in scotopic and photopic contrast space (contrast here is defined as $(S_{cf}-S_{Ref})/S_{Ref}$ and $(P_{cf}-P_{Ref})/P_{Ref}$ with S_{cf} / P_{cf} and S_{Ref} / P_{Ref} denoting the luminances of the comparison field and of the reference). Along one such line passing through the origin, the mesopic luminance contrast will be zero, and the border therefore minimally distinct, to the extent that border visibility or distinctness depends on luminance alone. For a photopic adaptation level the contour of constant border distinctness will form a nearly vertical line (solid lines in Figure 4). This is because under photopic conditions cone signals dominate: border distinctness will depend mainly on the contrast as seen by the cones, and a stimulus contrast seen only by the rods will have to be relatively larger to produce a noticeable change in border perception. Similarly, the line of constant border distinctness for a scotopic adaptation level will be oriented nearly horizontally (dotted lines in Figure 4). In this case since cones are not (or only to a small extent) involved, a large difference in photopic luminance is needed to create the same border distinctness. For mesopic adaptation levels the contour's orientation will be in between horizontal and vertical. Thus the orientation of the line of constant border perception represents the relative scotopic and photopic contribution to luminance. A vertical alignment of this isoluminance lines reflects pure cone vision and a horizontal orientation pure rod vision.

The goal of this experiment is to determine the orientation of the isoluminance line by minimally distinct border matches at photopic, mesopic, and scotopic adaptation levels. Thus, weights that describe the relative rod and cone contribution to border perception, which in this case corresponds to luminance, can be assigned to each adaptation level.

The border to assess was created by a centrally fixated round 12° disc on a uniform surround presented on a calibrated CRT-Monitor that was controlled by a Bits++ Graphics Card from Cambridge Research Systems (see Figure 5). The monitor ran at a refresh rate of 75 Hz and with a resolution of 1280×1024. The observers were seated 40 cm in front of the screen. At this distance the screen subtended a field of 44°×34°. The border matches between the disc and the surround were done under two different conditions as shown in Figure 5. Under the external reference condition the centrally fixated disc was the adjustable comparison field, whereas under the internal reference condition the surrounding acted as comparison field. The comparison field could be altered by the observer by key presses on a computer keyboard to meet the criterion of a minimally visible border between the two fields.
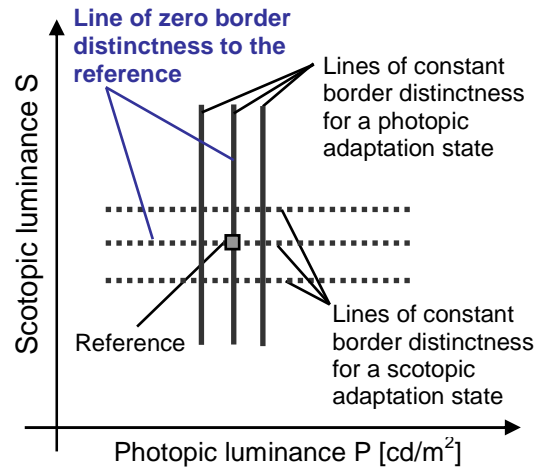
Figure 4: Hypothetical lines of equal border distinctness for a photopic (solid line) and scotopic (dotted line) adaptation state in S-P space. The contours show the scotopic and photopic luminances of the comparison field. The square indicates scotopic and photopic luminances of the reference field.

During each session **the reference field** was permanently set to a neutral equal energy white according to the CIE 10º color matching functions with (x,y)-chromaticity coordinates of (~0.34, ~0.33). The luminance (according to $V_{10}(\lambda)$) of the reference was set between photopic (42 cd/m^2) and scotopic (1.2 mcd/m^2) luminance levels (see Table 3 for a complete list). To provide mesopic and scotopic background luminance levels, calibrated neutral density filters (Lee filters, F299: 4 stops, F211: 3 stops, F210: 2 stops, and their combinations) were set in front of the monitor screen (see Appendix).
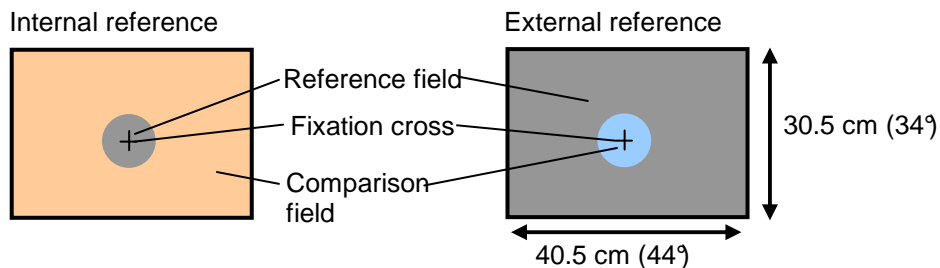
Figure 5: Sketch of the minimal distinct border stimulus. The visibiliy of the border between the inner 12° disc and the surround was minimized by adjusting either the surrounding field at a constant luminance of the disc (inner reference condition) or the disc at a constant surrounding field (external reference condition)

The **comparison field** was defined by the intensities of the 3 monitor guns: The green phosphor was kept constant at the level of the reference green phosphor ($g_{comp} = g_{ref}$). In most conditions the blue phosphor was kept constant for one setting, while the red phosphor was adjusted by key-presses of the observer. But at low adaptation levels the red phosphor was kept constant and the blue phosphor served as variable phosphor to keep the adjustment trajectory nearly orthogonal to the isoluminant line. These adjustment trajectories are straight lines with a constant slope in a plane where the abscissa is the photopic luminance and the ordinate the scotopic luminance (Figure 6). The constant phosphor (red or blue) was set to 2-5 intensities for each reference (e. g. to 0%, 30%, 70%, and 100% of the maximal luminance the gun can

generate). Each of these parameter combinations was presented 4 times in random order in one session for both the internal reference and external reference condition. Due to the offset of the three phosphors on the monitor mask, color artifacts can be visible, especially under high adaptation levels. To minimize the artifacts the border was slightly blurred by one pixel (= 2 arc min). Lindsey and Teller (Lindsey & Teller, 1989) found that an edge blur of up to 8 arc min does not change the spectral characteristics and additivity of border settings.

Photopic luminance P of reference according to $V_{10}(\lambda)$ (CIE 1964)	Scotopic luminance S of reference according to $V'_{10}(\lambda)$ (CIE 1951)	S/P ratio of the reference	(x,y) chromaticity coordinates of the reference		
			equal energy white (eew)	purple	green
42.2 cd/m²	90.6	2.15	0.34; 0.33	0.37; 0.22	0.32; 0.40
1.9 cd/m²	3.7	1.95	0.34; 0.33	0.36; 0.22	0.32; 0.43
0.43 cd/m²	0.81	1.90	0.34; 0.33	0.37; 0.22	0.32; 0.43
0.088 cd/m²	0.17	1.89	0.34; 0.33	0.37; 0.22	0.31; 0.43
0.044 cd/m²	0.081	1.86	0.34; 0.33	0.36; 0.21	-
0.021 cd/m²	0.038	1.83	0.34; 0.32	0.36; 0.21	-
0.011 cd/m²	0.018	1.70	0.36; 0.33	0.36; 0.20	-
1.2 mcd/m²	2.0 ·10⁻³	1.64	0.37; 0.34	0.55; 0.26	-

Table 3: Photopic and scotopic luminances of the reference fields. The S/P ratios of the dim references are lower because of the higher transmittance for long wavelength of the used filters. The small deviations of the chromaticity coordinates for the eew field from 0.33; 0.33 reflect changes due to a subsequent correction of calibration.

Purple and green condition: For the purple condition, instead of using a white equal energy reference, the green phosphor luminance was zero throughout, making the reference and comparison fields both purple. In addition also a green reference was used. Here, the green phosphor of the reference and the comparison field was set to a level as high as practicably possible, leading to a greenish adaptation field with the chromaticity of (0.32, 0.43) (see Table 3). The purple and the green references were set to yield the same ratio between photopic and scotopic CIE luminance levels as the equal energy white.

Further on, a control experiment was done under an adaptation level of 42 cd/m² with and without an achromatizing lens to examine possible influences of chromatic aberrations. Here a smaller disc with a diameter of 3.5° was used.

Observers: Seven observers (age between 18 and 35, mean: 28) with normal vision (normal color vision, Visual acuity of ≥ 0.8) took part in the experiment. The observers were instructed to adjust the comparison field via key presses on a keyboard until the border between the disc and the surround disappeared or was minimally distinct. During the adjustment they were asked to fixate a black cross in the middle of the disc. The timing of the experiment was solely determined by the observer. The adaptation period prior to the experiment ranged from 10 up to 45 minutes for the darkest adaptation level. During adaptation the observers got instructions and did some practice trials to get familiar with the setup. The experiments involving a purple and green background and the follow-up experiment with an achromatizing lens were done by two subjects only.

Some effects were observed that made a precise adjustment difficult especially under photopic and mesopic conditions. Under bright adaptation levels afterimages appeared that caused the

stabilized image to fade, when fixation was maintained too long (Troxler effect, Clarke, 1960). To minimize fading due to stabilization of the retinal image, a uniform field of the reference intensities was shown for 2-3 seconds after each matching was done. Further on, movements are encouraged during actual observation, fixation being carefully maintained only at the moment of making the final adjustment. In the following discussion of the results the named adaptation luminance is equivalent to the photopic luminance based on $V_{10}(\lambda)$ of the reference field. However it has to be noted that the state of adaptation is influenced by the luminance of both the reference field and the comparison field. Since the comparison field was varied in luminance as well as color, the state of adaptation changed during adjustment.

All luminance values in this chapter are based on the 10° CIE standard observers.

3.3   Results and Discussion

Representation of the data

The results are depicted in S-P contrast diagrams where the axes denote the scotopic and photopic luminance contrast formed between the reference and the comparison field. Recall that under the assumption that $V_{10}(\lambda)$ represents the cone sensitivity of the observer and that photopic MDB settings are based on luminance information only, a pure photopic response will result in a vertical straight line through the reference point in S-P contrast space (or S-P space). Correspondingly, a pure scotopic response leads to a horizontal straight line (see Figure 6). If the signals of the rods and cones add up linearly in the mesopic range, mesopic MDB adjustments will lead to a straight line through the reference with a negative slope.
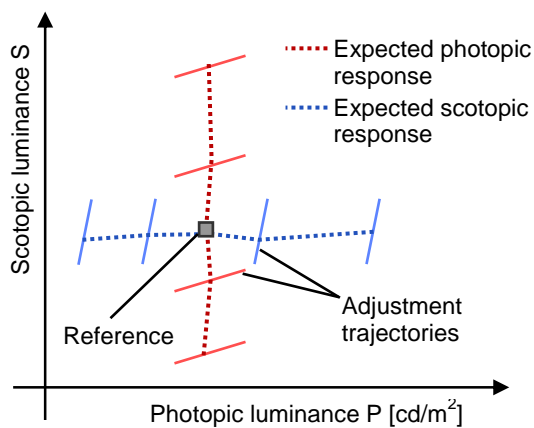
Figure 6: Hypothetical results for a pure photopic cone repsonse (red dotted curve) and a pure scotopic rod response (blue dotted curve). The red solid lines are example adjustment trajectories for constant green and blue phosphors. In this case the red phosphor was altered by the observer. The blue solid lines indicate adjustment trajectories for const. green and red phosphors. Here the blue phosphor was altered.
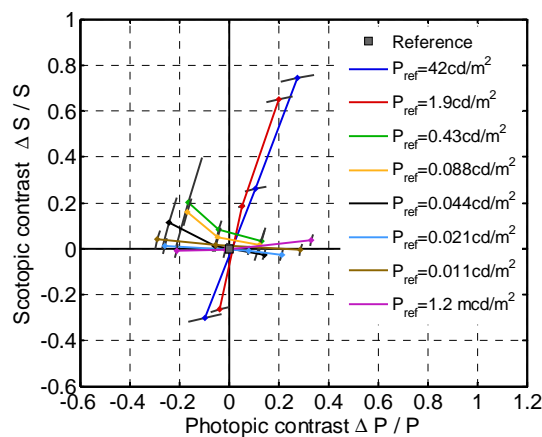
Figure 7: S-P contrast space showing the lines of minimum border perception for one observer and all tested adaptation levels. The data are averages between the internal and external reference condition.

Figure 7 shows the results of one subject in S-P contrast space. The data from the internal and external reference condition are averaged. The standard deviations are shown as black lines. The reference is represented by a gray square. Each line corresponds to one adaptation level, which here is equal to the luminance of the reference.

Calculating receptor weights

From the slope of the MDB curves in S-P space the relative weights for the photopic and scotopic responses can be retrieved. A simple linear modeling approach was used to calculate relative rod and cone weights in such a way that the weighted linear sum of photopic and scotopic luminance equals 1 as shown in Equation 7. S and P represent the luminance levels of the comparison field at minimum border setting made at one adaptation level. W_P' and W_S' denote the independent weights for the photopic and scotopic luminance, respectively.

$$1 = S \cdot W_S' + P \cdot W_P' \hspace{3cm} \text{Equation 7}$$

The constant value 1 is chosen arbitrarily, therefore the independent weights have no physio-logical meaning. The sum of the weights W_P' and W_S' was normalized to 1 ($1 = W_P + W_S$) to retrieve the relative weights W_P and W_S:

$$W_P = \frac{W_P'}{W_P' + W_S'} \hspace{2cm} W_S = \frac{W_S'}{W_P' + W_S'}$$

$$\text{Equation 8}$$

Hence, a relative cone weight W_P of 1 ($W_S = 0$) represents pure cone vision as defined by $V_{10}(\lambda)$ and vice versa, a relative rod weight W_S of 1 ($W_P = 0$) corresponds to pure rod vision as defined by $V'(\lambda)$.

Linearity measure

The linearity assumption of the model was verified by calculating the percent root mean square error ($RMSE_\%$) between a perfectly linear response and the experimentally measured response. For each setting, an error of prediction may be defined for the linear model from the ratio of the chosen stimulus intensity to the value predicted, which should ideally be 1. The deviation from 1 is the error of prediction expressed as a fraction of the reference luminance. The root mean square error from one observer ($RMSE_i$), and the average percent measure of linearity failure are expressed in Equation 9 and Equation 10:

$$RMSE_i = \sqrt{1/v \cdot \sum_{cf}^{v} \left[(W_P' \cdot P_{cf} + W_S' \cdot S_{cf}) / (W_P' \cdot P_{\mathrm{Ref}} + W_S' \cdot S_{\mathrm{Ref}}) - 1 \right]^2} \hspace{1cm} \text{Equation 9}$$

$$RMSE_\% = 100\% \cdot \frac{1}{N_{Obs}} \cdot \sum_{i}^{N_{Obs}} RMSE_i \hspace{2cm} \text{Equation 10}$$

In Equation 9 W'_P and W'_S are the independent weights of the cones and rods; P_{cf} and S_{cf} denote the photopic and scotopic luminance of the matched comparison field, these are the v S-P pairs that represent the curves in Figure 7. The number of measured points v for each curve is between 2 and 5. P_{Ref} and S_{Ref} are the photopic and scotopic luminance of the reference field. The number of observers N_{Obs} for this experiment is 7. The percent $RMSE_\%$ introduced by the assumption that the MDB data are linear is plotted in Figure 8. It shows that the average

linearity error is minor; it never exceeds 3.5% for all adaptation levels. The high degree of linearity makes it possible to average the slopes of the data for all subjects and to plot the results as straight lines (Figure 9). The linearity of the curves also rectifies the linear model described above. Hence, the mesopic response on which border distinctness depends can well be described as a linear addition of weighted cone and rod signals.
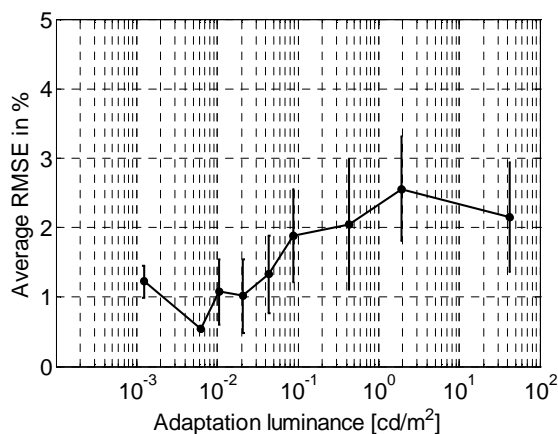
Figure 8: Linearity failure with ± standard deviation of the MDB data expressed as the percent RMSE% for all luminance levels.
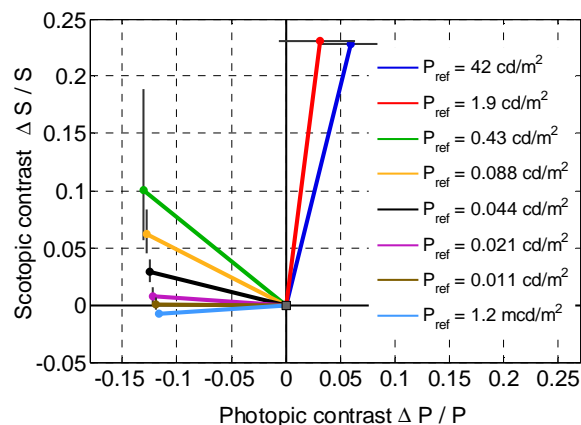
Figure 9: Lines of minimal distinct borders in S-P contrast space for the tested adaptation levels. The results of all observers and the external and internal reference conditions are averaged. The error bars are the standard deviations of the slopes.

Change of relative receptor weights with state of adaptation

The diagram in Figure 9 shows the averaged results across all observers and across the data of the internal and external reference condition in S-P contrast space. The mean was calculated by averaging the slopes for each observer's linearized response curve. The transition from a rod response to a cone response is depicted in the change of the slope of the lines from almost horizontal to vertical. The graph of Figure 9 shows at luminance levels of 0.01 cd/m^2 and below a purely scotopic response. With an assumed cone threshold of 0.1 td (Wyzecki & Stiles, 1982) the theoretical expected luminance of a purely scotopic response is between 3 mcd/m^2 and 5 mcd/m^2 for a 5 - 6 mm pupil. The high blue sensitivity is also reflected in the negative relative cone weights in Figure 10. The graph represents the average relative cone weights for all observers as a function of the photopic adaptation luminance. The slight positive slopes and the negative relative cone weights are apparent in five out of seven subjects at the very low adaptation levels can indicate a scotopic luminous efficiency function that differs from V'(λ), which can speculatively be attributed to a lower macular pigment density than is characteristic of the standard observer. As expected by the Purkinje shift, for increasing adaptation levels the importance of photopic contrast for the MDB settings raises.

Between the adaptation luminances of 0.43 cd/m^2 and 1.9 cd/m^2 there seems to be a nearly discontinuous change in the slopes of the MDB curves. In Figure 10 the curve of the relative cone weights shows a rather flat part with low cone weights for many subjects at this luminance range. A possible explanation is discussed below in the section about 'tangent bias'.

For the photopic level of 42.2 cd/m^2 the curve in Figure 9 shows an unexpected positive slope for all observers which implies a higher sensitivity for red than V$_{10}$(λ) suggests. For some observers this is also apparent at luminance levels as low as 1.9 cd/m^2. The positive slope

corresponds to cone weights above 1 in Figure 10, which means that bluish stimuli at the MDB isoluminance point have greater luminance than expected under the assumption that $V_{10}(\lambda)$ resembles the luminous efficiency of the eye. This effect could be due to a reduced effectiveness of blue light relative to red in MDB settings, as compared with flicker photometry, at light levels where rod contribution is negligible. One cause of such a discrepancy can be the loss of contrast in the blue-phosphor image as a result of chromatic aberration in the eye. Aberrations caused by the optical system of the eye are wavelength dependent. Under typical viewing conditions the eye is in focus for the middle wavelength range. As a consequence, short wavelength light leads to a blurred image on the retina. Hence short wavelength light might not or only to a limited extent contribute to border perception. This hypothesis was tested in a follow-up experiment with two observers (observer 1 with normal color vision and observer 10 a deuteranomalous trichromat) by correcting for chromatic aberrations with an achromatizing lens in front of one of the eyes. The other eye was covered with an eye patch. Since the achromatizing lens corrects for aberrations in the 14° central visual field, the border settings were done with a smaller disc with a 3.5° radius. At an adaptation level of $P_{adapt} = 42 \ cd/m^2$ and a circular adjustment trajectory (see section 'tangent bias') the relative cone weights were hardly affected for border settings with the achromatizing lens. Although the data of one of the observers are significantly different with and without the achromatizing lens, the direction and the minuscule size of the effect can not explain the cone weights greater than 1. The resulting average relative cone weights from 10 settings and the p-values for both observers are given in Table 4.
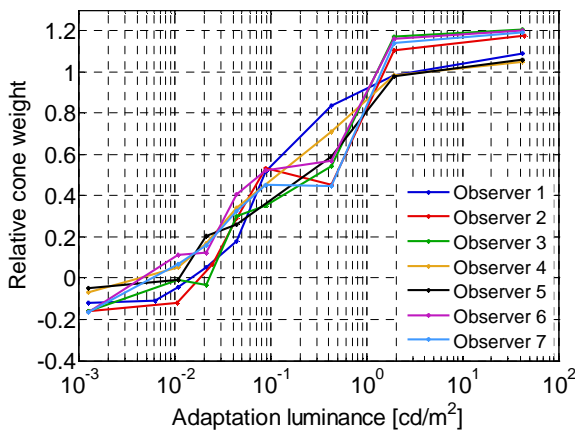
Figure 10: Relative cone weight over the adaptation luminance for all observers.
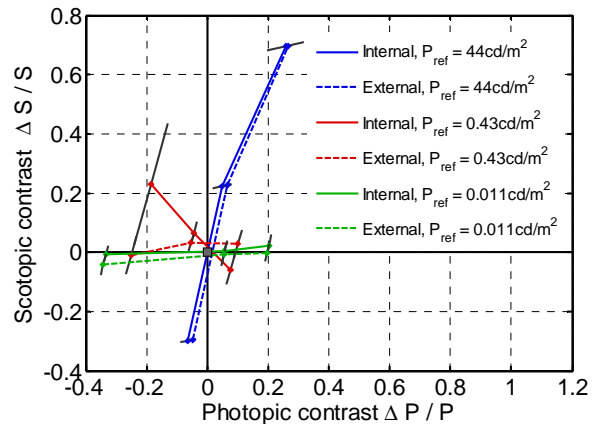
Figure 11: S-P contrast diagram with MDB curves for one photopic, mesopic and scotopic level (observer 2). The solid lines stand for the internal reference condition and the dotted lines for the external reference condition.

	No achromatizing lens	With achromatizing lens	p-value, 2-tailed t-test
Observer 1	$W_{P,woAL} = 1.11 \pm 0.07$	$W_{P,AL} = 1.14 \pm 0.07$	p=.24
Observer 10	$W_{P,woAL} = 1.04 \pm 0.02$	$W_{P,AL} = 1.08 \pm 0.04$	p<.01

Table 4: Comparison of the relative cone weights for border settings with and without an achromatizing lens.

Other reasons for the negative cone weights and for cone weights greater than 1 can be individual differences in receptor sensitivity and variations in macular pigment optical density. The macular pigment varies strongly between observers; the average density is given as 0.1 at

460 nm for a 10° field by the CIE (Stockman & Sharpe, 2000; CIE, 2006). It is suspected that with a standard deviation of 0.12 or higher the macular pigment optical density can be even higher than 0.10 in the periphery (Webster & MacLeod, 1988).

Comparing the internal and external reference condition

An effect that influences all MDB settings is the change of the adaptation level when adjustments of the comparison field are made. This may account for the different results between the internal and external reference condition. In Figure 7 and Figure 9 the MDB curves from the internal and external reference condition were averaged. Considering the two conditions separately shows that for most observers, in particular for high mesopic adaptation levels, the adjustments under the internal reference condition require a higher cone contribution compared to the external reference condition. At photopic and scotopic adaptation levels the differences are minor. However, at high mesopic levels (0.43 cd/m^2 and 0.088 cd/m^2) two of the subjects show strong discrepancies between the two conditions. An extreme case is depicted in Figure 11, which compares the MDB curves for the two conditions in S-P contrast space for three adaptation levels. The differences in the average cone weights between the internal and external reference condition over the adaptation luminance and the mean of the independent differences between all observers for each luminance level are illustrated in the two diagrams in Figure 12. The different receptor weights of the external and internal reference condition might be attributed to differences in adaptation of the rods and cones. For the interpretation of the results it is assumed that only the reference field determines the state of adaptation. This is a simplified assumption which does not account for the distinct rod and cone distribution over the retina. The uncertainty in determining the state of adaptation is surely a major drawback of minimum border settings. Nevertheless, the curves of Figure 10 show a broad agreement between the internal and external reference conditions for most adaptation levels and should not disqualify the MDB procedure as a measure of photopic luminance.
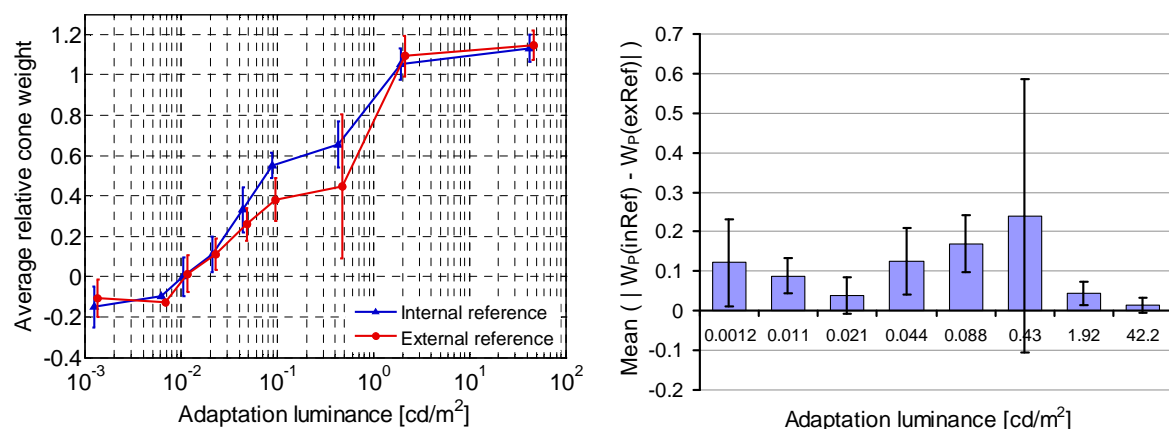
Figure 12: Left: The relative cone weights ± standard deviation for the internal and external reference condition vs. the adaptation luminance. The relative cone weight is averaged among all observers. Right: The average of the absolute differences of the cone weights between the two conditions for all adaptation luminance levels.

Tangent bias

In all of these experiments, the adjustment of either the red or the blue phosphor while the other two phosphors were kept constant led to a constant slope of the adjustment trajectory in S-P contrast space (see Figure 6). This setup introduces a potential bias in the measured orientation of the MDB contour. Figure 13 schematizes a hypothetical contour of constant border distinctness, along with the adjustment trajectories of red and blue phosphor. The contour is modeled as an ellipse centered on the reference point rather than as a straight line as shown above. The simple linear locus of MDB the setting points is expected if rod and cone signals add up linearly to determine mesopic luminance. The elliptical contour is an idealization of the behavior to be expected if rod and cone signals do *not* add up linearly in a perfectly additive manner to determine mesopic luminance, or if border distinctness does not depend on mesopic luminance alone, but can also be increased by chromatic contrast (Helmholtz, 1896; Chaparro et al., 1994). In that case the tilt of the ellipse is determined by the two apex points. The theoretical results of the minimum distinctness settings are shown as blue and red circles. The true apex point of the ellipse in S-P space can only be found if the adjustment trajectory is the tangent at the apex point. Hence every adjustment trajectory not perpendicular to the orientation of the MDB contour will introduce a bias in the results. A steeper adjustment trajectory (blue lines) will lead to an underestimation of the cone response. Correspondingly, a shallower adjustment trajectory (red lines) results in an overestimation of the cone response.
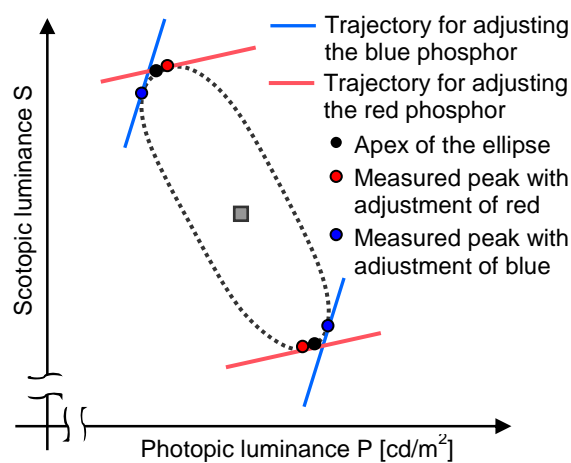
Figure 13: Schematic illustration of the tangent bias. The apex points of the ellipse (black circles) can only be found with a trajectory that is perpendicular to the orientation of the ellipse. The trajectories produced by the red and blue gun lead to points offset from the apex.
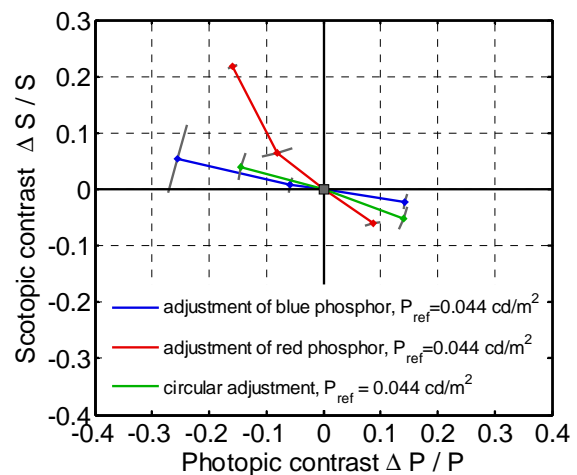
Figure 14: MDB data at the adaptation level of 0.044 cd/m² for Observer 4. The differences between the red and blue phosphor adjustment are due to tangent bias. External reference condition.

This bias is evident in the data shown in Figure 14 and Figure 15 which compare the MDB curves measured by adjustment of the red phosphor (red line) with the MDB curves measured by adjustment of the blue phosphor (blue line). From this it can be concluded that for the mesopic adaptation levels of 0.43 cd/m² and 0.09 cd/m² the true cone weights are higher than suggested by the curves measured by adjusting the blue phosphor. To quantify this bias the experiment was redesigned so that the adjustment was made by moving in a circle in S-P contrast space. This was realized by changing both, the red and the blue phosphor intensities at a constant green phosphor. With such a circular adjustment trajectory the tangent bias is

removed. Figure 15 shows the MDB results of the three different adjustment trajectories for an adaptation luminance of 0.43 cd/m^2 and 0.12 cd/m^2. The discrepancies are prominent and reflect differences in the relative cone weights of $\Delta W_{P,max} = 0.06$ for 0.43 cd/m^2 and $\Delta W_{P,max} = 0.36$ for 0.12 cd/m^2. The theory of the tangent bias shows that the weights between 0.43 and 0.09 cd/m^2 are underestimated, which can explain the saddle point in Figure 10.
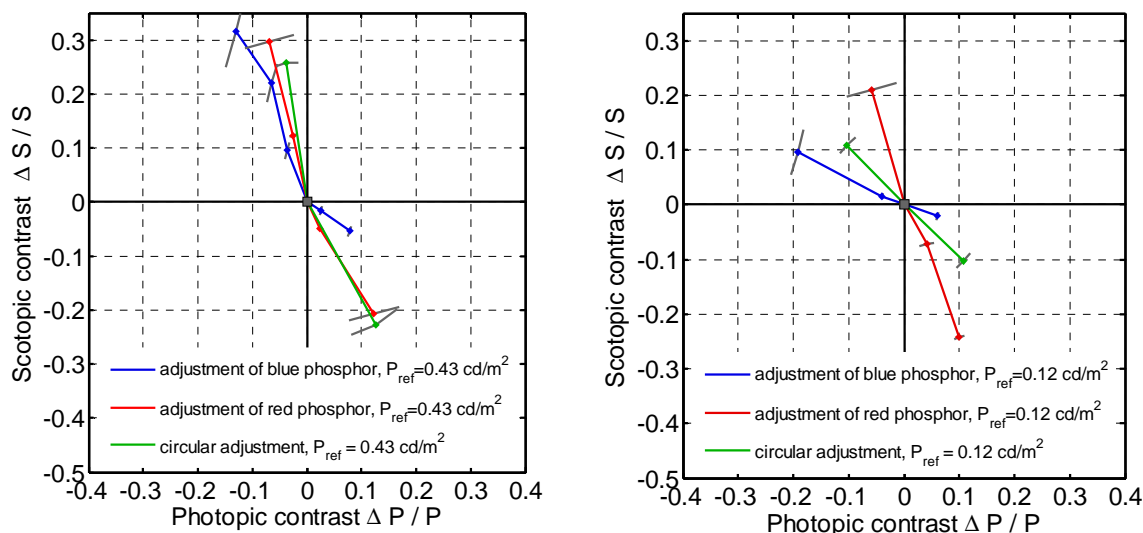
Figure 15: Comparison of MDB results in S-P contrast space for two adjustment trajectories for Observer 1. Blue lines: adjustment of the blue phosphor, red lines: adjustment of the red phosphor, green lines: circular adjustment in S-P contrast space. Left graph: internal reference condition at 0.43 cd/m^2 with calculated relative cone weights of $W_{P,b\_adjust} = 0.79$, $W_{P,r\_adjust} = 0.84$, $W_{P,circ} = 0.85$. Right graph external reference condition at 0.12 cd/m^2 with calculated relative cone weights of $W_{P,b\_adjust} = 0.48$, $W_{P,r\_adjust} = 0.84$, $W_{P,circ} = 0.66$.

However this explanation only holds, if loci of constant border distinctness are rather plump ellipses, for instance because chromatic signals are involved in border matches. This is unexpected in view of the good linear additivity found in these data and also in earlier results by Ingling and Drum (1973), Kaiser (1971), Wagner and Boynton (1972) and Boynton and Kaiser (1968). A detailed discussion of threshold contours is also given in chapter 5.

Change of rod and cone contribution with eccentricity

The characteristics of mesopic vision that rod and cone receptors act in concert and their distinct distribution over the retina lead to the assumption that mesopic luminance strongly depends on eccentricity. Since the fovea is dominated by cones a photopic response would be expected also under dim lighting conditions. In the periphery cone receptor density drops sharply to a low but constant level while rod receptor density increases and peaks around 14-20° off-axis (Curcio et al., 1990). Hence, peripheral vision will be mostly influenced by rods. As a consequence the luminance response at a mesopic light level can range from purely cone based to almost purely rod based depending on the position on the retina. Psychophysical evidence for the change of sensitivity with retinal position was found in many studies, e. g. Weale, 1951, Kishto 1970, Drum, 1980, Jamar, Kwakman, Koenderink, 1984.

To investigate the dependence of mesopic luminance on retinal eccentricity, the minimum border matches were done for a range of centrally fixated disc sizes at 0.044 cd/m^2 and

0.09 cd/m^2 with one subject. Though the standard deviation is substantially higher, there is a distinct decrease in cone weight for border matches from 1.5° to 14° off-axis (Figure 16). This decrease is comparable to the change of sensitivity in the periphery measured with other procedures (see chapter 4). Based on the results of Figure 16, eccentricity plays a very important part in setting the contributions of rods and cones: the 2-fold reduction in luminance that distinguishes the two curves of Figure 16 is compensated roughly by a doubling of the eccentricity.
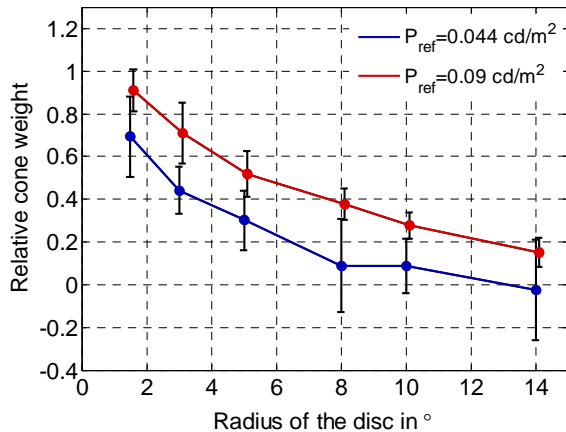
Figure 16: Relative cone weight vs. the radius of the disc in degrees. Each data point is the average of 10 measurements for observer 1, averages over internal and external reference condition.
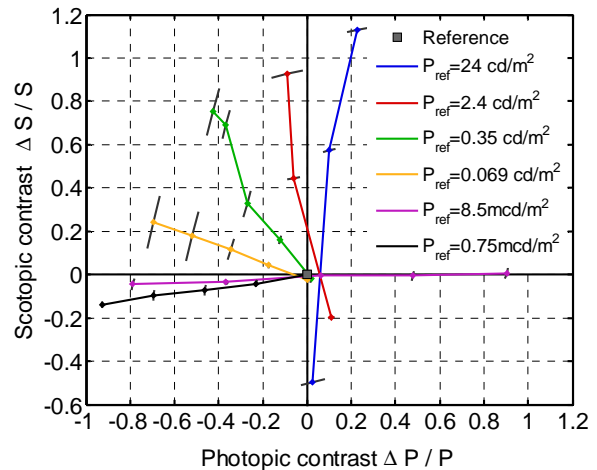
Figure 17: Purple reference, and purple comparison field, internal reference condition for observer 1

Comparison of an equal energy white, a purple and green adaptation field of equal photopic and scotopic luminance

The MDB experiment was also carried out with a purple and a green reference that was set to the same scotopic – photopic luminance ratio (S/P ratio) as the equal energy white (eew) reference. In the purple reference condition the comparison and reference fields were both composed of the blue and the red monitor gun only. This setting allows a comparison of photometrically identical but visually different conditions. The graph in Figure 17 depicts the MDB curves for the purple background for each adaptation level in S-P contrast space. To allow a comparison of the results Figure 18 illustrates the relative cone weights for the purple and eew condition. Note that the results in both diagrams were collected with straight adjustment trajectories by changing only the blue or the red phosphor. To avoid a potential bias the experiment was repeated with circular trajectories and an additional greenish background with chromaticity coordinates of (x, y) = (0.32, 0.43). The cone weights for the circular adjustment and the straight adjustment trajectories for all three backgrounds agree well (Figure 19). Some significant differences are apparent at high mesopic levels for the circular adjustment condition in Figure 19. However, given the high uncertainty that seems to accompany border matches in the periphery the deviations around 1 cd/m^2 can be regarded as minor.

The good agreement between the equal energy white, the green and the purple condition and the high linearity of the results suggest that border matches are based on the luminance pathway only. Thus, a mesopic luminance can be specified as a weighted sum of scotopic and photopic luminance. A contribution of achromatic opponent mechanisms seems unlikely. Based on these results a description of mesopic achromatic vision can be accomplished by a

linear two-parameter model, where the relative rod and cone contribution varies with luminance.
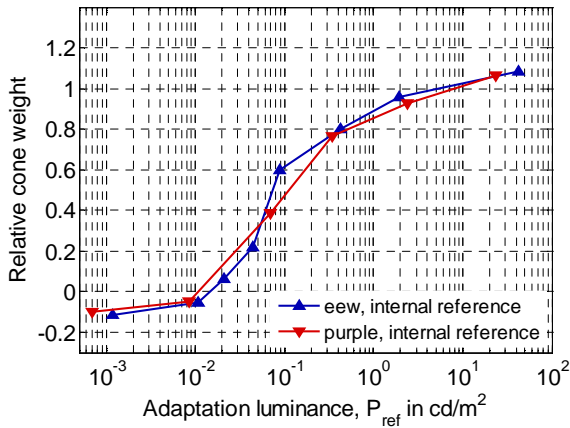
Figure 18: Purple and eew (equal energy white) condition with straight lines as adjustment trajectories, internal reference condition for observer 1
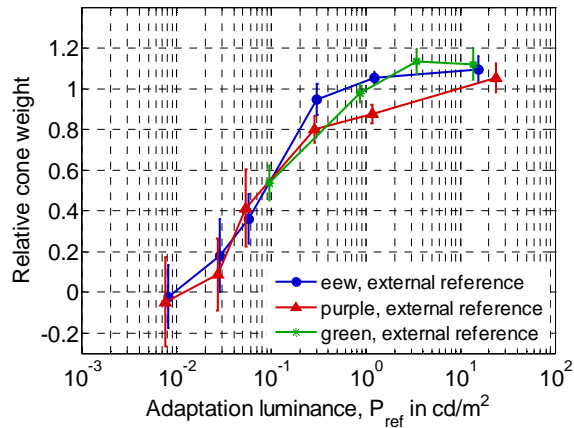
Figure 19: Comparison of the relative cone weights for the eew (equal energy white), the purple and green external reference. All data are from observer 1 measured with circular adjustment trajectories.

Modeling

The differences in sensitivity between the CIE standard observers and the psychophysically measured sensitivities that are evident in Figure 12 (left) as relative cone weights above 1 and below 0, make it difficult to model the results and to describe mesopic luminance. Therefore, the scotopic and photopic luminance definitions were redefined as sensation luminance to match the scotopic and photopic results of the tested observers. The photopic sensation luminance was redefined by weighting the luminance contribution of the blue and red phosphor to account for isoluminance between the reference and the matched test field at 42 cd/m².

$$P' = r\omega_{R,phot}P_R + gP_G + b\omega_{B,phot}P_B$$

Equation 11

Equation 11 shows the sensation luminance P' as the sum of the luminance contribution of all three phosphors. Here, P_R, P_G and P_B are the maximal photopic luminances the three phosphors can produce; R, G and B denote the phosphor intensities that are the linearized output voltages of the CRT monitor normalized between 0 and 1. The phosphor weights for the red and blue phosphor are $\omega_{R,phot}$ and $\omega_{B,phot}$, respectively. The green phosphor g is the same for both fields, hence does not influence luminance in this case. The phosphor weights were found to be $\omega_{R,phot}=1.32$ and $\omega_{B,phot}=0.22$. Scotopic sensation luminance was defined accordingly with the scotopic isoluminance match at 0.001 cd/m² ($\omega_{R,scot}=0.66$, $\omega_{B,scot}=1.06$).

The descent of the relative cone weight with dark adaptation based on scotopic and photopic sensation luminance, S' and P', respectively is shown in Figure 20 (red curve). For this W_P vs. logP curve a fit was obtained by minimizing the root mean square. Since the cone incremental threshold is constant below 40 td (2.5 cd/m²), it can be assumed that the cone contribution and thus the independent cone weight W_P' will be constant. On the other hand the rods will work above their absolute threshold in the Weber range. According to Weber's law the following equation will hold:

$$\Delta^* S \sim S$$

More generally we may allow for a power law dependence of sensitivity on illumination, rather than a strictly reciprocal one:

$$\Delta^* S \sim S^k \qquad\qquad\qquad \text{Equation 12}$$

Here, S is the scotopic background luminance and $\Delta^* S$ the incremental threshold for the rods. The exponent k is the slope of the TVI-curve (threshold versus intensity curve) for rods in log space (Wyzecki & Stiles, 1982). Hence, the TVI-exponent k represents the gradient of the rod adaptation mechanism with increasing intensity. For k = 1 Weber's law holds. If equal multiples of $\Delta^* S$ are equal in the luminance contribution from the rods (as found by MacLeod, 1974), the relation above holds also for intensities above threshold. The independent weight for the rods will be inversely proportional to the rod threshold, hence

$$W_S{}' \sim S^{-k} . \qquad\qquad\qquad \text{Equation 13}$$

With the independent rod weight $W_P{}'$ = const and the assumption that rods and cones do not interact, this relation can with Equation 8 be transformed to:

$$W_P = 1/\left(1 + c \cdot S^{-k}\right) . \qquad\qquad\qquad \text{Equation 14}$$

The parameters c and k were optimized iteratively by minimizing the root mean square error (RMSE) between the W_P vs. log(S) curve and the fitted curve (shown in Figure 20). With a TVI-slope of k=0.81 and c=0.41 the RMSE of the fit is 0.076. The TVI-slope of 0.8 the rod system is consistent with earlier results e. g. from Wyzecki and Stiles (1982).

In conclusion, the fitted curve can be described by

$$W_P = 1/\left(1 + 0.41 \cdot S'^{-0.81}\right) .$$

Comparing the MDB results of the eew background and the purple background for observer 1 (Figure 18) it is evident that with k_{eew}=0.99 and k_{purple}=0.97 the rod TVI-curves for both cases backgrounds do not differ. Sharpe et al. (1989) found that the rod sensitivity decreases due to interference by cone signals when red backgrounds are present, leading to an increase of the TVI-slope from 0.78 to 0.92. The increased rod sensitivity for red backgrounds was not found here, which can be explained by the monochromatic lights used by Sharpe et al. that produce a very high S/P ratio. Whereas the purple background used here shows a rather wide spectrum. However, the results confirm the suggestion that only S and P matter and show that rods obey roughly Weber's law.
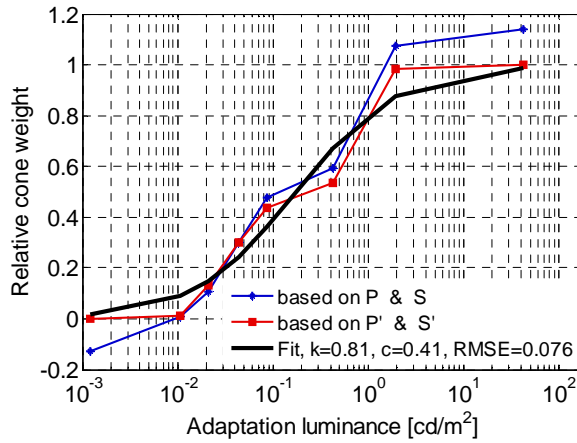
Figure 20: Relative cone weights based on the CIE luminances S & P and on sensation luminances S' & P'.

Change of rod and cone contribution with the S/P ratio of the reference

The question remains how the achromatic luminance information changes for different S/P ratios of the reference. The S/P ratio of the reference was altered by changing the scotopic luminance only and keeping the photopic luminance constant. It can be assumed, as was done above, that with the rods working in the Weber range ($\Delta*S/S$ = constant) Equation 13 will hold. With the additional assumptions that the incremental sensitivity of the cones does not change when photopic luminance P is changed within the mesopic range, Equation 8 and Equation 13 can be transformed to:

$$W_S/(1-W_S) \sim S^{-k}.$$

<div align="right">Equation 15</div>

Here, W_S is the relative rod weights. If only the scotopic luminance is changed to alter the S/P ratio, only the independent rod weights W'$_S$ will change while the relative cone weights W$_P$ remain constant. As a consequence a bluish reference with a high S/P ratio is expected to result in a decrease in relative rod weight. While a low S/P ratio, producing a reddish reference field, will lead to an increased relative rod weight.

These hypotheses were tested with a follow-up experiment. Minimum border settings were done with a reference field with S/P ratios ranging from 0.7 to 3.4 for four adaptation levels. The S/P ratio of the reference was altered by changing the scotopic luminance and keeping the photopic luminance constant. Figure 21 shows the course of the relative cone weights over a range of S/P ratios. An increase of relative cone weights (corresponding to a decrease of the relative rod weights) for increasing S/P ratios is evident for the two mesopic adaptation levels. The results are in agreement with the theory explained above. It has to be noted that for relative rod weights close to 0 or 1 a doubling of the independent rod weight due to a decreasing S/P ratio will only lead to a miniscule change in the photopic relative weight. This compression of the relative weights occurs if one of the independent weights is very large. Hence, a rather large change of the smaller independent weight will not change the relative weights in the same degree. Keeping that in mind, the TVI-exponent k can be estimated from weights not in close proximity to 0 or 1 for several S/P ratios with Equation 15. As a result, k averages around 1.35 for 0.027 cd/m^2 and 1.4 for 0.29 cd/m^2. TVI-exponents greater than 1 refer to a somewhat steeper slope of the TVI-curve than Weber's law suggests, but since it is not whether the upward deviation from 1 is statistically reliable, and since TVI-curve slopes

greater than 1 have not been reported in the mesopic range, the results could be taken as support for the Weber's-Law-based model where k = 1.
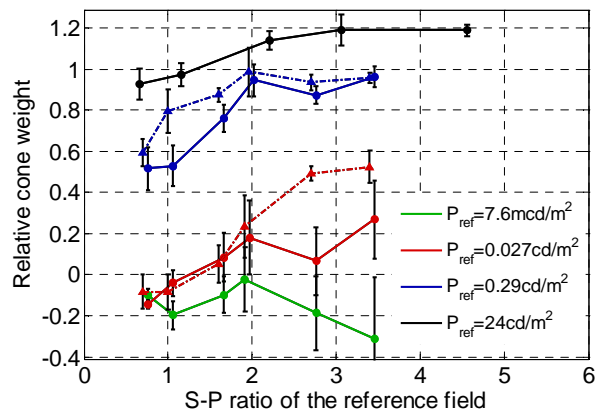
Figure 21: Relation between S/P-Ratio of the adaptation field (reference) and the relative cone weights for 2 subjects (solid curve: observer 1, dashed curve: observer 4). All data were collected with the external reference condition and a circular adjustment trajectory.

3.4   Summary and Conclusion

In this chapter the method of minimizing the distinctness of a border between a surround and a centrally fixated disc was described. MDB matches were done in the peripheral visual field 6° off-axis at adaptation conditions ranging from photopic to scotopic. It was shown that the method is also viable under dim lighting conditions and in the periphery. However, one has to consider some aspects in the experimental design to avoid unwanted side effects:

To prevent afterimages and fading due to the Troxler effect it is necessary to frequently alternate the test field with an intermittent adaptation screen as done by Kaiser (Kaiser, 1971). Also the way the chromaticity and the luminance of the comparison field are changed plays an important role. It was found that adjustment lines of different slopes in S-P diagram yield distinctly different results (tangent bias). To avoid this bias an adjustment trajectory perpendicular to the line of minimum border distinctness in S-P space has to be used. In contrast, chromatic aberrations seem to have only a minor effect on border settings with a CRT monitor. When conducting border settings with an internal and an external field, as it was done here, the definition of the adaptation level is ambiguous. At some mesopic conditions some subjects' data revealed differences in border settings with a constant central reference compared to a reference in the periphery. A possible way to minimize adaptation effects is to use an annulus as test field that can be adjusted by the observer. In that case, the luminance of the reference field should be changed in a way that the average luminance over the monitor is constant.

The decrease of relative cone weights with dark adaptation was described mathematically by optimizing two parameters that describes the steepness (TVI-slope k), vertical shift, and shape of the W_P vs. logS curve. With a slope close to 1 it was found that the rod system obeys Weber's law for border matches.

The MDB results show that under the most extreme photopic as well as scotopic adaptation levels tested the relative receptor contribution for most of the participating observers swung beyond a pure photopic and scotopic response as defined by $V_{10}(\lambda)$ and $V'(\lambda)$, respectively. The observed behavior reflects an increased sensitivity for red for the photopic case and under scotopic adaptation levels an increased sensitivity for blue compared to the CIE standard observers. The scotopic overshoot might be attributable to variations in macular pigment optical density. The photopic overshoot is more puzzling, but it may mean that MDB spectral sensitivity is simply more red-sensitive than the flicker sensitivity on the basis of which $V_{10}(\lambda)$ was defined. This explanation is surprising because earlier evidence suggests that the minimum border criterion and flicker photometry lead to very similar luminous efficiency curves as was found by Wagner & Boynton (1972) and Kaiser (1971).

MDB matches with the eew and purple reference; these are reference fields that yield the same photopic and scotopic luminance but have different chromaticities, show a high agreement in receptor weights. This and the high linearity between the rod and cone responses lead to the assumption that under dim light conditions border matches address only the luminance channel. A first modeling approach shows that a linear weighted sum of scotopic and photopic luminance is sufficient to describe the mesopic response under all adaptation conditions. This was confirmed by an identical TVI-slope of the rod system for the equal energy white background and the purple background.

Furthermore, minimum border adjustments with several colored references of different S/P ratios revealed the decreased effectiveness of rods relative to cones with an increase in S/P ratio expected on the assumption that rods work nearly in accordance with Weber's Law in the Weber range of the TVI-curve. Border perception is shown to depend also on the retinal position of the border. It was found that peripheral minimum border matches are possible and that the observed effect of the peripheral position on rod and cone contribution is in good agreement to results from minimum motion adjustments (see chapter 4).

Overall, it can be concluded that MDB is a viable method for assessing luminance in the mesopic adaptation range with some limitations that can be minimized by a suitable experimental design. A method that does not incorporate the disadvantages of the MDB method is described in the following chapter.

Chapter 4

Minimum motion under photopic, mesopic, and scotopic adaptation levels

4.1   Introduction and Background

When seen in rapid succession, separate images merge into one another and a single continuously moving image is experienced like in motion pictures or flip-books. The merged image appears to be smoothly and continuously moving if the succession rate exceeds the critical fusion frequency (50 Hz for foveal vision). The fusion of separate images to a continuous apparent motion is possible because the retinal signals persist for a short period after the stimuli disappeared (retinal lag). The importance of motion perception within the human visual system is obvious from developed mechanisms specialized to process moving targets. The visual system possesses retinal ganglion cells that act as motion detectors and cortical cells – mostly in the middle-temporal cortical area (MT) of the brain – that register a particular motion direction or velocity. These specialized cells treat successive non-moving stimuli e. g. from a flip-book as though they had moved. Gregory & Harris (1984) showed that such apparent motion and real motion are mediated by the same neural pathway and treated by the visual system the same way.

It has been suggested that motion perception is mediated by the luminance pathway and that color does not or only marginally contribute to motion (Anstis, 1970; Ramachandran & Gregory, 1978). However, other research shows that the red-green color opponent channel makes a contribution to or even inhibits motion perception (e. g. Derrington & Badcock, 1985; Cavanagh & Favreau, 1985; Cavanagh & Anstis, 1991).

In the case of particular interest here, successive images that generate apparent motion are of a sinusoidal grating, e. g. in sine and cosine spatial phase. The matching of corresponding points in the luminance in succeeding frames will generate leftward or rightward motion depending on the relative luminance of the sine and cosine. But if one grating is purely chromatic, with no variation in luminance, the direction of motion will be completely ambiguous: a 'motion null' is perceived. The method of nulling the apparent motion of a stimulus composed of homo-chromatic and heterochromatic sinusoids has been used to determine individual isoluminance ratios between two colors under photopic conditions (Anstis & Cavanagh, 1983; Cavanagh, MacLeod, Anstis, 1987; Kaiser, Vimal, Cowan, Hibino, 1989, and more). Anstis and Cavanagh (1983) described first a minimum motion (MinMot) technique to assess isoluminance between two colors and compared it with isoluminance settings by minimum flicker. They found very good agreement between the two methods and concluded that they address the same visual pathways. Thus Cavanagh et al. suggest that the mechanisms used for motion nulling respond to the linear sum of M and L cone signals only, hence are a measure of luminance resembling

flicker photometry in this respect (Eisner & Macleod, 1981). Here, luminance refers to what Kaiser called sensation luminance (Kaiser, 1988), meaning the individual luminance based on an individual spectral sensitivity, rather than photometric luminance (see chapter 2). Also Lee and Stromeyer (1989)found that S cone contribution is, if at all; only to a very small extent present. The notion of luminance is supported also by the high degree of additivity that was found in minimum motion data. The slight additivity failures of this method are within the same range of additivity failures of flicker photometry (Kaiser, Vimal, Cowan, Hibino, 1989). Thus, minimum motion and flicker photometric measures of sensitivity depend both on the summed activation of L and M cones under conditions where rods are excluded by the use of relatively high light levels or small fields.

The earlier findings with the minimum motion method mirror the responses of cone dominated vision between 10 cd/m^2 and 16 cd/m^2. The purpose of the present study is to determine the isoluminance ratio for photopic, mesopic, and scotopic adaptation levels at various eccentricities. The role of eccentricity in motion settings under various adaptation conditions has been studied by Anstis (2002). He found a linear increase of blue sensitivity with eccentricity at all adaptation conditions ranging from photopic to scotopic. Chien et al. (Chien, Teller, Palmer, 2000) compared the change of sensitivity between adults and infants with the minimum motion technique at photopic, mesopic and scotopic adaptation levels. The transition curve between photopic and scotopic levels showed no differences between the two groups and could be modeled as a sigmoid function.

4.2   The minimum motion stimulus

The minimum motion stimulus used here is a windmill-like colored annulus (Figure 22) that was presented on a CRT monitor.
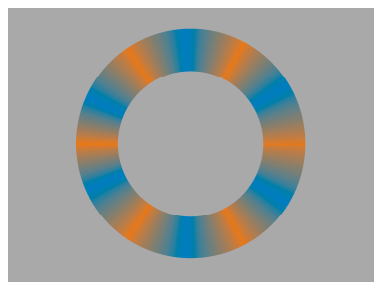
Figure 22: Minimum motion stimulus composed of red and blue sinusoidal waveforms on a uniform background.

The annulus is composed of two temporally and spatially varying sinusoidal gratings, a hetero-chromatic color grating and a homochromatic luminance grating, that are both modulated on the uniform background. The heterochromatic colored grating is formed by spatially inter-leaving two differently colored sine wave components, a test and a reference, in opposite spatial phase. Depending on the relative sensation luminance information of the two components of the chromatic grating, the stimulus appears to rotate clockwise or counterclockwise. When the

two luminance amplitudes match, the annulus will be perceived as neither moving rightward nor leftward; it will appear flickering. This state is called the motion null.

In the following paragraphs the composition of the stimulus will be discussed in more detail using a blue and red colored annulus as an example.

The **heterochromatic color grating** can be decomposed into two colored sinusoids changing in time and space with the same temporal and spatial frequency. One sinusoid is generated by modulating the red and the other by modulating the blue phosphor. The red and the blue sinusoidal gratings are 180º out of phase both in time and space. One of the phosphors is always modulated with the maximum possible range (here the red) while the amplitude of the other phosphor's sinusoid (blue) is varied by the observer until a motion null is perceived. In the illustrated case (the minimum motion point) the two phosphors are isoluminant.

The **homochromatic luminance grating** or 'luminance lure' is generated by modulating all three phosphors around the background level. The luminance grating changes with the same spatial and temporal frequency as the color grating. But now the phosphors are varied with no phase offset, thus producing a dark-light neutral gray grating that changes in luminance but not in chrominance. With the intention of keeping the space average in chromaticity of the whole stimulus constant at the chromaticity of the background, the color of the luminance grating is chosen to match the chromaticity coordinates of the background. The homochromatic luminance grating is offset by 90º to the heterochromatic grating in both space and time (that is, it is in quadrature with the colored grating). The maximum modulation amplitude of the luminance lure is kept constant at 8%.
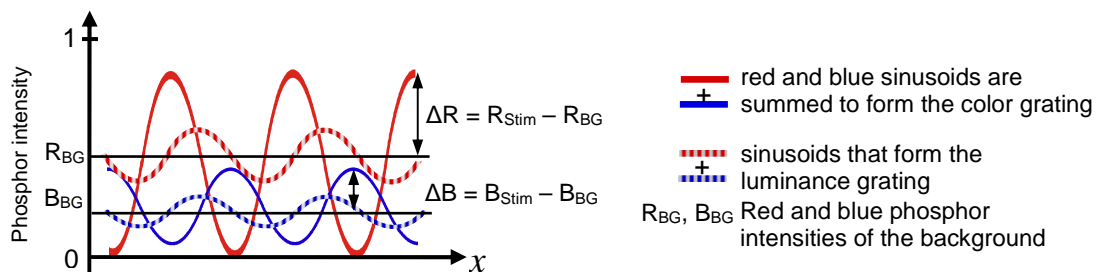
Figure 23: Shown are the red and blue phosphor intensities, modulated in space (x) around the background intensities R_{BG} and B_{BG}. In addition the sinusoids alternate in time around their space and time average luminance (= background luminance), hence every half time cycle the contrast reverses. The gratings change in time and space with the same temporal and spatial frequency. The sum of the striped gratings produce a homochromatic luminance grating that changes in intensity but not in chromaticity. The two solid gratings are offset from each other by 180º and form the heterochromatic grating.

Figure 23 depicts the described sinusoids that make up the annular test field. Angular position within the annulus is the relevant spatial coordinate and is shown by the x-axis. Each curve in Figure 23 shows the red and blue phosphor intensities over space at a particular moment in time. All gratings are modulated around the red and blue phosphor intensities of the background R_{BG} and B_{BG}. The phosphor intensities are the linearized output voltages of the CRT monitor normalized between 0 and 1. Thus a red phosphor intensity of 0.2 corresponds to 20% of the maximum CIE luminance the red gun can produce. The two solid curves in Figure 23 are summed to generate the color grating. Note that the amplitude of the red grating is chosen to be maximal ($R_{Stim,min}=0$). At a background level of $R_{BG} = 0.4$ or 0.6, a maximal modulation of 0.4 to both sides would be possible. The amplitude of the blue phosphor is not fixed and

changes with the mouse movement. The two striped gratings and a sinusoidal modulation of the green phosphor are superimposed in phase to create the gray luminance grating of the same chromaticity as the background. Hence, this luminance grating varies only in luminance. All sinusoids are counterphasing: each grating appears alternately in its initial spatial phase and in the opposite spatial phase and at intermediate times becomes uniform when the sinusoidal time course of its contrast crosses zero.

With a **simplified version of the stimulus** as schematized in Figure 24, the perception of motion will be explained. For simplicity the sinusoids are here replaced by square waves. Also for illustrative purposes, Figure 24 depicts one temporal cycle decomposed into 4 frames that are shown separated vertically and not superimposed as for the stimuli. In frame 1 at T_1 the color grating consisting of red and blue alternating patches is presented and at T_2 replaced by the gray luminance grating. Note that the offset from the color grating is ¼th of the cycle (phase shift of 90°). The rapid switch between the two gratings lets the red patch seem to move towards one of the neighboring gray patches of the luminance grating. If the luminance of the red patch is smaller than that of the blue patch the red patch will jump toward the darker patch of the luminance grating, to the left (black arrows). Conversely, when the luminance of the red patch is higher than that of the blue patch the red patch will jump toward the brighter patch of the luminance grating, meaning, to the right (light gray arrows). Frame 3 and frame 4 show again the red-blue color grating and the gray luminance grating reversed in contrast (shifted by 180°) compared to frame 1 and frame 2, respectively. Again, each patch will appear to jump towards the right or left patch of the next frame depending on its luminance amplitude. T_1 to T_4 represent one temporal cycle of the stimulus and are repeated endlessly. This causes the impression of continuous motion. But if the sensation luminance of the red and blue patches is equal, there is no preference for either motion direction and the annulus will not rotate but flicker.
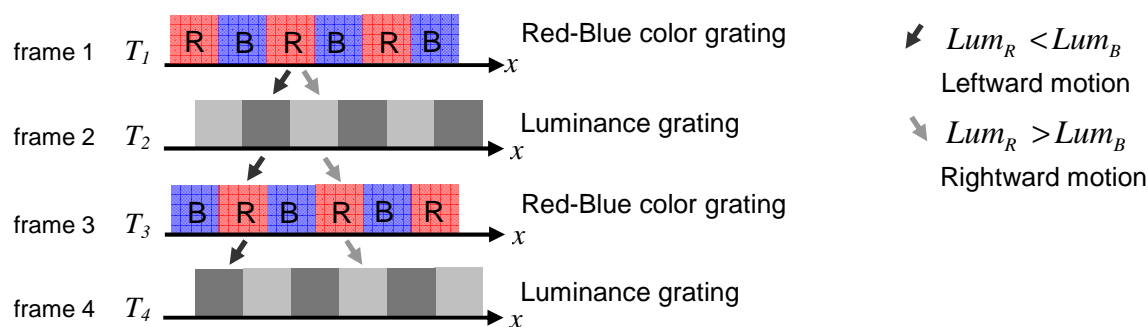
Figure 24: One time cycle of a simplified version of the stimulus, decomposed in four time frames $T_1 - T_4$. At T_1 and T_3 the heterochromatic color grating (here depicted as square wave) is presented followed by the homochromatic luminance grating at T_2 and T_4 offset by a quarter of a spatial period. Between T_1 & T_3 and also between T_2 & T_4 the signals undergo a periodical contrast reversal, which is repeated in subsequent periods. The apparent motion is leftward when the red patch of the color grating is dimmer than the blue patch. As a consequence the red patch seems to 'move' toward the left, dimmer patch of the luminance grating (dark arrows). A rightward motion is perceived when the red patch is brighter than the blue patch and therefore 'moves' toward the brighter patch of the luminance grating (gray arrows). (figure adapted from Cavanagh, MacLeod, Anstis, 1987)

For the windmill stimulus of the experiment the spatial square waves were replaced by spatial sinusoids, and the temporal modulation was introduced by periodically reversing the contrast of the color grating with a sinusoidal modulation in time from T_1 through T_4 until at T_5 it reverts to the grating shown at T_1. The luminance grating is varied sinusoidally in the same way. When

the two counterphasing gratings are combined, the intensity of each phosphor at each pixel varied sinusoidally in time. This creates a smoother impression of motion than is possible with the square-wave stimulus of Figure 3, and it also has the advantage of allowing systematic exploration of the effects of spatial and temporal frequency on the contribution of rods and cones to mesopic luminance.

Figure 25 illustrates how the stimulus can be decomposed into its chromatic and achromatic components. In each inset the abscissa shows the space dimension x, e. g. pixels on the monitor. The color grating can be decomposed in a luminance component (achromatic) and a chrominance component as shown in the second diagram of each row. The chrominance component is present for any setting of the relative luminance of the red and blue phosphors, since they are always in opposite spatial and temporal phase (black curves in the second columns graphs). But luminance modulation only appears in the color grating if and only if the red and blue phosphors have different amounts of luminance information (case A and B). Whenever the achromatic component of the blue and red sinusoids cancel each other (case C), the luminance profile of the chromatic grating is uniform (light gray curves in second column's graphs) and produces no motion effect by its interaction with the luminance lure. Only the interaction of the luminance component of the heterochromatic color grating with the homochromatic luminance grating results in the perception of motion.
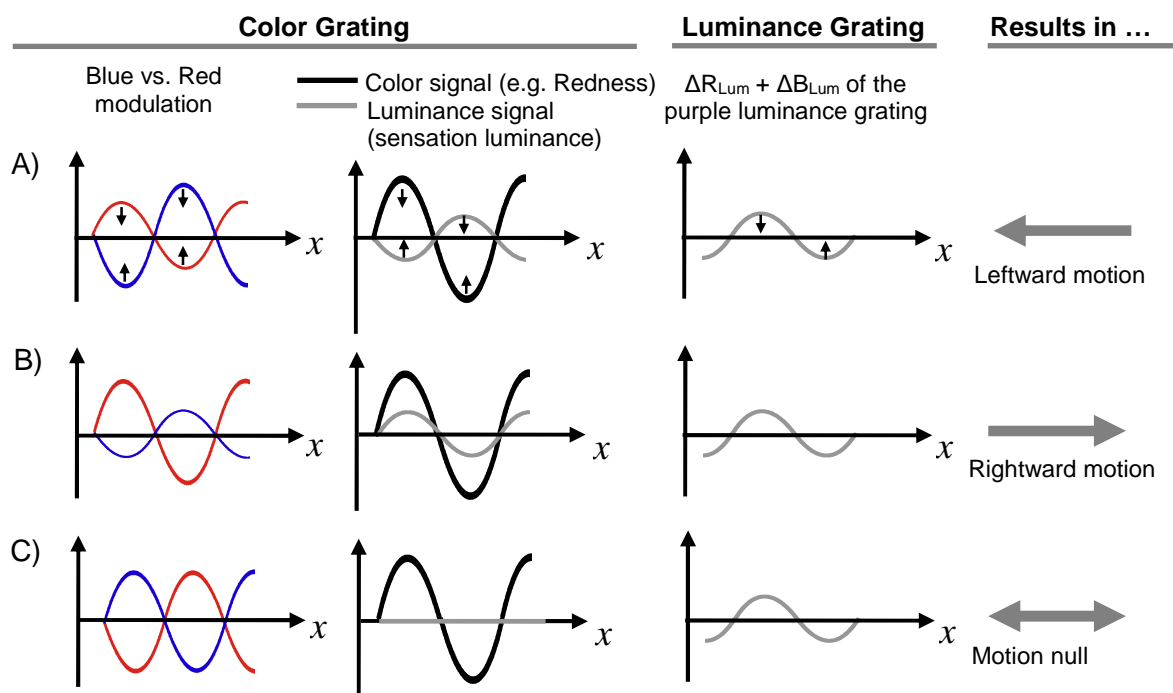
Figure 25: Composition of the stimulus: The graphs express (in the left panels) the modulations of the red and blue intensity over space and (in the center panel) their decomposition in chromatic (black curve) and achromatic luminance (grey curve) information. The change over time is suggested by the black arrows. Case A: The blue color grating is brighter than the red: the interaction of the resulting achromatic information of the color grating and the subsequently appearing luminance grating (right panels) lead to perceived leftward motion. Case B: The red color grating is brighter than the blue, the interaction of the resulting achromatic information of the color grating and the luminance grating lead to perceived rightward motion. Case C: The red and blue grating contain the same luminance information, which is canceled out, leading to motion null. (graphs adapted from Cavanagh, MacLeod, Anstis, 1987)

A spatiotemporal grating can be described by the product of sinusoids in time and space. Since there is a 180° phase shift between the two colored gratings as shown in Figure 23 and Figure 25, the basic components of the red and blue color gratings can be expressed by $\cos(2\pi x f_S) \cdot \cos(2\pi t f_T)$ and $-\cos(2\pi x f_S) \cdot \cos(2\pi t f_T)$. Here, f_S and f_T denote the spatial frequency and the temporal frequency of the gratings, respectively. Given that the luminance grating is shifted by 90° in time and in space compared with the color gratings, it can be described by the product of the sine over time and the sine over space: $\sin(2\pi x f_S) \cdot \sin(2\pi t f_T)$. From this, the variation of the red phosphor can be expressed as:

$$R(x,t) = P_R + \frac{1}{2}P_R \cdot m_R \cdot \cos(2\pi x f_S) \cdot \cos(2\pi t f_T) + \frac{1}{2}P_R \cdot m_{Lum} \cdot \sin(2\pi x f_S) \cdot \sin(2\pi t f_T) \quad \text{Equation 16}$$

Likewise for the blue phosphor:

$$B(x,t) = P_B - \frac{1}{2}P_B \cdot m_B \cdot \cos(2\pi x f_S) \cdot \cos(2\pi t f_T) + \frac{1}{2}P_B \cdot m_{Lum} \cdot \sin(2\pi x f_S) \cdot \sin(2\pi t f_T) \quad \text{Equation 17}$$

The luminance of the background generated by the blue and red phosphor is denoted by P_B and P_R, respectively, whereas m_{Lum} is the modulation amplitude of the homochromatic luminance grating ('luminance lure') and m_R and m_B determine the modulation amplitude of the red and blue sinusoids of the color grating. Here, m_R is fixed at a level that allows maximum modulation of the red phosphor and m_B is varied by the observer. The green phosphor is set to the level of the background and not altered:

$$G(x,t) = const. = P_G$$

In Equation 16 and Equation 17 the sinusoidal terms generate the luminance grating with an amplitude of $m_{Lum} \cdot (P_R + P_B)/2$. It has to be emphasized that the amplitude of the luminance grating is fixed at all times with $m_{Lum} = 0.05$ whereas the ratio of the amplitudes between the red and the blue components of the color grating is variable.

The space- and time-average photometric luminance of the annulus for each phosphor in the above equations is equal to the background luminance levels, $P_R + P_B$. Since the two gratings are modulated on the adaptation background, at any time the space average of the photopic CIE luminance of the stimuli matches the photopic CIE luminance of the background. Therefore local adaptation causing side effects as it was evident in the MDB experiment is avoided.

4.3   Experimental Design

As mentioned in the last section, our minimum motion stimulus created chromatic modulation using the red and blue phosphor of a CRT monitor. This ensures maximum visibility under photopic and scotopic conditions since the scotopic and photopic systems are most selectively responsive to the red and the blue phosphor.

To provide background luminances ranging from photopic to scotopic levels, neutral density filters (Lee filters, F299 4 stops, F211 3 stops, F210 2 stops, and their combinations) were set in front of the monitor screen (Figure 26). The output of the CRT monitor was calibrated to linearize the luminance output of each phosphor. Also the spectral radiance of the monitor

guns as well as the filter spectral transmissions was measured. The monitor was controlled by a Bits++ graphics card from Cambridge Research Systems, which allows generating stimuli with a 14-bit-precision in intensity (2^{14}=16384 intensity steps) per color.

The uniform background was set to an equal energy white (eew) at eight luminance levels (see Table 3 in chapter 3). In addition to the equal energy white background two subjects were tested with a purple background (x, y $\approx$ 0.37, 0.22) of the same S/P ratio as the equal energy white. Under this condition the green phosphor was set to 0 for the background and the stimuli. At the scotopic luminance of 2.4 mcd/m^2 only the purple background was used, because the equal energy white (eew) background didn't offer a high enough range for modulation of the red phosphor to find a motion null. In addition, several colored backgrounds with S/P ratios ranging from 0.7 to 3.4 were used by keeping the photopic luminance constant and altering the scotopic luminance of the background alone. To allow for peripheral and near foveal matches, the radius of the annulus ranged from 1° to 18°. The given radii are the mean of the inner and outer radii. The relative thickness of the rings was set to 15% of the radius, except for the smallest two stimuli, whose thickness was set to 30% of their radii. This maintains visibility and allows minimum motion settings at dimmer light levels. For each stimulus at least 5 repeated settings were done. For the main part of the experiment the spatial frequency of the annulus was kept constant at 1 cpd (cycles per degree) for all stimuli sizes, by setting the number of windmill segments accordingly.

When working in the mesopic range one has to consider the different temporal properties of the cone and rod pathways as described in chapter 2. The temporal frequency of the annulus was kept constant at 2 Hz for the main experiment. This driftrate is low enough to avoid appreciable phase lags between rod and cone signals that can complicate the time cancellation between rods and cones (MacLeod & Stockman; 1987), yet high enough to give the impression of a smoothly rotating annulus. An overview of the stimulus parameters and the variables is shown in Table 5.
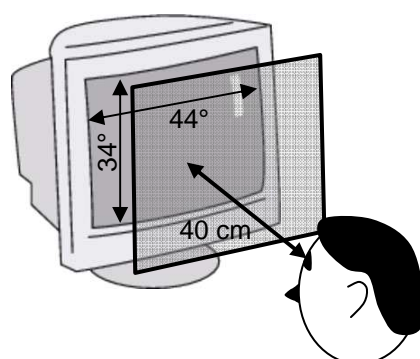
Figure 26: Schematized test-setup: CRT monitor with ND-filter, the widths and the heights of the monitor screen are 44° (40.5 cm) x 34° (30.5 cm) at a viewing distance of 40 cm.

The duration of dark adaptation varied from 10 minutes for the photopic condition to 45 minutes for the dimmest condition. During dark adaptation the observers got instructions and got familiar with the stimulus and the adjustment process. The observer's head was positioned in a distance of 40 cm from the screen in a chinrest. The subjects were asked to fixate a fixation

spot in the middle of the screen and to move the mouse to adjust the m_R (keeping m_B fixed at its maximal value) until a motion null is found. The data collection for all adaptation levels was divided in 4 sessions spread over several days. In each session the data for 1-3 adaptation levels were collected.

Dependent variables	
Isoluminance ratio between the blue and red phosphor, that is the fraction of the red phosphor that has to be added to the eew background to match the added fraction of the blue phosphor to the eew background: ΔR/ΔB	

Independent variables	
Background / adaptation luminance P_{adapt}	P_{adapt} = 0.0024 … 42 cd/m²
	Equal energy white (x, y) = (0.34, 0.33)
	or purple (x, y) = (0.37, 0.22)
	S/P ratio ≈ 1.7 … 2
Annulus radius / eccentricities θ	1° / 2° / 5° / 10° / 14° / 18°
Driftrate f_T	2 Hz (occasionally 0.5 Hz … 4 Hz)
Spatial frequency f_S	1 cpd (occasionally 0.5 cpd … 5 cpd)

Parameters & conditions	
Thickness of annulus	15% of radius, 30% of radius for the 1° and 2°
Repetition of each stimulus condition	5 or more
Fixation	Fixation spot in the middle of the stimulus

Observers	
9 subjects	8 subjects took part in the main experiment,
	1 further subject took part only in 2 follow up experiments
	visus ≥ 0.8, normal color vision
	Age: 18-36 (5 ♂, 4 ♀)

Table 5: Overview over the experimental parameters and conditions

Presentation of the results and calculation of relative receptor weights

For each setting we recorded the ratio of ΔR/ΔB at motion null (Figure 23). Here, ΔR and ΔB are the differences in the linearized phosphor intensity between the maximum amplitude of the grating and the background, expressed as a fraction of the maximum phosphor intensity. In the results section this ratio is expressed as the ratio of luminance values that are isoluminant. The ratio between the two phosphors' luminances at equal luminance will be called 'isoluminance ratio' further on.

As in chapter 3 relative rod and cone weights were calculated under the assumption that the rod and cone signals add up linearly. The S and P values in Equation 7 in chapter 3 are here the luminance amplitudes of the red and blue phosphors of the color grating at isoluminance. An isoluminance ratio of 1 will result in the relative cone weight of 1. Analogously an isoluminance ratio around 14 is identical to a scotopic isoluminance ratio, hence leads to a relative rod weight of 1 and a cone weight of 0.

4.4   Results and Discussion

Effect of adaptation level and eccentricity

Figure 27 and Figure 28 show the results for all eight subjects at three eccentricities. The vertical axis depicts the isoluminance $\Delta P_R / \Delta P_B$ ratio between the red and the blue phosphor on a log scale; the horizontal axis shows the adaptation luminance based on $V_{10}(\lambda)$ (the photopic adapting or background luminance, based on the large-field photopic luminous efficiency curve for the CIE 1964 supplementary standard observer). An isoluminance ratio of 1 reflects a pure photopic adaptation state if $V_{10}(\lambda)$ is the underlying sensitivity function. The Purkinje shift is reflected by the increased isoluminance ratio for decreasing adaptation levels. At the lowest tested luminance a photometrically photopic isoluminance ratio of 14 is identical with a scotopic isoluminant state. The scotopic and photopic isoluminance ratios are shown as gray horizontal lines in Figure 28. Figure 27 only includes the photopic isoluminance lines. For demonstration purpose the curves for the 1.9° annulus are shifted up by one log unit. To resolve the error bars an insignificant horizontal shift has been applied to each observer's curve. The error bars represent ± 1 standard deviation of at least 5 settings per person. It can be seen that the red-blue sensitivity does not change considerably within the ±1°- fovea over the tested range of adaptation levels. At levels below 0.1 cd/m² the adjustment was more difficult or not feasible at all. The 2° radius data, however, do show an increase of blue sensitivity for lower adaptation levels, though they don't reach a pure scotopic response at the lowest tested level of 0.01 cd/m². The average isoluminance ratios for the two smallest stimuli at 42 cd/m² are slightly below the theoretical photometric unity (0.63 and 0.85). This is attributed to an increased red sensitivity within a 2° - 4° visual field compared to $V_{10}(\lambda)$. A conversion of the luminance to luminance values based on the $V_2(\lambda)$ luminous efficiency function leads to an increase of the isoluminance ratios for the 0.95° and 1.9° stimuli from 0.63 and 0.85 to 0.92 and 1.24, respectively. This shows that foveal photopic luminance can be best described by $V_2(\lambda)$, whereas $V_{10}(\lambda)$ accounts best for the photopic results between 2° and 5° off-axis as expected.

For the periphery at 18° the isoluminance curve is shifted towards higher isoluminance ratios indicating an increased blue sensitivity. The scotopic isoluminance ratio is approached already at 0.1 cd/m², a luminance where the 2° radius isoluminance setting remains closer to photopic than scotopic equality. Below that luminance, the blue sensitivity increases further to a level that reliably exceeds expectations based on the standard scotopic luminous efficiency curve V'(λ).
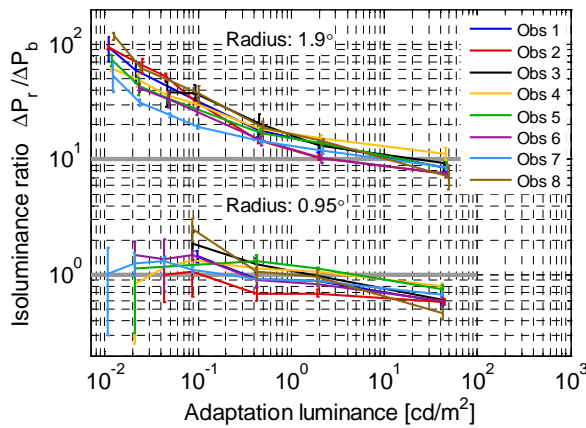
Figure 27: Isoluminance ratios for stimuli with 0.95° and 1.9° radius. The curves for the 1.9° stimulus are shifted up by one log unit for illustration purpose. Each line stands for the average data for one subject.
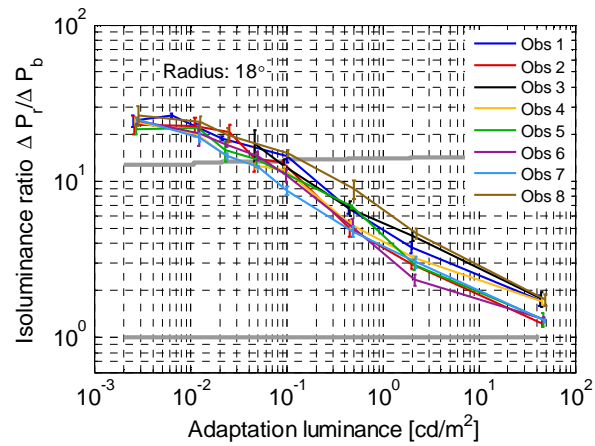
Figure 28: Same as previous figure for a stimuli radius of 18°. Here the upper gray line indicates scotopic and the lower gray line photopic isoluminance. Below an adaptation luminance of 0.05 cd/m² the isoluminance ratio exceeds scotopic isoluminance for all observers.

The average relative cone weights and the standard deviations between subjects are plotted as a function of adaptation luminance and the stimulus radius in Figure 29 and Figure 30, respectively, with the other independent variable as a parameter in each case. The graphs show the continuous decline of cone weight for lower adaptation levels. It is evident that the more eccentric the stimuli, the wider the luminance range over which the rods dominate vision. An exception is the very small stimulus, where the cones define vision alone at all levels.

The influence of eccentricity is highest at mesopic adaptation levels, when rods and cones are both active. Between 0.021 cd/m² and 0.088 cd/m² vision is dominated by the cones in the fovea and by the rods at 18° off-axis. This effect is expected, since it is determined by the different spectral sensitivity of the receptors and their distinct distributions over the retina (Curcio et al., 1990). The effect of eccentricity at various adaptation conditions with a similar stimulus as used here was examined earlier by Anstis (2002). He found that blue sensitivity increases linear with eccentricity and the darker the adaptation level the steeper the slope of the eccentriccity function. The slope of the eccentricity function increased by a factor of 2 to 4 for each decrease of one $\log_{10}$ unit of luminance. However, here, at 42 cd/m² the blue sensitivity measured as isoluminance ratio $\Delta P_R / \Delta P_B$ increases linear with the log of the radius in degrees. At lower adaptation levels the isoluminance ratio increases more rapidly as with the log of the radius.

The relation of the data to the standard V'(λ) function at low adaptation levels is surprising. For the 18° annulus, settings consistent with V'(λ) are made at a luminance of 0.06 cd/m² and negative weights are obtained at lower luminances. Yet at 0.011 cd/m² and lower luminances, no color was visible in the test field. These negative cone weights are therefore unlikely to be due to cone intrusion. The CIE V'(λ) function is based on data collected at 8 degrees eccentricity (Wald, 1945) or with a 10 degree radius bipartite field (Crawford, 1949). One might expect agreement with the present data for a field radius between 5° and 10°. However, the results suggest that rod sensitivity in the peripheral retina favors short wavelengths to a greater degree than expected on the basis of V'(λ). A possible explanations might include observer variation in scotopic luminous efficiency functions compared to V'(λ), but this is unlikely since both the present group of 8 observers and Crawford's group of 50 subjects on which V'(λ) was

based are relatively homogeneous. Another possibility is that some blue-absorbing macular pigment is still present at a radius of 10°.

Macular pigment in the periphery might also account for the dependency of receptor weights at pure photopic and scotopic light levels. The graphs in Figure 29 and Figure 30 illustrate that the influence of eccentricity for a pure rod adaptation level of 2.4 mcd/m² is decreased compared to a mesopic adaptation luminance but not diminished to a negligible level. The differences in cone weights between the 5° radius ($W_P \sim -0.1$) and the bigger annuli ($W_P < -0.2$) are surprising, given that at this luminance vision is determined by rods alone and that the sensitivity of the rods is constant over the peripheral visual field. Also the upper curve in Figure 30 shows that for the photopic adaptation level cone weights drop off slightly with increasing eccentricity. The small decrease for peripheral stimuli might be due to rod activity at 42 cd/m². Rods begin to saturate around 2.0 $\log_{10}$ scotopic trolands (sc td) ($\approx$ 1.6 log phot. td $\approx$ 3 cd/m²) but are not completely saturated until 120-300 cd/m² (3.0 log10 sc td $\approx$ 2.6 log phot. td $\approx$ 45 cd/m²) (Aguilar & Stiles, 1954, Hayhoe, MacLeod, Bruch, 1976, Stockman & Sharpe, 2006). This allows the assumption that the rods might have some minor influence on minimum motion perception in the periphery at the photopic luminance of 42 cd/m². Another likely basis for this shift is the reduction in macular pigment density with eccentricity. On the basis of the color matching functions of Stiles and Burch (1955), Stockman, MacLeod and Johnson (1993) estimate a macular pigment peak density of 0.15 for a full 10° field. The estimate of a standard deviation of 0.12 in peak macular pigment density among observers for a 10° field by Webster and MacLeod (1988) could suggest an even greater mean density than this. So it is not surprising that the scotopic and mesopic luminous efficiency functions continue to shift at large eccentricities. The isoluminance ratios under purely scotopic and purely photopic conditions change by roughly the same factor with eccentricity; this also supports the macular pigment hypothesis.
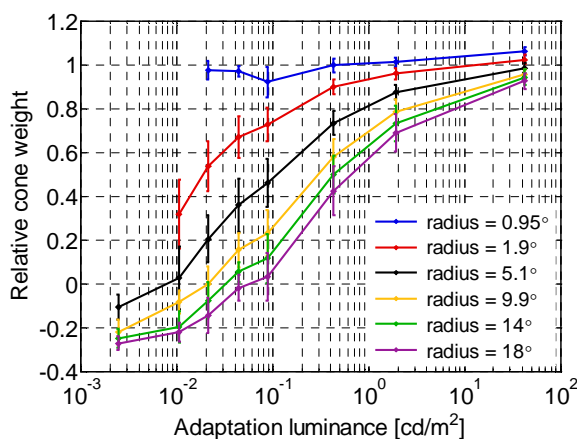
Figure 29: Relative cone weights for increasing adaptation luminance. Parameter is the radius of the annulus. The error bars are the ± standard deviations of 8 subjects.
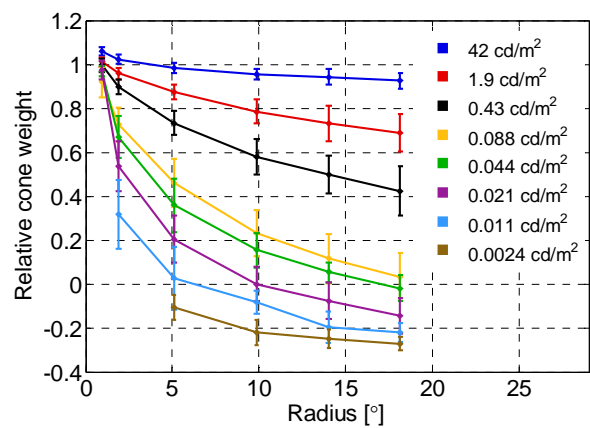
Figure 30: Relative cone weights vs. annulus radius. The parameter is the adaptation luminance and the error bars are the ± standard deviations of 8 subjects.

The data in Figure 29 and Figure 30 can be summed up by defining the luminance of equal rod and cone contribution for a particular eccentricity, which will be called 'mesomesopic' luminance. The results in Figure 31 show a remarkable shift of the mesomesopic luminance of equal rod–cone contribution from 0.85 cd/m² to 0.02 cd/m² with eccentricity. This

demonstrates the extent to which the position of the stimuli influences perception under mesopic adaptation levels. The strong effect can be explained by the distinct distribution of rods and cones across the retina. Central vision is determined by the cones alone also at mesopic light levels due to the absence of rods in the fovea; whereas with eccentricity the relative amount of rods in the retina increases, so does their influence on vision.
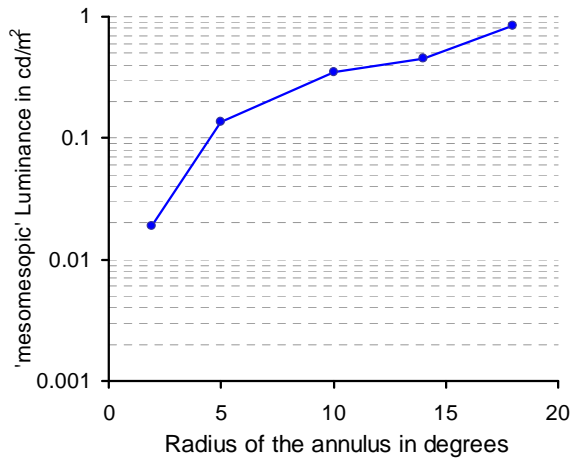
Figure 31: The mesomesopic luminance over the radius of the annulus. The mesomesopic luminance is the luminance of equal rod and cone contribution.
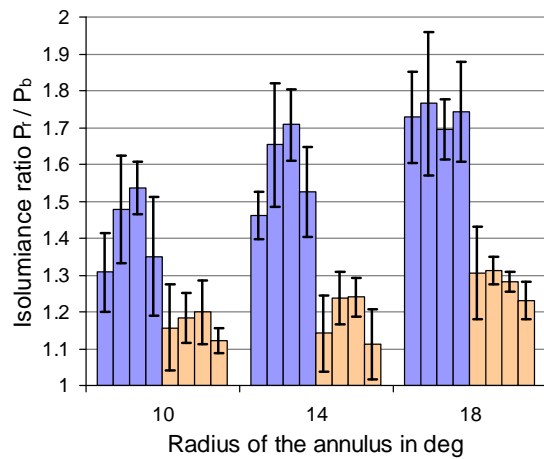
Figure 32: Isoluminance ratios at 42 cd/m² for radii of 10°, 14°, and 18°. Each bar represents one subject. The error bars are the single ± standard deviation. The two colors represent the two groups that might reflect different variants of L-cone pigments.

Taking a closer look at the isoluminance ratios of the individual observers at 42 cd/m², it appears that they may fall into two groups with distinct photopic sensitivity. Especially the isoluminance ratios (IR) for the 18° and 14° annulus radii seem to separate in two groups (IR: 1.3 vs. 1.7 and 1.2 vs. 1.6, respectively). A plausible idea is that this disparity might be due to variations in L-cone pigments. The two polymorphic variants of L-cones pigment incorporating alanine vs. serine, result in a shift of a few nm of the absorbance spectrum. The shift has been estimated as 2.7 nm (Sharpe, Stockman, Jaegle, Knau, Klausen, Reitner, Nathans, 1998) or perhaps more (4.3 nm (Merbs & Nathans, 1992), 7 nm (Asenja, Rim, Oprian, 1994)). This hypothesis does not, however, survive quantitative scrutiny. Let us assume a shift of 3 nm in L cone peak excitation between observers with serine and alanine forms of the normal L cone pigment. The relative excitation of L cones (which are the main source of photopic luminance, and of bimodal variation in normal colour vision) by the blue and red phosphors changes by about 3% per 1 nm shift in the peak absorption (Golz & MacLeod, 2003, Table 6). This suggests that the serine /alanine polymorphism of the L pigment, with its attendant shift in wavelength of peak absorption by about 3 nm, will change the photopic relative luminance of the red and blue phosphors by about 10%. The individual variation revealed at large eccentricities in Figure 32 is of much greater magnitude, and therefore probably has a different origin, such as either continuous or discrete individual variation in the relative contributions of the L and M cones to photopic luminance.

Comparison of an equal energy white and a purple field of equal photopic and scotopic luminance

The question arises whether the two quantities, scotopic and photopic luminance, are sufficient to describe a mesopic luminance response. This is by no means clear a priori, since four photoreceptor types (three cones, one rod) combine in ways not well understood to determine mesopic luminance, which in principle may be a function of all four photoreceptor excitations rather than just the photopic and scotopic values of the stimulus. To test this point, the equal energy white field was replaced by a purple field of the same S/P ratio. If the sum of the scotopic and photopic spectral luminosities is the only quantity that determines mesopic luminance information, the equal energy white and the two colored fields should elicit the same mesopic response. Two subjects were tested with adaptation levels from photopic to low mesopic. Figure 33 shows the relative cone weights for the eew (equal energy white) and purple background of equal S/P ratios. In both graphs the solid lines stand for the equal energy white background and the dashed lines for the purple background. For both observers the cone weights from the purple reference and the equal energy white reference agree very well. A two-way ANOVA gives the following results:

Observer 1: $p_{1.9°} > .05$; $p_{5°} < .01$; $p_{10°} > .05$; $p_{14°} > .05$

Observer 9: $p_{1.9°} < .01$; $p_{5°} > .05$; $p_{14°} > .05$

Though the statistical comparison of the weights shows for some stimulus sizes significant differences between the two conditions, the differences are minor and the results can be regarded as being in good agreement between the purple and the equal energy white background. The found differences might reflect individual deviations from the $V_{10}(\lambda)$ luminous efficiency curve that are more pronounced near the fovea than in the periphery.

a)   b)
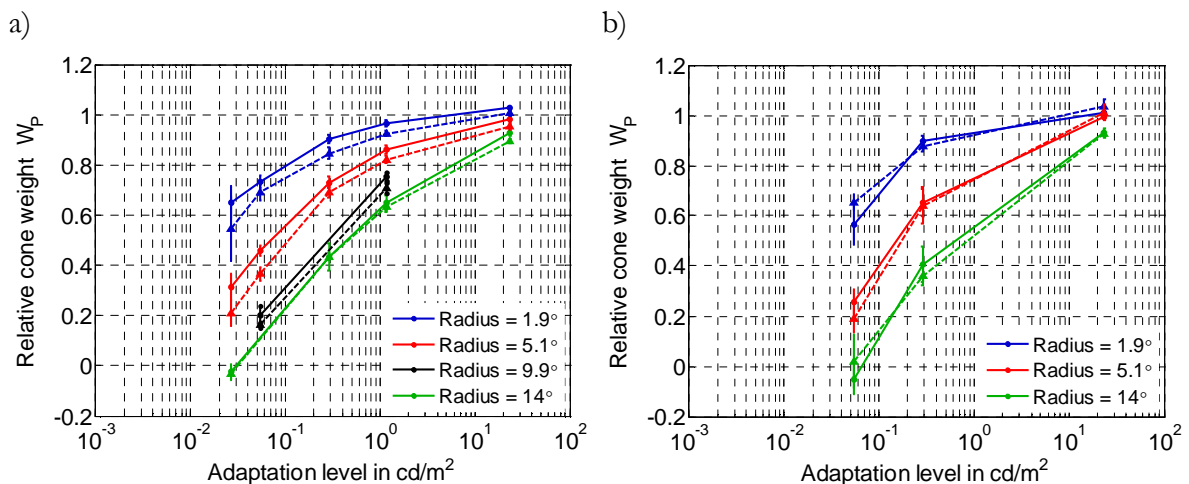
Figure 33: Comparison of the relative cone weights for a gray equal energy white background and a purple background for several stimulus radii. a) for observer 1 and b) for observer 9

Altogether, the results support the interpretation of a mesopic luminance based on rod and cone achromatic luminance information only that determine minimum motion settings under all adaptation conditions. Therefore the results can be described as a linear weighted sum of scotopic and photopic luminance based on the scotopic luminous efficiency function $V'(\lambda)$ and the photopic 10°-luminous efficiency function $V_{10}(\lambda)$.

Modeling

The curves in Figure 29 were modeled mathematically as it was described in chapter 3 for the MDB data. Also here, the scotopic and photopic sensation luminances were defined by weighting the red and blue phosphors accordingly for each of the curves separately, with the aim to avoid negative relative cone weights and cone weights exceeding 1. The phosphor weights for the photopic sensation luminance, relative to those of the standard 10° observer are $\omega_{R,phot}$=0.87…0.97 and $\omega_{B,phot}$=1.04…1.31. Scotopic sensation luminance was defined with weights of $\omega_{R,scot}$=0.75…0.90, $\omega_{B,scot}$=1.1…1.26. The given range of weights results from multiple tested stimuli radii. Figure 34 shows as a function of adaptation luminance the average relative cone weights based on the CIE standard observers (blue curve) and based on the average photopic and scotopic sensation luminance (red curve) for a stimulus radius of 14°.

As described in the chapter 3, the following assumptions can be made to simplify the modeling of the data: i) under mesopic and low photopic light levels rods work nearly in accordance with Weber's Law, that is with incremental sensitivity inversely proportional to the k power of background luminance, with k not far below 1; ii) the cone incremental threshold is constant at dim adaptation conditions and iii) the proportional relation between rod incremental threshold and rod background luminance to the power of k (Equation 12 in chapter 3) is also valid for modest multiples of rod thresholds (MacLeod, 1974).

With these assumptions the descent of the relative cone weight with dark adaptation based on the scotopic and photopic sensation luminance, S' and P', respectively can be described with Equation 18. Here, W_P is the relative cone weight, S the scotopic adaptation luminance, c is a constant and k is the TVI- exponent that determines the slope of the rod TVI-curve in Weber range. For k=1 Weber's law holds.

$$W_P = 1/\left(1 + c \cdot S^{-k}\right) .$$

Equation 18

The parameters c and k were optimized iteratively to minimize the root mean square error (RMSE) between the experimental W_P vs. logS curve and the fitted curve from Equation 18 (red and black curves in Figure 34) for each annulus diameter separately. The fitted curves for the annulus radii between 2° and 18° are shown in Figure 35 with their corresponding slope parameter k and the root mean square error. With k between 0.68 … 0.78 the rod TVI-slopes agree well with values found earlier with detection of flashes (Aguilar & Stiles, 1954; Barlow, 1957; Sharpe, et al., 1989). Table 6 summarizes the values of k for all conditions.

Comparing the TVI-slopes of the MDB data in chapter 3 with the minimum motion results of a similar eccentricity, the results show good agreement, although the k of the MDB data (k_{MDB}=0.81) is slightly higher than that resulting from the minimum motion data (k_{MinMot}=0.75).
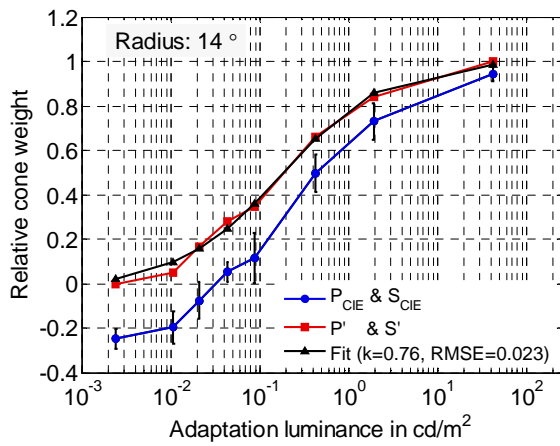
Figure 34: Relative cone weight vs. photopic adaptation luminance for an eccentricity of 14°. The weights are based on the CIE photopic and scotopic luminous efficiency functions (blue curve) and the sensation luminance P' and S' (red curve).
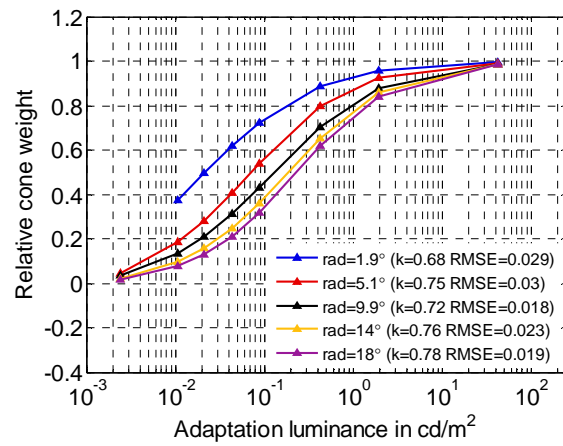
Figure 35: The fitted relative cone weights based on the average photopic and scotopic sensation luminance for stimuli radii between 2° and 18°.

The agreement between photopic and scotopic values needed for isoluminance for a neutral gray and a purple field (Figure 33) is reflected similar calculated TVI-slopes for the two backgrounds (Table 6). The calculation was based on the CIE scotopic luminance and the photopic sensation luminance for both backgrounds, because the lowest tested luminance level of 0.027 cd/m² and 0.054 cd/m² do not reflect pure rod vision and can not serve as a baseline to define scotopic sensation luminance.

Radius of the Annulus in °	AVG of Observers 1 to 8	Observer 1		Observer 9	
	EEW	EEW	Purple	EEW	Purple
2	0.68	0.69	0.62	1.04	0.71
5	0.75	0.73	0.85	0.97	1.18
10	0.72	0.83	0.84		
14	0.76	1.07	1.06	7.5	2.0
18	0.78				

Table 6: TVI-slopes k of the rod system for stimuli radii between 2° and 18°: The 2nd column shows TVI-slopes of the average W_P vs. logS curves. For observer 1 and 9 k is compared for the equal energy white (EEW) background and the purple background. The k values of the last 4 columns are based on the CIE scotopic luminance and photopic sensation luminance.

The small decrease in rod sensitivity for red backgrounds that was found by Sharpe et al. (1989) was not consistently evident in the data shown here (see Table 6). Sharpe et al. used mono-chromatic lights with a wider range of S/P ratios than the CRT used in this experiment can produce. Since their increase of the rod TVI-slope was relatively small, the spectral composition of the stimuli used here do not incorporate high enough S/P ratios to detect small differences in rod adaptation.

The influence of the S/P ratio of the stimulus field on the red-blue isoluminance ratio

In a direct experimental test of whether the S/P ratio of the field influences mesopic luminance, the scotopic luminance of the field was increased by changing its color, while the photopic luminance was held constant. With a constant cone response over all S/P ratios tested, the results should reflect the consequences of rod adaptation. With the same assumptions drawn in

the previous section, the independent weight for the rods will be inversely proportional to the rod threshold:

$$W_S / (1 - W_S) \sim S^{-k},$$

where W_S and S are the relative rod weight and the scotopic adaptation level, respectively. This relation makes it possible to estimate the TVI-slope k for the rod system at a constant photopic adaptation level. If only the scotopic luminance is changed to alter the S/P ratio, only the independent rod weights W'_S will change, but not the independent cone weight W'_P. As a consequence, a bluish reference with a high S/P ratio is expected to result in a decrease in rod sensitivity (at a constant photopic field luminance) and a consequently reduced relative weight for scotopic luminance differences. Likewise a low S/P ratio, producing a reddish reference field, will lead to an increased relative rod weight.

It has to be noted that for relative rod weights close to 1 the independent rod weight is large relative to the independent cone weight. Hence, a doubling of the independent rod weight due to a decreasing S/P ratio will only lead to a miniscule change in the photopic relative weight. The same is true for relative rod weights close to 0 and relative cone weights close to 1. This compression of the relative weights occurs if one of the independent weights is very large. Hence, a rather large change of the smaller independent weight will not change the relative weight in the same degree. Keeping that in mind, the TVI-exponent k can not be estimated from weights in close proximity to 0 or 1 as shown in Figure 36.

To test for the influence of various S/P ratios on the isoluminance ratio, minimum motion settings were done with reference fields with S/P ratios ranging from 0.7 to 3.4 for five adaptation levels between 0.007 cd/m² and 24 cd/m². Each of the settings was repeated 5 times. Figure 36 to Figure 38 show the course of the relative cone weights over a range of S/P ratios for the two tested observers.

An increase of relative cone weights (corresponding to a decrease of the relative rod weights) for increasing S/P ratios is evident for the two mesopic adaptation levels. The results are in agreement with the theory explained above. While the cone weight at mesopic adaptation levels raises with increasing S/P ratio, the weights at the photopic condition are close to 1 and do not change in the same manner due to the compression of the relative weights. Thus, the rod TVI-slopes were estimated for all mesopic conditions from the weights at the highest and lowest tested S/P ratio. Table 7 gives an overview of all values. Most of the TVI-exponents are with k = 1.00 … 1.75 greater than 1 and refer to a somewhat steeper slope of the TVI-curve than Weber's law suggests and than was found in the main results explained earlier. These high values of k for the experiment with a constant photopic luminance and a changed scotopic luminance are surprising since the TVI-slopes for rods estimated from the isoluminance ratios between 2.4 mcd/m² and 42 cd/m² were found to be mostly below 1 (see Table 6); agreeing well in this respect with earlier data. A process whereby cones suppress rod sensitivity, of the kind documented by Makous & Boothe (1974) and by Sharpe et al. (1989) could account for these higher exponents.
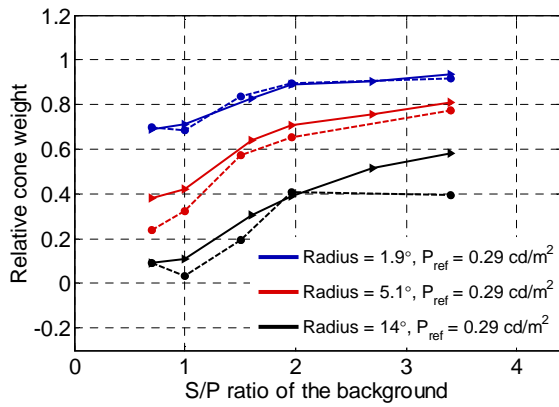
Figure 36: Relative cone weights as a function of S/P ratio of the background at a constant photopic luminance of at 0.29 cd/m². Solid lines are for observer 1 and dashed lines for observer 9.
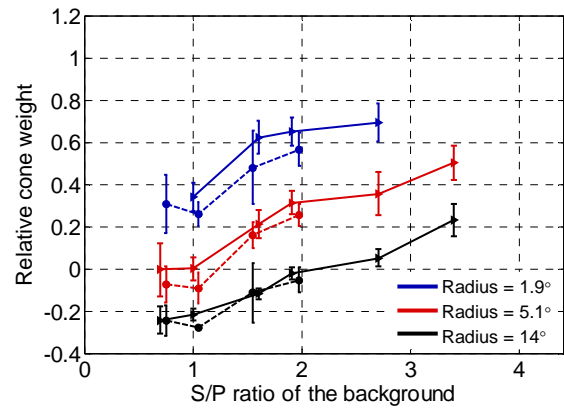
Figure 37: Relative cone weights as a function of S/P ratio of the background. Solid lines are for observer 1 who was tested at 0.027 cd/m² and dashed lines for observer 9 at a background luminance of 0.054 cd/m².
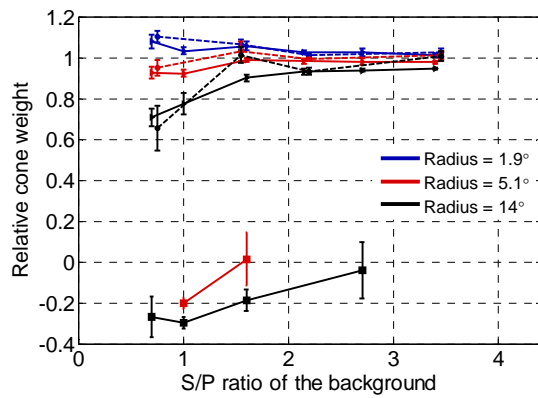
Figure 38: Relative cone weights vs. S/P ratio for the adaptation levels of 8 mcd/m² (2 lower curves) and 24 cd/m² (6 upper curves) for two observers. Solid lines are for observer 1, dashed lines for observer 9.

P_{adapt} [cd/m²]	Radius [°]	TVI-slope k
Obs 1		
0.027	2	1.48
0.027	5	1.75
0.29	2	1.16
0.29	5	1.22
0.29	14	1.68
Obs 9		
0.054	2	1.07
0.29	2	1.00
0.29	5	1.51
0.29	14	1.19

Table 7: The estimated TVI-exponent k for mesopic adaptation conditions.

Change of red-blue isoluminance ratio with spatial and temporal frequency

For all data shown above the temporal frequency of the grating was fixed at 2 Hz. This driftrate is low enough to allow the rods to participate in motion perception and to avoid noticeable phase disturbances between the rod and the cone signals (MacLeod, Stockman, 1987). These interferences that can lead to complete cancellation at 7.5 Hz occur due to the sluggishness of the rod system compared to the cone system (MacLeod, 1972).

With regard to temporal contrast sensitivity functions the rod and cone systems' curves show low pass or band pass characteristics depending on the adaptation level and spatial frequencies. In general, the peak sensitivity for several temporal frequencies shifts from 20 Hz to 5 Hz with dark adaptation (Kelly, 1961).

The influence of spatial and temporal frequencies on equiluminance matches between a white and a color grating were done earlier by Anstis and Cavanagh (1983). Their results showed that with increasing spatial frequency (0.6 to 5 cycles per degree (cpd)) the luminous efficiency, relative to a minimum flicker match with white, increases for red, stays about the same for green, and drops for blue. However, the temporal frequencies between 0.9 and 15 Hz don't seem to reveal a significant influence. These results could be reproduced by Cavanagh and

colleagues (Cavanagh, MacLeod, Anstis, 1987) with temporal frequencies between 0.5 Hz and 7.5 Hz and spatial frequencies between 0.5 and 12 cpd (cycles per degree). Their results show that for color pairs involving blue, 20-30% more blue was needed at increased spatial frequencies. The authors test and exclude the hypothesis that this is due to an influence of S cones on the minimum motion settings, and attribute the shift instead to the blue-absorbing macular pigment: since the foveal retina on which we depend for detection of the highest spatial frequencies is covered by macular pigment, motion nulls at high spatial frequencies show reduced blue sensitivity. Changing the temporal frequency between 0.5 and 7.5 Hz showed no or a minor influence when blue was present.

Temporal frequencies used in the present experiment are all in the range of maximum sensitivity to the rod and cone system. The results for a mesopic luminance level of 0.09 cd/m^2 show that temporal frequencies between 0.5 Hz and 5 Hz had little or no effect on minimum motion isoluminance ratios between blue and red (Figure 39). At 5 Hz the stimuli appeared to flicker which made the nulling of motion difficult and indicates that the mutual interactions between rods and cones interfere with vision at this temporal frequency.

The results agree with studies by Anstis & Cavanagh (1983) and by Cavanagh et al. (Cavanagh, MacLeod, Anstis, 1987, Cavanagh, Anstis, 1991) though their data were collected under photopic conditions. Both studies revealed only a little or no effect of temporal frequency. Cavanagh et al. found an effect only for the red–green grating. Here, 7-9% more green was required to match the red at 7.5 Hz compared to 0.5 Hz (Cavanagh, MacLeod, Anstis, 1987). The limited influence of temporal frequency on the rod weight is suprising given the evidence of more limited sensitivity of the rod system to high temporal frequencies (Kelly, 1961; Conner, 1982).
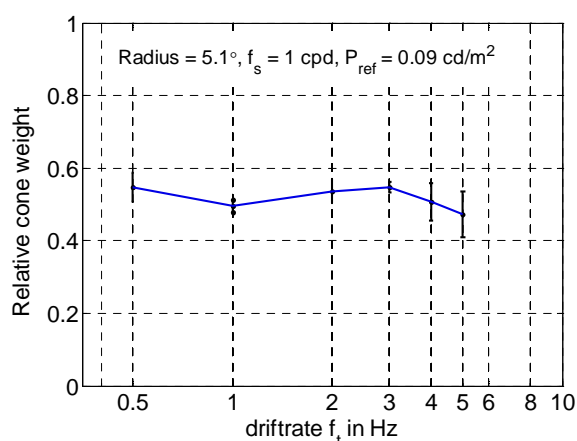
Figure 39: Relative cone weights for an adaptation luminance of 0.09 cd/m² as a function of temporal frequency. All data points are averages from 5 measurements from observer 1. The stimulus' spatial frequency was constant at 1 cpd.

The spatial frequency of the stimulus was varied between 0.5 cpd and 8 cpd. Spatial resolution of the cone system is known to be higher than that of the rod system when foveal cones are compared with extrafoveal rods, or when cone vision at high light levels is compared with rod vision at scotopic levels. But there is little evidence about the relation between rod and cone spatial resolution when conditions of stimulation and retinal location are comparable (though see D'Zmura & Lennie, 1986). Such a comparison may be made by considering the behavior of

the rod and cone weights in the present experiment as a function of spatial frequency. The results support the conclusion that rod and cone vision differ in spatial resolution when tested with similar stimuli. Figure 40 and Figure 41 show that for the mesopic adaptation conditions a distinct increase of the relative cone weights occurs at higher spatial frequencies. The relative increase of cone weights is similar for near foveal and peripheral stimuli. At 0.01 cd/m² a sharp increase of cone weight between 2 cpd and 4 cpd was found, showing that even under this very dim conditions the cones play a substantial role at high spatial frequencies. Spatial frequencies above 4 cpd could not be resolved at the mesopic luminance levels tested. At intermediate mesopic levels, a clear increase in cone weight appears as spatial frequency is increased. Although clearly present, the increase is modest in size, at amounting to at most a factor of two in the range 1 to 4 cpd. The differences in the spatial sensitivity curves for peripheral rod and foveal cones vision suggest a much greater difference in sensitivity between 1 and 4 cpd. Like the results of D'Zmura and Lennie (1986), this shows that rod and cone resolution are not profoundly different when measured under the same conditions (same luminance and eccentricity).
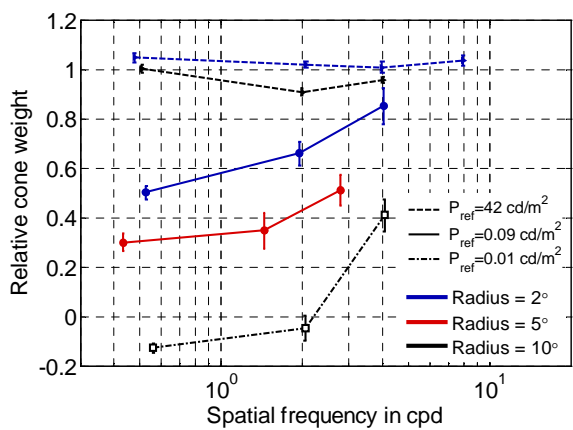
Figure 40: Relative cone weights as a function of spatial frequency. All data points are averages from 5 measurements from observer 9. The stimulus' driftrate was constant at 2 Hz.
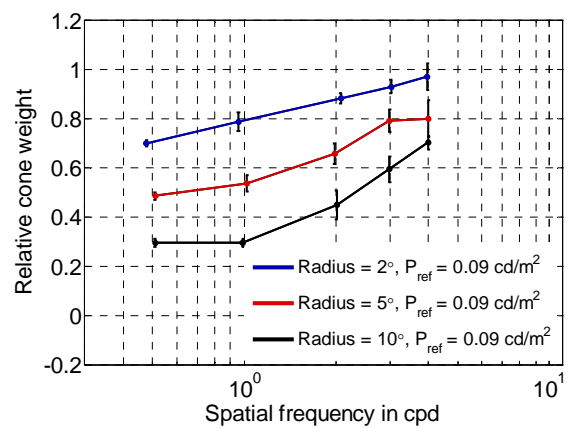
Figure 41: Relative cone weights for an adaptation luminance of 0.09 cd/m² as a function of spatial frequency. All data points are averages from 5 measurements from observer 1. The stimulus' driftrate was constant at 2 Hz.

At photopic adaptation levels the change of cone contribution with spatial frequency is smaller compared to lower light levels; the change at a photopic adaptation luminance is solely due to the L and M cone response (two upper curves in Figure 40).

4.5 Summary and Conclusions

The method of minimum motion as described here with low temporal and spatial frequencies is a suitable procedure to assess luminance at any adaptation level ranging from photopic to scotopic. Finding a motion null is a sharp criterion, for foveal stimuli as well as peripheral stimuli, which leads to a high reproducibility and low intra-individual standard deviations between several settings. Since the annulus stimulus is modulated upon the background in a way that the temporal and spatial average of luminance is equal to the background, the adaptation state is constant over time and space. Flicker photometry fails at mesopic conditions

because rod-cone and rod-rod phase lags arise at frequencies around 7.5 Hz and 15 Hz, respectively. However, minimum motion photometry can be done at frequencies between 0.5 Hz and 4 Hz, where such phase lags are not problematic.

The results of the minimum motion method show that near foveal vision ($\pm$ 1°) can be described with only the cone response at all intensities where settings are possible. From 2° off-axis to 18° off-axis the mesomesopic luminance, the luminance level of equal rod and cone contribution to luminance shifts from 0.02 cd/m^2 to 0.85 cd/m^2. Also at pure photopic and scotopic adaptation conditions an increased blue sensitivity was found with increasing eccentricity, which was ascribed to changes of macular pigment optical density. At photopic levels the isoluminance ratios agreed with the $V_{10}(\lambda)$ luminous efficiency function for eccentricities between 2° and 5°. For more peripheral and photopic stimuli sensitivity to blue increases beyond the sensitivity described by $V_{10}(\lambda)$. At scotopic level of 0.0024 cd/m^2 and also at 0.011 cd/m^2 the blue sensitivity was higher than expected on the basis of the CIE scotopic standard observer $V'(\lambda)$. For far peripheral stimuli scotopic isoluminance based on $V'(\lambda)$ was reached at 0.06 cd/m^2, decreasing to 0.008 cd/m^2 for stimuli with a radius of 5°.

Motion settings using differently colored adaptation fields with the same S/P ratio (ratio of scotopic to photopic luminance) show no differences in isoluminance ratio. This suggests that the individual scotopic and photopic sensitivity functions are sufficient to describe achromatic luminance at all light levels.

The decrease of the relative cone weights with decreasing adaptation luminance was modeled as a sigmoid function described by two parameters that were iteratively optimized. It was found that the estimated slopes of the rod TVI-curves agree well with earlier data from detection threshold experiments. The slopes varied between 0.68 and 0.78 and increased with eccentricity.

When comparing relative cone weights from mesopic adaptation backgrounds of the same photopic luminance but different scotopic luminance the greater S/P ratio is associated with a decreased effectiveness of rod stimulation. The relative decrease is equal for several eccentricities. Besides the influence of eccentricity and S/P ratio, also the spatial and temporal frequency of the stimulus was examined. Mesopic luminance determined by minimum motion is not influenced by temporal frequencies between 0.5 and 5 Hz at 0.09 cd/m^2. However, an increase of spatial frequency reveals an increased cone contribution for all tested eccentricities.

Chapter 5

Contrast thresholds of peripheral objects in the mesopic range

5.1   Introduction and Background

Detecting obstacles is crucial when driving under twilight conditions, therefore this chapter will be devoted to detection threshold contrasts of peripheral objects under dim light conditions. The primary basis for detecting an object is usually the luminance contrast between the object and its background, though differences in color may also contribute to detection as noted in Chapter 2. In addition, the ability to perceive and detect objects depends on numerous parameters that describe the environment, the object and the state of the eye. Most influential are the state of adaptation, as well as the size, duration and the position in the visual field of the object to be detected (Blackwell, 1946, Bouman, 1950). The state of adaptation itself depends on the luminance and the spectral properties of the surround and the objects.

The behavior of thresholds with dark adaptation is characterized by the Purkinje-shift, which manifests in the relative change of threshold contrasts to long and short wavelength stimuli. Also the effect of eccentricity (e. g. Kishto, 1970, Drum, 1980b, Drum, 1980a, Kuyk, 1982, Pearson & Swanson, 2000) largely depends on the state of adaptation and the spectral composition of the stimuli. Under mesopic and photopic conditions long wavelength stimuli exhibit a low detection threshold in the fovea which increases strongly the further peripheral the stimuli appears. In contrast, thresholds of short wavelength stimuli are high in the fovea, a consequence of a central foveal tritanopia; and opposed to thresholds of reddish stimuli, the thresholds to short wavelength stimuli decrease with eccentricity in the parafovea around 2-3° until they maintain a relatively constant level or increase slightly for high adaptation conditions. Under scotopic conditions thresholds for spectrally different stimuli diverge still more with eccentricity. Rod thresholds of the fovea centralis are high and decrease beyond the central rod-free area. While thresholds to bluish stimuli fall off toward the periphery owing to the high rod density, reddish stimuli lead to an increase in threshold with eccentricity due to the low sensitivity of the rods to long wavelength (Kishto, 1970).

In contrast to the previously described criteria of minimal distinctness of borders and minimum motion in chapter 3 and chapter 4, the detection of objects at threshold is determined by the luminance system as the sum of the L and M cone and the red-green opponent system that responds to the difference between the L and M cones signals (King-Smith & Carden, 1976, Thornton & Pugh, 1983, Chaparro, Stromeyer, Kronauer, Eskew, 1994). The contribution of color to contrast perception is also evident down to low mesopic light levels (Walkey et al., 2005); and especially the contribution of the red-green channel decreases sharply with

eccentricity (Mullen & Kingdom, 2002). In comparison to the luminance channel the red-green opponent channel was shown to be more sensitive in detection (Chaparro et al., 1993).

This chapter presents three methods to measure contrast thresholds contours in S-P contrast space that are applicable in any adaptation condition. The described contrast experiments aim at the understanding of how rod and cone contributions change with dark adaptation and eccentricity and to which extent rods and cones cooperate to detect an obstacle. Further on, several approaches on mesopic photometry mostly based on brightness matches were applied to the threshold data, to test whether these approaches can describe mesopic contrast perception.

5.2 Detection thresholds for flashed stimuli

5.2.1 Experimental Design

A LCD projector was used to present a uniform gray background, as well as the stimuli and a tracking task. The background was projected on a screen in 3.20 m distance of the observer. Figure 42 shows a sketch of the test setup. The uniformity of the background was ensured by an inverse luminance mask of the luminance the projector produces on the screen. The adaptation luminance of the background P_{ad} was set to four fixed adaptation levels between 0.012 cd/m² and 7.4 cd/m². Table 8 gives an overview over the S/P ratios and chromaticity coordinates of the backgrounds. For the photometric measurements a LMT Luminance camera L1009, a LMK color 98-3 from TechnoTeam, and an OPTRONIC OL770 spectroradiometer was used. All given photopic luminance values are based on the 2° CIE spectral luminous efficiency function. The stimuli were circular targets of 0.7° diameter presented in four colors (green, blue, red, and gray). The discs which were incremented on the background appeared on a horizontal line at θ = 2°, 6°, 10°, and 14° to the right and in the center of fixation at θ = 0°. Because the targets were superimposed on the background, the low contrast stimuli were desaturated. Each stimulus was shown twice in each of the six different contrast steps.

Background luminance P_{adapt}	average S/P ratio	CIE x-y coordinates
0.012 cd/m²	2.90	0.31 , 0.21
0.077 cd/m²	2.84	0.27 , 0.28
0.73 cd/m²	2.78	0.27 , 0.30
7.4 cd/m²	2.70	0.27 , 0.30

Table 8: Luminance, S/P ratio and CIE x-y coordinates of the backgrounds

To avoid falsified results due to the expectations of the subject for horizontal stimuli, on roughly 10% of trials stimuli were also shown at alternative positions in the periphery. The stimuli were presented for 500 ms each in randomized order over trials. The time in between two subsequent stimuli was randomly chosen between 1 and 5 s. If the object was seen the test person was supposed to push a button. For each stimulus it was recorded whether the stimulus was seen or not. To ensure fixation to a defined spot on the background, a tracking task was presented, which consisted of a thin red ring of 0.9° in diameter and a small red ball within the

circle. The ball moved spontaneous in a random way, but could be controlled with a joystick. The observer's task was to keep the ball with the joy-stick in the middle of the red circle. 40 subjects between 18 to 36 years with normal color vision (Ishihara Test) and a visual acuity of at least 1.0 (Snellen: 20/20) took part in this study. After an adaptation time of 10 min each person started with a training session of 15 minutes to get familiar with the joystick and the test design. All of the subjects were tested at two adaptation levels, which lead to 20 datasets for each condition. A questionnaire was used to assess the level of difficulty to accomplish the tracking task and the previous experience in using a joystick on a 5-point scale. Table 9 summarizes all dependent and independent variables for the detection threshold experiment. Here, in contrast to the experiments described in the two previous chapters, the 2° CIE luminous efficiency function was used as basis for photopic luminance.

Dependent variables	
Incremental threshold	$\Delta P_{th} = P_s - P_{adapt}$
Independent variables	
Background luminance (adaptation lum.) P_{adapt}	0.012 / 0.077 / 0.73 / 7.4 cd/m^2
Stimuli eccentricities θ	0° / 2° / 6° / 10° / 14°
Color of the stimuli	blue, green, red, grey
5×4×4=80	80 stimuli-background situations
6 contrast levels	480 stimuli-background-contrast situations
Parameters	
Subjects	2×20 totally (20 for each P_{adapt})
Age range	18 – 36 years
Visus	1.0 normal color vision
Gender	m / f
Stimulus size	0.7°
# of repetition of stimuli	2
Duration of the stimuli	0.5 s
Tracking task	keep the ball in the circle push a button if stimuli seen

Table 9: Variables and parameters for the detection contrast experiment
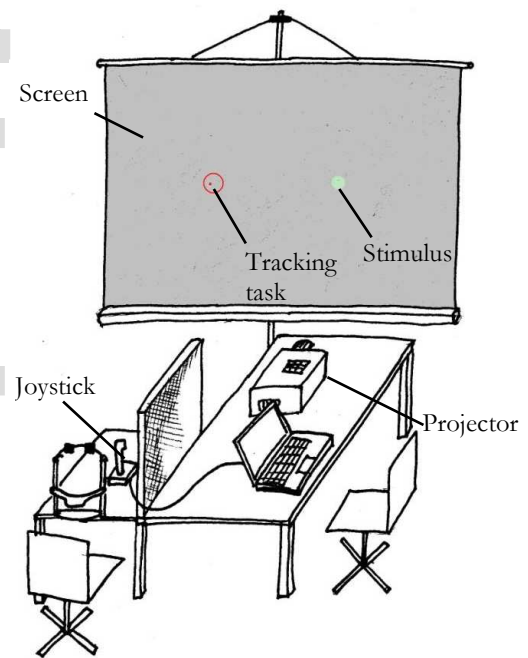
Figure 42: Sketch of the test setup

5.2.2 Results and Discussion

The average threshold contrast per run was determined by averaging the contrasts of the stimulus with the highest contrast that was not seen anymore and the stimulus with the lowest contrast that was still seen. The detection threshold contrasts of the two runs for each condition were averaged for every observer and from that the luminance threshold increments ΔP_{th} were calculated. Figure 43 and Figure 44 show the photopic incremental contrast thresholds of all adaptation conditions as a function of stimulus eccentricity for the four stimuli colors. The curves are slightly horizontally offset to differentiate between the error-bars which represent ±1 standard deviation. The absolute shift in incremental threshold shows the decreased absolute sensitivity towards higher adaptation levels. The photopic threshold differences at the two higher adaptation luminances (7.4 cd/m^2 and 0.73 cd/m^2, the dashed curves in Figure 43 and Figure 44) show a steady increase of thresholds with eccentricity for the red, green and gray stimuli, whereas the incremental threshold for the blue disc remains constant at a somewhat lower level. For the two lowest adaptation levels the Purkinje shift is

more evident. As expected, due to the increased short wavelength sensitivity, the threshold for blue objects remains nearly constant or decreases at low luminance levels over all tested peripheral positions, whereas the threshold difference of red objects increases with eccentricity. The change of sensitivity for the red stimuli relative to the blue target increases with decreasing background luminance. The behavior of the green and gray stimuli thresholds is similar for increasing eccentricities at all adaptation conditions, which is consistent with the findings of Kishto (1970). A small dip around 10° for the blue, green and gray stimuli at 0.077 cd/m² is evident in the data, which was also found by Kishto, though only at scotopic levels for one of his two observers.

The graphs reveal a clear increase in thresholds with foveal presentation at each adaptation level. This effect is unexpected, since given that the fovea is the most sensitive area of the retina under photopic conditions, a lower threshold would be expected at photopic levels. Under dark adaptation a raise in foveal threshold can be explained by the lack of rods in the central most part of the fovea and the decreased response of cones. However, the effect seems to be consistent over all conditions, therefore another likely explanation is that the tracking task disturbed the detection of the discs in the fovea. The results from a prior control experiment to verify the range of contrasts for each condition confirm this assumption. This experiment was done with two observers at eccentricities ranging from 0° to 14° in 1°-increments and without a tracking task at otherwise identical conditions. The results show an increased threshold close to the fovea only for the blue target, whereas the thresholds for the green, blue and gray target do not increase near the fovea.
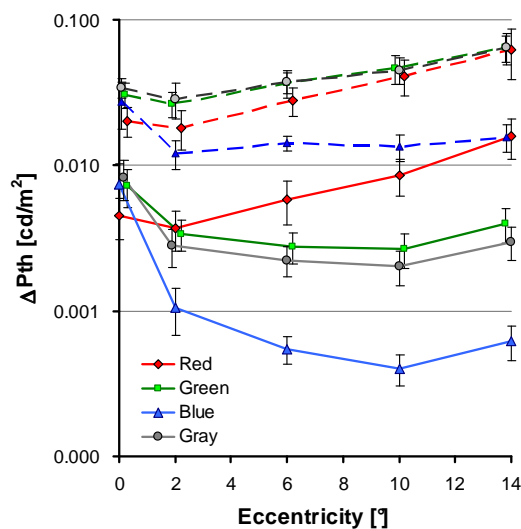
Figure 43: Luminance threshold increments on a log scale for adaptation levels of 0.012 cd/m² (lower four solid curves) and 0.73 cd/m² (upper dashed curves)
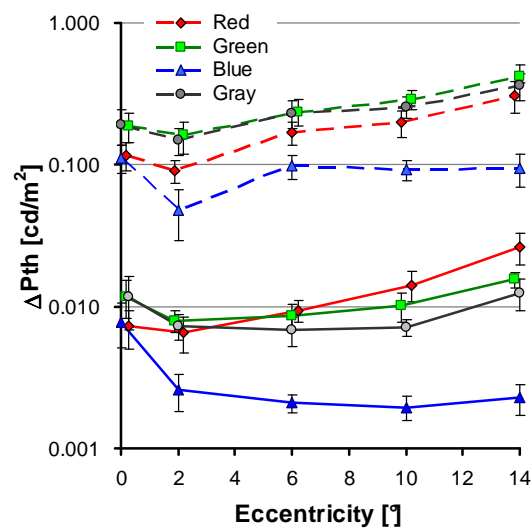
Figure 44: Luminance threshold increments on a log scale for adaptation levels of 0.077 cd/m² (lower four solid curves) and 7.4 cd/m² (upper dashed curves)

An analysis of variance (ANOVA) revealed no differences between observers between 16-25 years and 26-32, gender and the rated subjective difficulty of the task. Also the comparison of the results between frequent users of joysticks and novices show no differences in thresholds. This rejects the speculation that the tracking task might have stressed subjects with little experience using a joystick.

The experimental design chosen for this study might raise the objection that sensitivity is different in the upper and lower and nasal and temporal visual field, with lower thresholds found in the nasal and upper retina than the temporal and lower retina (Kishto, 1970). However, the differences found are minor and would probably not be detectable by averaging between datasets from 20 observers. The effect has been found significant and pronounced only in the far periphery beyond 30° off-axis (e. g. Grigsby & Tsou, 1994).
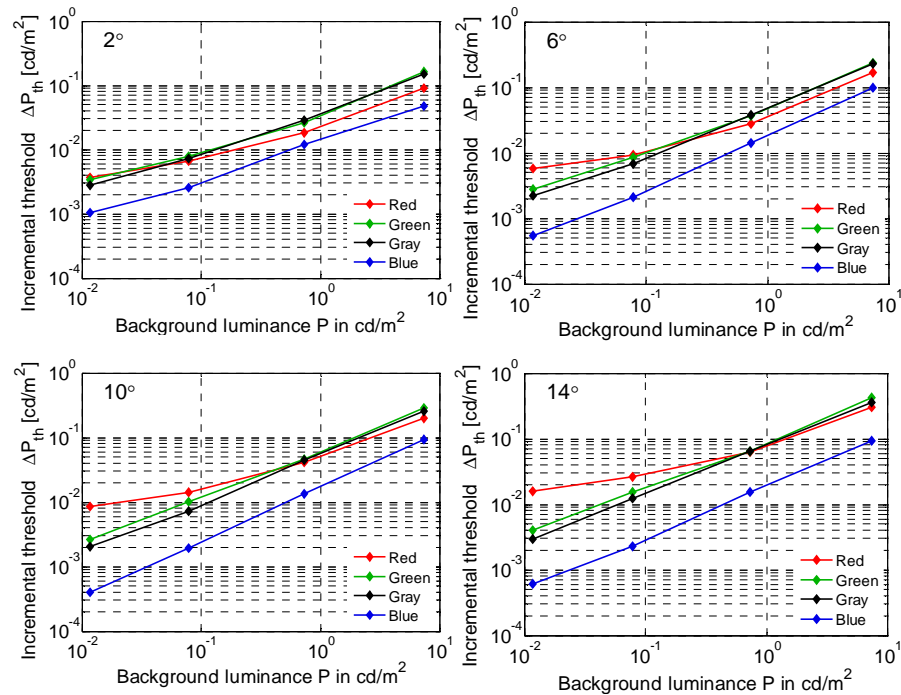
Figure 45: Luminance threshold increments as a function of background luminance for stimuli positions from 2° to 14°.

The graphs in Figure 45 show the TVI-curves of the results, this is threshold luminance difference of the four colored stimuli as a function of adaptation luminance for several eccentricities. Over a large range the log threshold increases linearly with the log of the background illumination, implying a power law relation. The foveal data are not shown here due to a possible interference with the tracking task and the resulting uncertainties. The slope for all eccentricities and colors were calculated by minimizing the mean squared error and plotted against the eccentricity, as shown in Figure 46. Because the threshold for the red stimuli seems to deviate from the power law at the lower luminances, the TVI-slope k of the red stimuli was calculated without the threshold value at the lowest adaptation level for 10° and 14° and without the threshold values at the lowest two adaptation levels for 6° and 2°. The Weber's law holds when the slope k in a log-log plot (the exponent of the power law) is 1. With k values between 0.57 and 0.85 here, the range of the estimated slopes agrees with data found by Barlow (1957) and Sharpe et al. (1993). However, the differences of the slopes between the four colors in the periphery raise some questions. The TVI-slope is consistently lower for the detection of red objects, indicating a slow increase of threshold increment for increasing adaptation levels, whereas the slope for the detection of the blue object is highest. The increase of sensitivity to short wavelength stimuli for decreasing adaptation luminance happens earlier than the sensitivity change for long wavelength objects. These differences in slope reflect the Purkinje-effect,

which can also explain the rise and the separation of different k values between 2° and the more peripheral positions. Due to the sensitivity shift the threshold for short wavelength stimuli reaches absolute threshold at a higher luminance than the threshold curve for long wavelength stimuli, resulting in a steeper decrease of the TVI-curve for bluish stimuli. Near the fovea the Purkinje-effect is less evident. The TVI-slopes represent to a high degree cone vision, therefore the k values which are based on the photopic luminous efficiency function are equal.
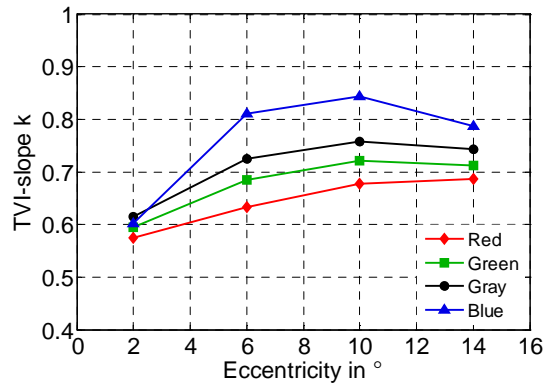
Figure 46: Change of TVI slope k with eccentricity for all four colors

Figure 47 and Figure 48 show the threshold data in S-P contrast space for the lowest and highest adaptation luminance. Each curve can be regarded as an iso-contrast-contour and is made up of four data points from one tested eccentricity. The almost vertical alignment of the foveal thresholds shows the limited dependence on rod vision also under dimmest light levels. At the lowest adaptation luminance the threshold lines decrease in slope to an almost horizontal orientation, reflecting an increase in rod influence with eccentricity. These trends agree with the results found in the two previous chapters.

Similar curves were measured with direct brightness matches under various adaptation levels (Palmer, 1966) and under photopic conditions with the detection of flashes (Chaparro et al., 1994) and with motion detection (Stromeyer et al., 1995). Such a detection contour forms an ellipse in cone contrast or S-P contrast space, if positive and negative threshold contrasts in both axes dimensions were measured. The orientation of the ellipse is the direction of lowest sensitivity and mirrors the contribution of rods and cones when drawn in S-P contrast space, whereas the elongation (the length) and the size of the contour reflect the sensitivity (see also chapter 2). Since the thresholds that were presented are limited to stimuli of four colors shown with positive contrast, all data points assemble in the first quadrant of S-P contrast space. This limited database does not allow fitting a threshold ellipse; however with reservations due to the test design one can estimate the relative rod and cone contribution and a parameter indicating to which extent rod and cone signals sum up.
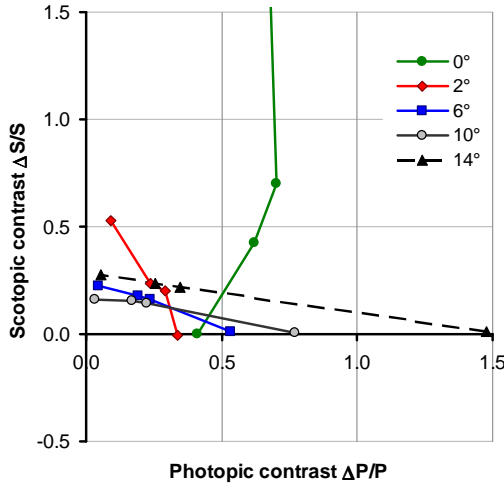
Figure 47: Photopic contrast threshold versus scotopic contrast threshold for adaptation levels of 0.012 cd/m².
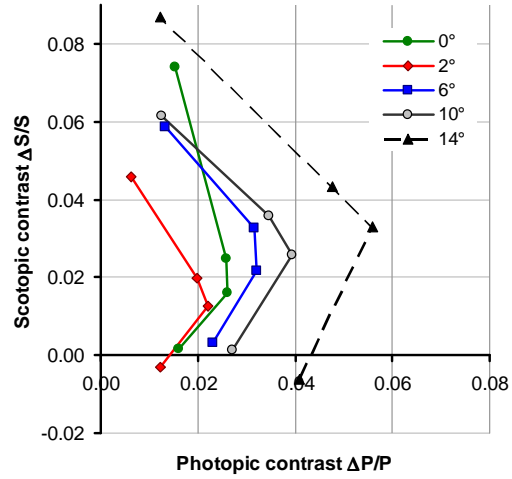
Figure 48: Photopic contrast threshold versus scotopic contrast threshold for adaptation levels of 7.4 cd/m².

Modeling

The results are described by a model in which the relative weights of the photopic and scotopic incremental thresholds as well as a parameter n vary with luminance. The additional parameter n accounts for the degree of cooperation between rods and cones at threshold. In this implicit mechanistic model suitably weighted signals from the photopic and scotopic system have to sum to a constant value at threshold and each signal varies as the n-th power of the relevant stimulus signal. The independent rod and cone weights W'_P and W'_S, respectively and the parameter n were optimized to fit Equation 19.

$$1 = (\Delta S \cdot W'_S)^n + (\Delta P \cdot W'_P)^n$$

Equation 19

Here, ΔP and ΔS are the photopic and scotopic thresholds for detection, respectively, whereas W'_P and W'_S are the optimal independent cone and rod weights. Consequently, $(W'_P \cdot \Delta P)^n$ can be regarded as the fraction of the total threshold signal contributed by the photopic system and similarly $(W'_S \cdot \Delta S)^n$ is the fraction contributed by the scotopic system. The exponent n gives an indication to which extent rods and cones cooperate with each other (see Figure 3 in chapter 2). For n=1 the rod and cone signals cooperate fully and the linear sum of rod and cone signals has to meet a threshold value to perceive a stimulus. For n=2 rod and cone signals would add up quadratic as Helmholtz suggested for cone signals (Helmholtz, 1896). The larger the exponent n the more independent do rods and cones contribute to perception. For very large n values the rod and cone response separately have to exceed a certain threshold to perceive a target. In this case there is no cooperation between the receptors.

The fitting criterion is the root mean square between the predicted thresholds and the measured thresholds:

$$RMSE = \sqrt{1/4 \sum^{4} \left[1/n \cdot \log_{10}((W'_P \cdot P)^n + (W'_S \cdot S)^n) \right]^2}$$

Equation 20

Here the root mean square is taken over the sum of four values, one for each of the four colored stimuli used. The best fitting independent weights were scaled such that the sum of W'_P and W'_S is 1 resulting in the relative weights W_P and W_S. With the assumption that the influence of the tracking task on foveal thresholds was equal for all stimuli, the foveal data are included in

the calculation of receptor weights. The iteratively optimized weights W_P and the corresponding exponents n are shown in Table 10. For the dimmest conditions the estimated exponents are close to unity. For background levels of 7.4 cd/m² and 0.73 cd/m² the exponent was fixed to 1. When vision is dominated by either the rods or the cones n becomes difficult to determine.

P_{adapt}	0.012 cd/m²		0.077 cd/m²		0.73 cd/m²		7.4 cd/m²	
Eccentricity	n	W_P	n	W_P	n	W_P	n	W_P
0°	1.7	1	13	0.93	[1]	1	[1]	0.97
2°	1.4	0.84	>20	0.86	[1]	0.95	[1]	0.94
6°	1.3	0.57	2.2	0.75	[1]	0.91	[1]	0.92
10°	1.6	0.40	1.7	0.65	[1]	0.86	[1]	0.90
14°	1.0	0.38	1.7	0.60	[1]	0.86	[1]	0.88

Table 10: Relative cone weights W_P and exponents n for four different luminance levels. For the two highest adaptation luminances only the weights were optimized; the exponent n was fixed to 1 assuming linear summation of rod and cone signals.

The course of the relative cone weights with increasing eccentricity is shown in Figure 49. In the fovea and 2° off-axis detection is dominated by the cone system even at mesopic adaptation conditions. For peripheral detection the rod influence increases with decreasing adaptation levels but never reaches a pure scotopic state. Comparing the threshold experiment with the minimum motion experiment discussed in chapter 4 reveals that the relative cone weights from the detection experiment are higher and decrease less with decreasing adaptation level. The 'mesomesopic luminance' defined here as the adaptation level at which rods and cones contribute equally to perception, in this case detection threshold, is at 0.024 cd/m² and 0.033 cd/m² by a factor of 10 lower than the analogous mesomesopic luminances of minimum motion. A possible reason for the higher cone influence can be the contribution of the chromatic information to the detection of objects. The red-green and blue-yellow opponent signals might allow the cone system to detect objects at dimmer light levels than would be possible if only luminance information is present.
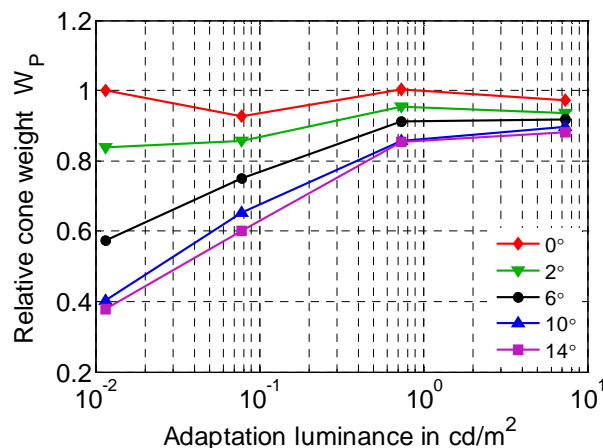
Figure 49: Relative cone weights for all stimulus eccentricities according to the nonlinear summation of rod and cone signals.

Comparison with other detection and brightness based mesopic models

The discrepancies between detection thresholds of red and blue targets in the mesopic range reflect the sensitivity shift towards shorter wavelengths due to rod activation. In practical photometry when a photometer head with $V_2(\lambda)$ sensitivity is used the measurements do not account for the sensitivity change due to dark adaptation. This leads to an underestimation of short wavelengths and an overestimation of long wavelengths with respect to luminance and detection thresholds. However, since $V_2(\lambda)$ is based on luminance only, one can not expect it to explain detection threshold data even under photopic conditions. The color-opponent signals and under dimmer light levels the rod signals play an important role in the detection of obstacles, which are both not accounted for by photopic luminance.

Some approaches have been undertaken to describe the Purkinje shift with the goal to generate a photometric system that is suitable for all adaptation conditions. Most of these approaches are based on brightness matches between the two halves of a bipartite field subtending to the periphery (Palmer 1966, Palmer, 1968, Kokoschka 1977, 1980, Sagawa & Takeichi, 1986, Nakano, Ikeda, 1986, Trezona, 1991). Two approaches use performance based measures like reaction times (Rea et al. 2004) and detection and recognition thresholds (Goodman et al., 2007) to describe a mesopic equivalent to luminance. These models take photopic and scotopic luminance and partly the chromaticity coordinates as input parameters to calculate an equivalent, or 'mesopic' luminance. The basis for the comparison of different mesopic approaches are the presented detection thresholds and the assumption that equal visibility should result from equal differences in the 'mesopic luminance' values delivered by the model. Ideally the thresholds for all stimulus colors should be the same when expressed as differences in mesopic luminance as defined by the model. When the incremental thresholds for different colors are expressed in mesopic units, the variation among these values is a measure of the model's error in predicting the detectability of differently colored objects under dim adaptation conditions.
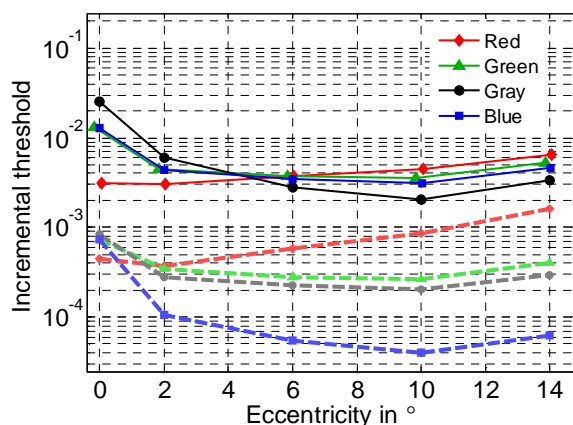
Figure 50: Photopic incremental thresholds based on $V_2(\lambda)$ (dashed curves) and mesopic incremental threshold by Kokoschka (1980) (solid curves) for 0.012 cd/m² as a function of stimulus eccentricity. The photopic curves are shifted down one log unit. Note that the y-axis shows photopic luminance units for the dashed lines but mesopic units based on Kokoschka for the solid lines.

Figure 50 shows the photopic incremental thresholds as measured in the described experiment as dashed lines for the adaptation level of 0.012 cd/m². The data are based on the photopic luminous efficiency function $V_2(\lambda)$ and are identical to those shown in Figure 43. The solid

curves represent the same dataset but here photopic thresholds units were converted to mesopic incremental thresholds units according to Kokoschka's model (Kokoschka, 1980). The graphs show clearly that for peripheral detection the mesopic incremental threshold curves for the four colored stimuli depart less from each other than the thresholds based on $V_2(\lambda)$. Thus, the mesopic units from the Kokoschka model are able to give a better representation of the equal level of visibility than the thresholds based on $V_2(\lambda)$.

The root mean square difference of the log threshold increments $RMSE_{Log\Delta M}$ was used as a measure of the degree to which the model can describe visual detection in the mesopic adaptation range:

$$RMSE_{Log\Delta M} = \sqrt{\frac{1}{N}\sum_{i}^{N}(\log\Delta\hat{M} - \log\Delta M_i)^2}$$ Equation 21

Here, ΔM_i is the mesopic incremental threshold for the i_{th} of the four colors calculated as the difference between the mesopic luminance of the background and the mesopic luminance of the stimulus at threshold. The average of the mesopic incremental thresholds for the four colors under one condition is $\Delta\hat{M}$. Small values of RMSE indicate that the mesopic threshold increments for the four colored stimuli are close to each other; hence the model correctly describes the shift of sensitivity under dim adaptation levels that leads to a lower threshold for blue targets compared with red targets. Figure 51 and Figure 52 show the root mean squared errors for the two lowest adaptation levels for various mesopic models. For comparison, the black bar represents the root mean squared error of the prediction thresholds based on the photopic luminous efficiency function $V_2(\lambda)$.
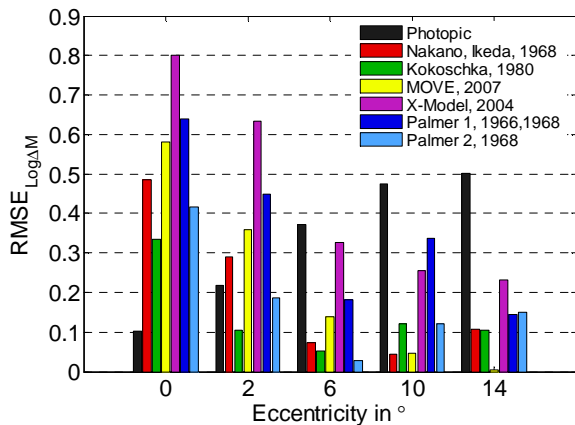
Figure 51: Root mean square error of prediction of the log mesopic thresholds for various mesopic models for the adaptation level of 0.012 cd/m².
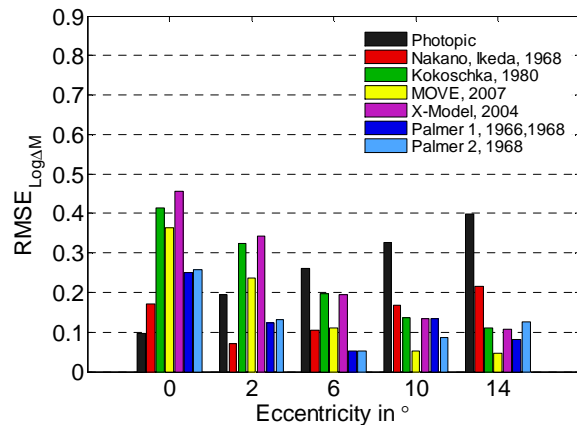
Figure 52: Root mean square error of prediction of the log mesopic thresholds for various mesopic models for the adaptation level of 0.077 cd/m².

The lower RMSE values for the mesopic models compared to the photopic model indicate that the mesopic threshold contrasts of all models have a better correlation to detection of peripheral objects than photopic luminance. But for foveal and near foveal objects the photopic luminance is the more suitable measurement criterion. The general trend shows that, not surprisingly, the further apart from the fovea a stimulus appears the larger are the failures of photopic luminance to describe thresholds. For peripheral detection the $RMSE_{Log\Delta M}$ values of all the implemented mesopic approaches are below the photopic $RMSE_{Log\Delta P}$. Though the

mesopic models are mostly based on peripheral detection or brightness matches with larger bisected fields, only luminance - and not the eccentricity - is a parameter of the models. Most of the models are optimized for peripheral vision 10° off-axis, which is reflected in the low $RMSE_{Log\Delta M}$ values around this eccentricity. At an adaptation luminance of 0.73 cd/m^2 the trend is similar to those shown at the lower adaptation levels, though the differences among the mesopic $RMSE_{Log\Delta M}$ and the photopic $RMSE_{Log\Delta P}$ are smaller. The highest adaptation luminance of 7.4 cd/m^2 is considered by most of the mesopic approaches as photopic. Hence, the $RMSE_{Log\Delta M}$ is close to or identical with the photopic $RMSE_{Log\Delta P}$, only Palmers enhanced model and the MOVE approach show consistently lower $RMSE_{Log\Delta M}$ values for peripheral thresholds under this level. Furthermore, the largest differences between the several models are found in the mid to low mesopic adaptation range. This is consistent with the results reported by Rea et al. (2004).

A limitation of the validity of this comparison might be that most models are based on brightness matches and not detection thresholds. The question arises how mechanisms for detection and brightness perception compare to each other and whether detection can be regarded as a special case of brightness perception when the standard itself is at threshold, as was suggested by Guth, Donley, and Marrocco (1969). However, experimental evidence contradicts this notion; Drum (1980b) found a different behavior for threshold luminance and luminance required for constant brightness for light and dark adapted receptors with eccentricity. The discrepancies between thresholds and brightness perception seem to decrease towards the far periphery.

Despite of the different nature of the two tasks the mesopic models of photometry can explain the peripheral detection of colored stimuli quite well. The decreased $RMSE_{Log\Delta M}$ values compared to $RMSE_{Log\Delta P}$ show that the correlation is good between most of the proposed mesopic luminance models and peripheral detection. On average the highest $RMSE_{Log\Delta M}$ values are found for the X-Model which is based on reaction times. This failure can be explained by the differences between a reaction time task and a detection task. The opponent color channels are said to be too slow to contribute to reaction times (Guth, 1964) whereas the possible influence of the opponent channels on detection is clear. However, some evidence exist that there is only a minor contribution of the opponent channels to reaction time measurements (Walkey, Harlow, Barbur, 2006; Walkey et al., 2007). The differences between the mechanisms of these two methods seem to be more pronounced than the differences between brightness matches and detection thresholds.

Most of the models are based on the 10° V(λ) function (Rea et al., 2004) and the 10° CIE tristimulus values (Kokoschka, 1980) or on photopic and scotopic luminous efficiency curves based on brightness matches (Ikeda, Nakano, 1986). The luminance values of the detection experiment were measured with the LMK color, a luminance camera from TechnoTeam which has the 2° CIE Color matching functions (CIE, 1931) implemented. Therefore all the calculations are based on the 2° tristimulus values $X_{2°}$, $Y_{2°}$, $Z_{2°}$, which leads to an underestimation of the photopic luminance of short wavelengths, both outside of the fovea where the foveal macular pigment is less dense and also at the fovea where the CIE color matching functions are slightly in error (Stockman, MacLeod and Johnson, 1993). Consequently, the 10° luminance of the background gray is 7.5% higher than the 2° luminance indicated by $V_2(\lambda)$.

5.3 Threshold contrast contours for detection and motion discrimination

Contrast threshold contours for the detection of a counterphasing grating and for the identification of motion direction with drifting grating stimuli have been measured under photopic conditions (Stromeyer et al., 1995). Here, a similar approach was used to determine contrast threshold contours under mesopic conditions in the periphery.

5.3.1 Experimental Design

In the disc detection experiment described in section 5.2 only stimuli of positive contrasts were used. Hence, in S-P contrast space only the first quadrant was addressed. In the second quadrant, something new happens: the scotopic and photopic systems are stimulated with changes of opposite sign, so their luminance contributions may cancel. To measure a contrast contour in the two upper quadrants of S-P contrast space two other detection experiments were carried out with a modified version of the minimum motion stimuli described in Chapter 4. If not noted differently the annulus had a diameter of 10° calculated as the average between the outer and inner diameter and was centrally fixated. The width of the stimulus was set to be 30% of the radius. In contrast to the minimum motion task previously described, here, the ratio of the blue and red phosphors that generate the color grating was fixed, but the absolute modulation amplitude of the color gratings was changed by the observer. Two criteria were used for adjustment: the just noticeable appearance of the annulus, (detection threshold) and the clear identification of the rotation direction (motion discrimination threshold).

The fixed ratio between the red and blue phosphor determines the direction of modulation in the S-P contrast plane. By choosing a set of constant red-blue ratios and adjusting only the amplitude of modulation, the adjustment trajectories are radii from the origin of the S-P contrast plane (from the reference) to the outside at a set of corresponding orientations. The thresholds were determined for 9 different red-blue ratios (S/P ratios) that resulted in angles in S-P contrast space between 0° and 178°. The modulation of the luminance grating (luminance lure) referred to in chapter 4 was here set to zero for the detection task, so that the stimulus became a simple counterphasing red/blue grating. For the motion discrimination task a lure was introduced but was kept at the lowest possible value (3-5%) that could generate an impression of motion at the low adaptation levels (for more details see chapter 4.2). At high adaptation levels even without a color grating (modulation amplitude of the color grating = 0) the luminance lure was visible and made it more difficult to detect the motion direction of the stimuli. Without the luminance component the stimulus consists of superimposed blue and red counterphasing sinusoids that are 180° out of phase in time and space. This stimulus seems to flicker, rather than move, as the red and blue bars switch places.

Threshold contours were measured for several adaptation levels between 0.013 and 42 cd/m^2 with a constant temporal frequency of 2 Hz and spatial frequency of 1 cpd. In addition the temporal and spatial frequencies were varied between 1 and 4 Hz and between 0.5 and 4 cpd (cycles per degree), respectively, at a constant adaptation luminance of 0.09 cd/m^2. Two observers took part in this experiment: one observer with normal color vision (Observer 1) and one deuteranomalous trichromat (Observer 10).

All luminance values shown in the Results section are based on the 10° luminous efficiency function.

5.3.2   Results and Discussion

Figure 53 and Figure 54 show the threshold contours in S-P contrast space for several adaptation luminances for the detection and motion discrimination criterion, respectively. The data points are averages of 5 settings from observer 1. The contour lines outside of the graphs are adjustments where no clear rotation direction was visible at the highest possible modulation of the color gratings. As described above and in chapter 2, the threshold contours form ellipses that are defined by their elongation (dimensions) and orientation (direction of lowest sensitivity) in contrast space. The dimmer the adaptation level, the more oriented are the contours towards the abscissa, reflecting an increased rod influence. Comparing the contours for the two criteria shows that the detection ellipses are consistently wider than the motion discrimination ellipses; more contrast is needed to detect the motion direction than to just detect the stimulus (see also Figure 55).

Figure 53 shows that for observer 1 the orientation of the photopic ellipse is slightly positive indicating a higher red sensitivity than $V_{10}(\lambda)$ would suggest. For this observer the trend was also found in the photopic MDB data ($W_P=1.09$ for a 6° off-axis border, chapter 3). Interestingly the positive orientation of the threshold contour is not evident in the motion discrimination data at 42 cd/m^2 (Figure 54); it was also not evident in the minimum motion results of that observer ($W_P = 0.95$ at 5.1° off-axis, chapter 4). Do the methods tap different channels of the visual system after all? This question will be addressed below.
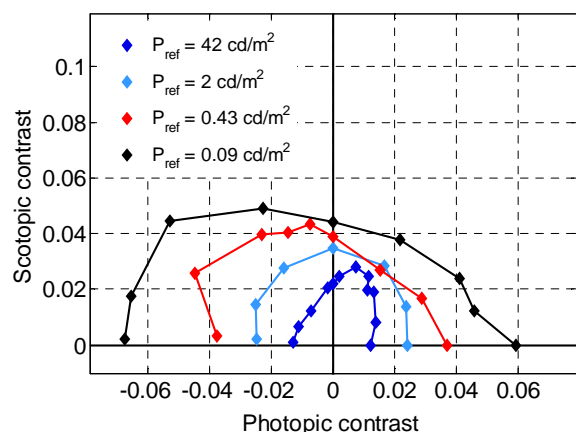
Figure 53: Detection threshold contours for observer 1 at several adaptation levels (2 Hz, 1 cpd).
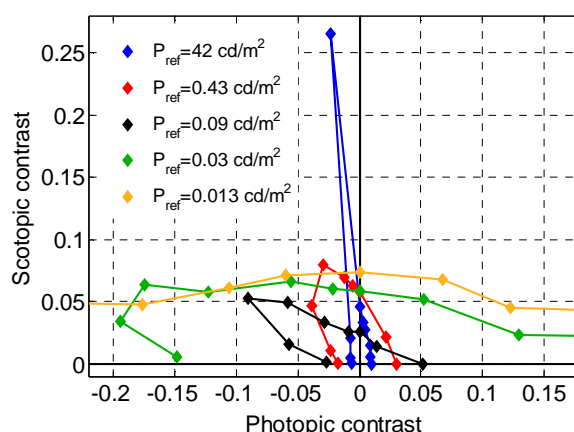
Figure 54: Motion direction threshold contours for observer 1 at various adaptation levels (2Hz, 1cpd), the luminance lure was 5%, only for 42 cd/m² a lure of 3% was used.

The receptor weights were estimated by modeling the contours as ellipses in contrast space. The fitting was optimized by minimizing the mean square of the $\log_{10}$ differences between the prediction of contrast thresholds and the measured contrast thresholds at different directions in S-P contrast plane. One can assume as a working hypothesis that the long axis of the ellipse is the direction of mesopic isoluminance, where the luminance modulation in nulled. From the

orientation of the long axis of the ellipse, the relative weighting of rod and cone stimulation S and P for mesopic luminance can be calculated so that the weighted sum of the scotopic and photopic luminances is constant:

$$1 = S \cdot W_S' + P \cdot W_P' \qquad\qquad \text{Equation 22}$$

Here S and P is a pair of scotopic and photopic luminance values that is on the axes of least sensitivity. W_P' and W_S' denote the independent weights for the photopic and scotopic luminance, respectively. The weights were normalized such that the sum of W_P' and W_S' is 1 resulting in the relative weights W_P and W_S. Figure 56 compares the relative cone weights as a function of the adaptation luminance for the detection task, the motion discrimination and minimum motion criteria for the same observer and eccentricity. All three criteria agree well under mesopic adaptation conditions (0.09 cd/m²). For photopic adaptation luminances the cone weights for the detection task are distinctly higher compared to weights from motion discrimination. This might be due to the fact that the detectability of chromatic contrast increases relative to luminance contrast at high luminances. The close proximity between the weights from minimum motion and motion discrimination points to the assumed exclusive involvement of the luminance channel.

Figure 55 compares two mesopic threshold contours from Observer 10, a deuteranomalous trichromat, measured with the methods of detection and motion discrimination at 0.09 cd/m². As for the normal observer, for this observer the motion discrimination ellipse is more elongated than the contrast detection ellipse. The long axis of the motion discrimination ellipse is more than three times wider compared to the short axis. The differences in elongation are more pronounced for observer 1 with normal color vision. If the detection threshold on the long, isoluminant axis of the ellipse is set by chromatic contrast in the absence of luminance variation, this difference is not unexpected, since the chromatic signals are less strong in the red/green deficient observer. Because of the strong elongation of the ellipses their orientations are more clearly defined in this observer. The ellipse orientations are close together with estimated cone weights of 0.68 and 0.72 for detection and recognition of motion direction.
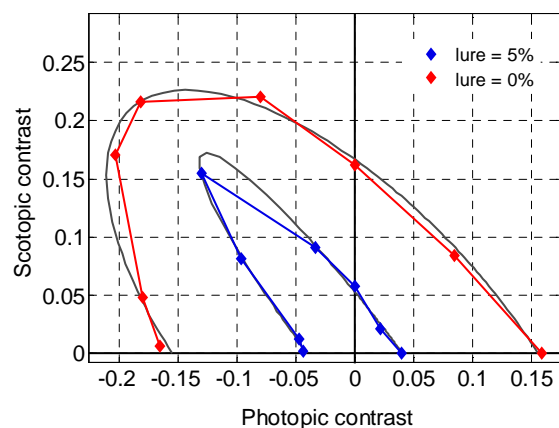
Figure 55: Threshold contours for motion discrimination (lure=5%) and detection (lure=0%) at 0.09 cd/m² for the deuteranomalous observer. The spatial and temporal frequencies of the stimulus are 1 cpd and 2 Hz. The gray lines show the fitted ellipses.
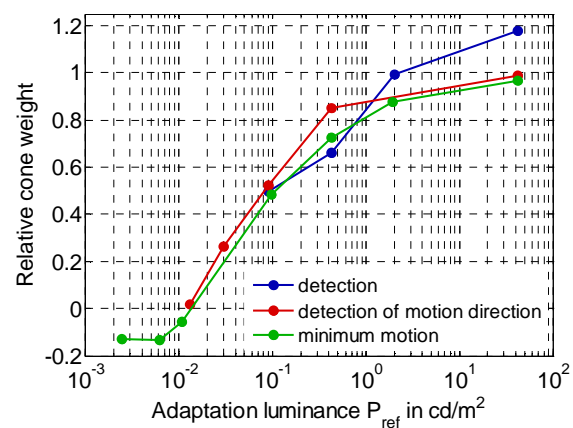
Figure 56: Relative cone weights as a function of adaptation luminance for detection task (lure=0%), motion discrimination (lure=5%) and minimum motion with an annulus of 5° radius for observer 1 (1 cpd and 2 Hz).

Some of the motion discrimination contours drawn in the following figures form two parallel straight lines rather than a closed ellipse. For lines exceeding the graph the gamut of the monitor was not sufficient to allow for a confident detection of motion. As the graphs show, the threshold points are assembled in two lines whose slopes can be regarded as having the orientation of lowest sensitivity, that is, the direction of constant mesopic luminance. Along a line from the origin in contrast space parallel to the threshold lines the difference in mesopic luminance between the adaptation field and the stimulus is zero. These very narrow ellipses suggest that the criterion of motion discrimination taps the fast luminance channel only. In the direction of constant luminance, motion detection is difficult or impossible because differences in luminance to aid detection are not present.

Influence of spatial frequency

The different spatial and temporal properties of the rod and the cone system make the measurement of mesopic vision especially interesting and challenging. The peak sensitivity for photopic cone vision is between 10 and 20 cpd as opposed to around 0.9 cpd for rod vision (Kelly, 1961, D'Zmura & Lennie, 1986). Combined rod and cone excitation lead to a spatial sensitivity function that envelopes the rod only and cone only sensitivity functions (D'Zmura & Lennie, 1986). The peak of this sensitivity function shifts towards lower frequencies for darker adaptation levels (Kelly, 1961). For the mid mesopic luminance level at which the threshold data were collected the highest sensitivity might be around 3-5 cpd (Kelly, 1961, D'Zmura & Lennie, 1986). As a consequence of different spatial sensitivities and different spatial rod and cone distributions on the retina the peak sensitivity shifts towards shorter spatial frequencies with eccentricity (Kelly, 1984).

The influence of spatial and temporal frequencies at a constant mesopic adaptation luminance of $0.09 cd/m^2$ was examined with one observer. The detection contour was measured with 1 cpd and 3 cpd as shown in Figure 57. It is evident that the threshold increases substantially for the increased spatial frequency of 3 cpd. A model that accounts for photopic and scotopic contributions to threshold contrast as described above shows an increase in the relative photopic weight W_P from 0.5 to 0.78, while spatial frequency increases from 1 cpd to 3 cpd, conforming the notion that the cone system possesses the highest acuity, whereas the rod system is not able to resolve finer details. If the annulus is doubled in radius from 5° to 10° at a constant spatial and temporal frequency, the threshold ellipse gets wider (blue curve in Figure 57). More cone contrast and at the same time less rod contrast is needed to detect the stimuli. In this case modeling reveals a decrease in cone contribution from 0.5 to 0.28. The weights are in proximity to the cone weights from the minimum motion criterion (Chapter 4), which decrease from 0.48 to 0.16 for the same observer under similar conditions.

Figure 58 shows threshold contours for the motion discrimination criterion under constant temporal frequency and variable spatial frequency. Here only at 1 cpd could a closed contour be measured. For other spatial frequencies, the monitor gamut was not sufficient to lead to an unambiguous perception of motion for the isoluminant direction. The resulting narrow contours support the idea that unlike simple contrast detection the motion discrimination task involves only luminance information, as was discussed above. With an increase in spatial frequency above 1 cpd, the orientations of the threshold contrast lines become more vertical, hence the influence of rod contrast decreases. The relative cone weights for detection and motion discri-

mination are summarized in Figure 59 as a function of spatial frequency. The decrease of the cone weights from 4 to 1 cpd agrees with the cone weights from the detection task. However, the very low spatial frequency of 0.5 cpd leads to a small increase of cone contribution to 0.61. The peak sensitivity for the rods is close to 1 cpd; a lower spatial frequency might lead to a decrease of rod sensitivity and therefore to an increase in the relative cone weight.
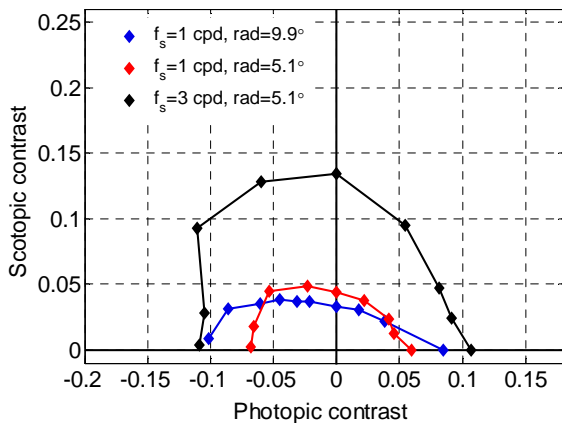
Figure 57: Threshold contours for the detection task measured at 0.09 cd/m². The radius of the stimulus was 5° for the red and the black curve and 10° for the blue curve with a temporal frequency of 2 Hz.
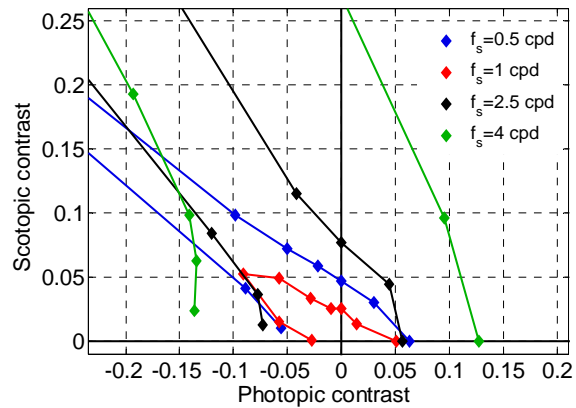
Figure 58: Threshold contours for the motion discrimination task measured at 0.09 cd/m². The radius of the stimulus was 5° with a temporal frequency of 2 Hz.
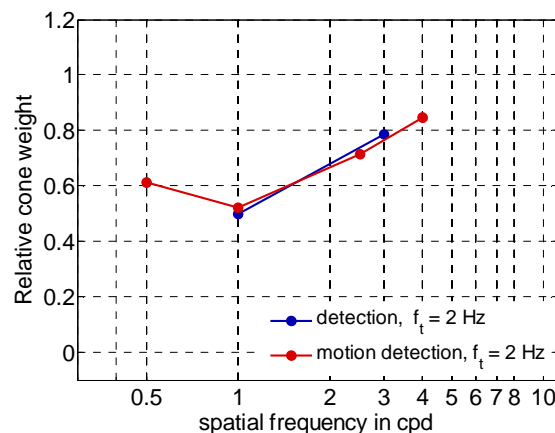
Figure 59: Relative cone weights as a function of spatial frequency for the detection task and the motion discrimination criterion at 0.09 cd/m². The radius of the annulus was set to 5° with a temporal frequency of 2 Hz.

Influence of temporal frequency

The photopic temporal sensitivity curves measured at the optimal spatial frequency are low-pass curves that fall off steeply around 5 Hz (Kelly, 1984). By comparison rod vision is more sluggish (MacLeod, 1972), but speeds up at mesopic light levels, where a second, faster rod mechanism comes into play (Conner & MacLeod, 1977; Sharpe & Stockman, 1999).

Rod temporal sensitivity depends on the adaptation level and the resulting activation of the two rod channels. The slower, more sensitive channel that is active at scotopic light levels exhibits a temporal sensitivity curve that has a low-pass characteristic with a drop-off at frequencies higher than 7 Hz. While the faster rod channel, active at mesopic light levels shows a band-pass

characteristic with the peak sensitivity between 5 and 10 Hz (Sharpe, Stockman, MacLeod, 1989, Snowden, Hess, Waugh, 1995).

Temporal frequencies at 4 Hz and below were tested because slow temporal changes are not expected to reveal rod-cone interference like enhancement or cancellation. Figure 60 shows the effect of temporal frequency for the detection task for a constant spatial frequency. Figure 61 and Figure 62 show the threshold contours of two different constant spatial frequencies for the motion discrimination criterion. The thresholds for the detection task increase for increased temporal frequencies; however the thresholds seem to rise to the same extent for the rods and the cones. Hence, the orientation of the contours does not change for the range of temporal frequencies tested here. The same trend is evident in the motion discrimination contours. As mentioned above, the ellipses for the motion discrimination task seem to be strongly elongated; along the direction of constant mesopic luminance no clear motion direction was evident. For 2.5 cpd also the absolute contrasts do not seem to be affected by changes of temporal frequency. The constant orientation is also reflected in the relative cone weights shown in Figure 63.
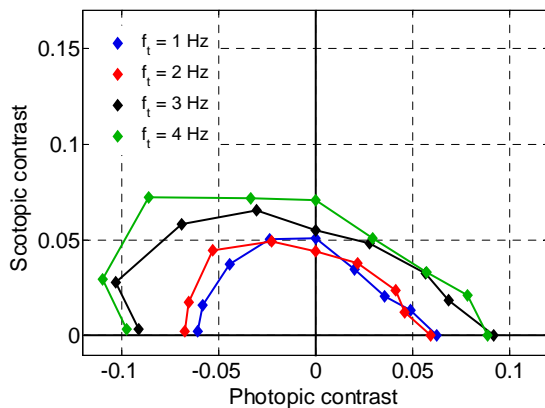
Figure 60: Threshold contours with the criterion of detection at 0.09 cd/m². The radius of the stimuli was 5° with a spatial frequency of 1 cpd.
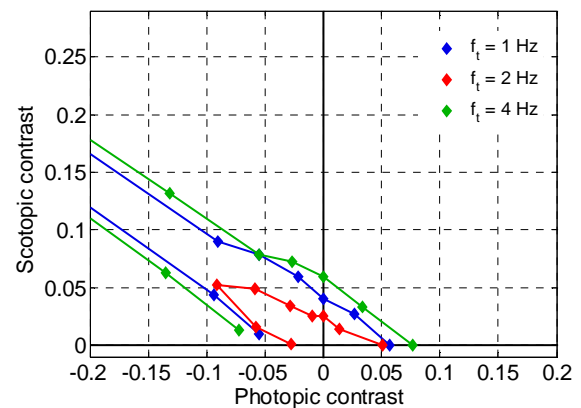
Figure 61: Threshold contours with the criterion of motion discrimination at 0.09 cd/m². The radius of the stimuli was 5° with a spatial frequency of 1 cpd.
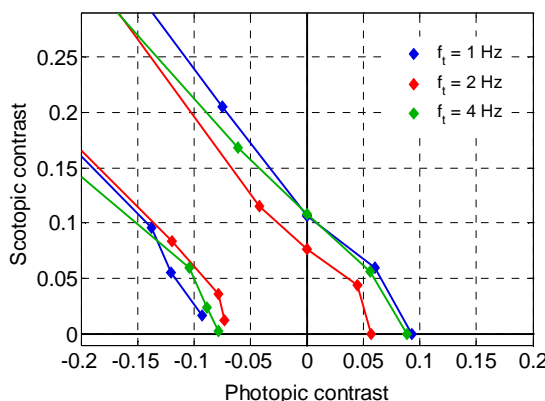
Figure 62: Threshold contours with the criterion of motion discrimination at 0.09 cd/m². The radius of the stimuli was 5° with a spatial frequency of 2.5 cpd.
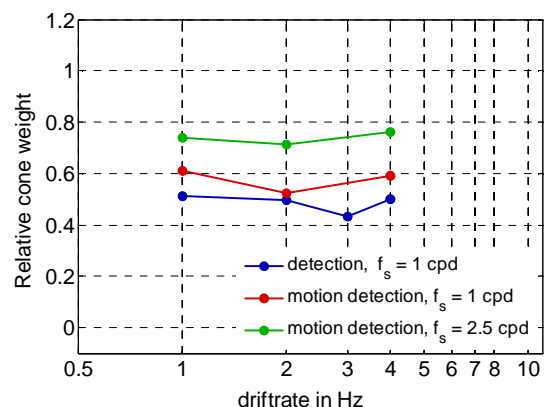
Figure 63: Relative cone weights as a function of temporal frequency for the detection task and the motion discrimination and MinMot criterion. The radius of the annulus was 5°.

Overall the results are comparable with minimum motion settings made at various temporal and spatial frequencies described in chapter 4. Since changes in spatial and temporal frequency seem to have the same influence on motion discrimination and minimum motion as well as on the detection of a counterphasing stimuli, one might conclude that the color opponent signals have no or only a minor influence on spatial and temporal vision in the mesopic range.

5.4   Summary and Conclusions

This chapter describes three methods to measure contrast threshold contours: the detection of flashes, detection of a flickering annulus, and the detection of motion direction of a rotating annulus. All of these criteria proved to be applicable under adaptation conditions ranging from photopic to low mesopic. Threshold contrasts represented in S-P contrast space form elliptic contours defined by their size, elongation, and orientation. With iterative modeling of these ellipses, the orientation, i.e. the direction of zero luminance contrast with the reference, was estimated and used to determine the relative contribution of rod and cone luminance to threshold.

The detection thresholds of 500 ms flashes were examined as a function of eccentricity, color and adaptation level. The incremental thresholds of the peripheral visual field decrease linearly for all colors with the decreasing log of the adaptation luminance. Especially for darkest adaptation levels the thresholds increase with eccentricity, strongest for the red stimuli and moderately for green and gray. The thresholds to the blue stimuli were the lowest for all peripheral positions and relatively constant over eccentricity. The differences in threshold between the colored stimuli increased with decreasing luminance. The increase of foveal contrast thresholds for all colored stimuli was attributed to the interference with the tracking task. The estimated slopes of the TVI-curves were below unity for all conditions, as was also reported earlier (e. g. König & Brodhun, 1903, Barlow, 1957). The TVI-slope was somewhat lower for the 2° stimuli compared to the more peripheral ones. In addition, the color of the stimulus had a pronounced effect on the TVI-slopes, with increased slopes for the bluish stimulus. The dependency on eccentricity and color can be attributed to the Purkinje-shift.

The results of the flash detection experiment were modeled as a non-linear sum of weighted rod and cone responses. Despite some reservations and uncertainties due to the small number of data points in S-P space, it can be concluded that a linear addition of rod and cone contrasts can describe detection under mesopic adaptation conditions (0.012 cd/m^2 and 0.077 cd/m^2). A comparison of the relative cone weights from flash detection and minimum motion shows that data from the flash detection experiment lead to increased cone weights for all peripheral stimuli. However, the constant relative cone weight close to 1 for foveal vision under all light conditions was also found in the minimum motion results. The foveal thresholds can be regarded as cone dominant and less affected by the Purkinje-shift due to the absence or the small amount of rods under photopic and mesopic adaptation levels.

The data of the flash detection experiment were used as a basis to compare earlier approaches on mesopic photometry based on brightness matches, detection thresholds and reaction times. Despite the different methods the models are based on, the mesopic contrasts provide an

improved description of detection contrasts compared to the photopic contrasts for peripheral stimuli. Foveal or near foveal stimuli are best described by photopic luminance. It has to be noted that none of the existing models evaluated incorporate an eccentricity parameter, therefore they can not account for different contrast thresholds over the visual field.

Experiments on the detection of a flickering annulus and the discrimination of motion direction of a rotating annulus reveal quite different threshold contours. While the detection contours are wider both in photopic and scotopic contrast, the motion discrimination contours are more elongated in the direction of constant mesopic luminance. The motion discrimination results resemble to a high degree results from the minimum motion experiment (chapter 4), whereas the detection weights are close to the results from minimum motion only under mesopic conditions. At higher luminances the differences are pronounced.

Threshold contours for several temporal frequencies do not show a shift in the orientation of the ellipse meaning that high temporal frequency limits threshold for rods and cones roughly to the same extent. In contrast, an increase in spatial frequency of the annulus leads to a remarkable change of orientation towards a higher cone influence. The fine contours of the stimulus hinder the rods from contributing to detection, whereas the cones dominate vision at higher spatial frequencies due to their ability to resolve fine patterns.

The narrowing of the motion discrimination contours and their close proximity to minimum motion data in their dependence from adaptation luminance, spatial and temporal frequency support the idea that the method of motion discrimination taps the luminance channel only. It was also reported earlier that color does not support perception of motion (Ramachandran & Gregory, 1978). The present results extend the finding that chromatic information is not very relevant for motion perception to mesopic conditions.

Overall the consistency of the results for the motion discrimination method and the minimum motion method suggests that these two methods address the same visual channel, namely the luminance channel only. Detection of flashed stimuli and the detection of a flickering annulus however, are influenced by both luminance and chrominance information.

Chapter 6

Summary and Conclusion

Visual perception in the mesopic adaptation range is of particular interest for lighting applications like street, automotive, and emergency lighting. With the intention to safe energy and costs a photometric model for the mesopic adaptation range that enables a perception based evaluation of an illumination system is desired. However, due to the physiological characteristics of the visual system mesopic vision is very complex and so far there is no satisfying unified model to describe mesopic perception.

This thesis presents results from three extensive psychophysical experiments, namely minimum motion (MinMot), minimally distinct borders (MDB), and threshold contrasts for flashes to study the change in the relative contribution of rods and cones. In addition exploratory studies were conducted to measure threshold contrasts of counterphasing stimuli and motion discrimination thresholds. The focus of all these studies lies on near foveal and peripheral vision under adaptation levels ranging from photopic to scotopic.

It is shown here that the applied methods are viable to assess peripheral and near foveal vision under all lighting conditions. The minimal distinct border method showed some unwanted side effects like afterimages, fading of the test field due to the Troxler effect and the described tangent bias. Compared to motion nulling at low spatial and temporal frequencies, minimizing border distinctness and finding a motion discrimination threshold by adjustment seem to be less sharp criteria which result in higher standard deviations.

To obtain relative rod and cone weights, the results of the MDB and MinMot method were modeled with the assumption that rod and cone signals combine linearly. The decrease in cone weights with dark adaptation can be described with a sigmoid function whose shape depends on the eccentricity of the stimulus. The steepness of the sigmoid function in W_S-logP space describes the mechanism of adaptation and reflects the exponent of the rod TVI-curve. It was found that the estimated slopes of the rod TVI-curves agree well with earlier data from detection threshold experiments. The modeled TVI-slopes from the minimum motion data increased with eccentricity, and agree well with the TVI-slope of the MDB data.

Comparing the relative cone weights of the MDB and minimum motion experiments for mesopic and scotopic adaptation levels for 5-6° extrafoveal vision reveals a close proximity. However, cone weights under photopic adaptation luminances are slightly higher for border settings than for motion nulling. The modeled receptor weights of both methods depend strongly on stimuli eccentricity under mesopic conditions. The results of the minimum motion method show that for vision from 2° off-axis to 18° off-axis the luminance level of equal rod and cone contribution to luminance increases strongly by more than one log unit. Yet, near foveal vision ($\pm$ 1°) can be described with only the cone response at all intensities. The relative cone weights derived from the MDB experiment at photopic adaptation levels reveal a slightly increased sensitivity for red lights compared with the photopic standard observer $V_{10}(\lambda)$. For

both methods the relative cone weights under scotopic conditions show an increased blue sensitivity compared to V'(λ), which might be ascribed to changes of macular pigment optical density. Also the small but consistent change of receptor weights with eccentricity for pure photopic and scotopic light levels that was evident in the MinMot data was attributed to macular pigment in the periphery.

Reference fields of different chromaticity but identical ratios of scotopic to photopic luminance (S/P ratio) show a good agreement in receptor weights for both motion and border nulling. This and the high linearity between the rod and cone responses evident in the MDB data suggest, though not conclusively, that the sum of the weighted individual scotopic and photopic luminance is sufficient to describe achromatic luminance at all light levels.

When comparing relative cone weights from mesopic adaptation backgrounds of the same photopic luminance but different scotopic luminance the greater S/P ratio is associated with an increased sensitivity and a decreased weight for rod receptors. This behavior is expected on the assumption that rods work nearly in accordance with Weber's Law in the Weber range of the TVI-curve. The relative decrease of rod weights was found to be equal for a wide range of eccentricities. Moreover, it was shown that mesopic luminance determined by minimum motion is not influenced by temporal frequencies between 0.5 and 5 Hz at mid mesopic light levels. However, an increase of spatial frequency reveals an increased cone contribution for all tested eccentricities. This effect can partly be explained by the rod's increased receptive field size and the inability to resolve fine details.

Furthermore, several threshold criteria were applied for peripheral vision under a variety of adaptation levels: the detection of flashes, the detection of a counterphasing flickering annulus, and the threshold for discriminating the direction of motion for a counterphasing rotating annulus. The detection thresholds of 500 ms flashes were measured as a function of eccentricity, color and adaptation level. The differences in threshold between the colored stimuli for the tested adaptation conditions reflect the Purkinje shift with decreasing thresholds for bluish stimuli. The results of the flash detection experiment were modeled as a non-linear sum of weighted rod and cone responses that vary with the n-th power of the relevant stimulus luminance. A comparison of the relative cone weights from the flash detection and minimum motion experiment show that data from the flash detection experiment lead to higher cone weights for all peripheral stimuli. However, the constant relative cone weight close to 1 for foveal vision under all light conditions was also found in the minimum motion results. As in the minimum motion and MDB experiments the estimated slopes of the TVI-curves were for all conditions below unity. The peripheral position of the stimulus and its color have an effect on the TVI-slope, which reflects the Purkinje-shift.

In addition to the three mentioned studies, explorative experiments on the detection of a flickering annulus and the discrimination of motion direction of a rotating annulus were carried out to determine threshold contours for positive and negative cone contrasts. The threshold contours of both methods exhibit pronounced differences. While the detection contours resemble thick ellipses in photopic and scotopic contrast space, the motion discrimination contours are more elongated in the direction of constant mesopic luminance. The motion discrimination results resemble to a high degree results from the minimum motion experiment, whereas the weights from the detection criterion are only under mesopic conditions close to the results from minimum motion.

The effect of temporal and spatial frequency on motion discrimination thresholds is similar to the minimum motion results: a moderate increase in temporal frequency from 1 to 4 Hz has no influence on the threshold for rods and cones. In contrast, an increase in spatial frequency of the annulus leads to higher cone influence.

The strong elongation of the motion discrimination contours, and their close proximity to MDB and minimum motion results in their dependence from adaptation luminance, spatial and temporal frequency support the idea that the method of motion discrimination taps the luminance channel only. This conclusion is in agreement with earlier findings from Ramachandran and Gregory (1978). The present results extend to mesopic conditions the finding that chromatic information is not much relevant for motion perception.

The results suggest the existence of a common luminance pathway that carries achromatic luminance information. Hence, the mesopic luminance for a certain stimuli eccentricity and spatial frequency can be described as a linear sum of photopic and scotopic achromatic luminance. Since spatial frequency (object size) and eccentricity have a high influence on luminance, any mesopic model should incorporate these parameters. Detection of flashed stimuli and the detection of a flickering annulus however, are influenced by luminance and chrominance information. Here, a simple linear model might not be rectified.

Existing models of mesopic photometry describe mesopic detection contrasts to a limited extent since they do not account for the strong dependence of perception on eccentricity. Especially for peripheral stimuli the mesopic contrasts provide an improved description of detection contrasts compared to the photopic units.

Generally, a model of mesopic vision to improve practical applications is difficult to develop, partly because vision in the mesopic domain is complex and it depends on multiple parameters. But, for practical purposes one might neglect temporal phase lags if temporal changes are below 5 Hz, which is surely true for most natural visual scenes. Secondly, the size of objects influences strongly how well we can detect them; therefore the parameter of object size or spatial frequency has to be considered in a model of photometry. However, since the size of objects one encounters e. g. on the street is difficult to foresee, a practical photometric model will give only a rough prediction of luminance with respect to object size. Even more prominent is the effect of the position at which obstacles appear in the visual field.

How can the findings of this thesis be used to improve lighting installations? Foveal and near foveal perception can be regarded as cone dominant and less affected by the Purkinje-shift due to the absence or the small amount of rods under photopic and mesopic adaptation levels. Therefore, a photometry based on photopic sensitivity is sufficient for foveal perception also at low light levels. However, the contribution of cones to achromatic luminance is minor for perception in the far periphery at 10° or further off-axis. Therefore, any perception based description of mesopic vision needs to account for the strong influence of rods for extrafoveal vision and for the considerable effect of object size (spatial frequency).

This requirement imposes challenges on the development of a system of mesopic photometry. In night time driving the perception of objects in the periphery is very important, since most objects (e. g. pedestrians, animals or turning cars) appear first in the periphery. Generally, one can assume that after the detection of a peripheral obstacle the fixation changes towards this object. Consequently one goal is to enhance peripheral perception. A possible scenario for automotive nighttime lighting is to allow for improved peripheral perception by the street

lighting system that enables illumination of the pedestrian sidewalks and areas directly adjacent to the street. Here, a rod favoring, bluish illumination (e. g. metal halide lamps) would be preferable. Conversely, to enhance foveal perception an illumination supporting the cones with increased photopic luminance is favored. This can be realized by the headlamp system of the car.

These considerations show that both photopic and scotopic luminance is important in night time driving. The notion to generally increase scotopic luminance with bluish light sources like LEDs is therefore not always supportive.

Appendix

A Calibration of the monitor used for the MDB and MinMot experiments

An Iiyama 19" CRT monitor was used to present the stimuli and background for the MDB and MinMot experiments. The monitor was set to a resolution of 1280x1024 with 72 Hz. The use of a CRT Monitor is preferred over a LCD Monitor (or projector) due to their superior temporal response, color gamut and luminance precision properties.

The spectrum of the three phosphors was measured with a Photo Research PR-650 Spectro Scan spectroradiometer with a resolution of 4 nm. The measurement area was a disc in the middle of the screen surrounded by an equal energy white background at 50% of the maximum luminance. The intensity of the colored disc was also set to 50% intensity of the maximum available intensity of the phosphor. The spectrum of the three phosphors and the white is shown in Figure 6. Figure 7 shows the additivity failure of the RGB phosphors of the CRT monitor in % according:

$$FA_{i,\%} = \frac{L_{i,red} + L_{i,green} + L_{i,blue}}{L_{i,white}} \cdot 100$$

$FA_{i,\%}$ is the percent additivity error at the i_{th} wavelength, L_i is the spectral radiance for the i_{th} wavelength for the red , green and blue phosphor, $L_{i,white}$ is the spectral radiance for the i_{th} wavelength for a white signal when all three phosphors are active to the same extent.
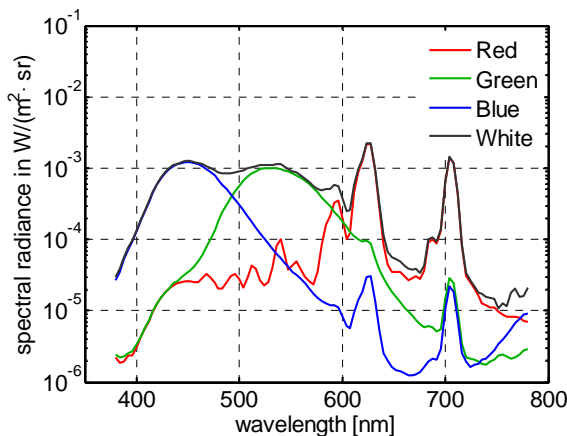
Figure 64: Spectra of the monitor phosphors and the combination of all three phosphors.
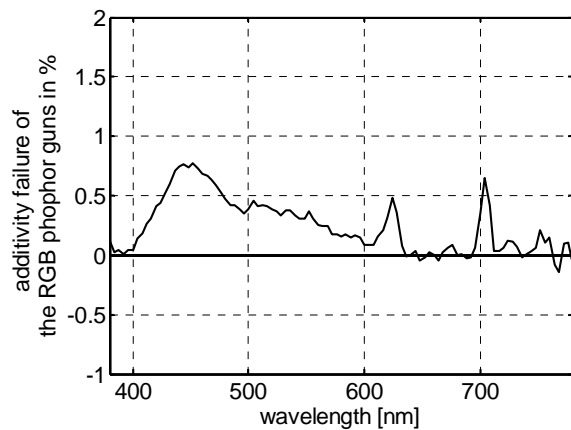
Figure 65: Additivity failure of the RGB phosphors over wavelength

The intrusion of infrared radiation in the visible range within the PR-650 device was tested with infrared filters and no measureable intrusion was found.

The spectral radiance was used to calculate transformation matrices that transform the RGB values into the cone excitations L, M, and S; the photopic and scotopic luminance; and the CIE tristimulus primaries for each phosphor level. The photopic luminances for the 2° field were

double checked with a LMT Luminance meter L1009 (LMT Lichtmesstechnik) and agreed very well. The gamut range of the CRT monitor in terms of photopic and scotopic luminance is shown in Figure 66.
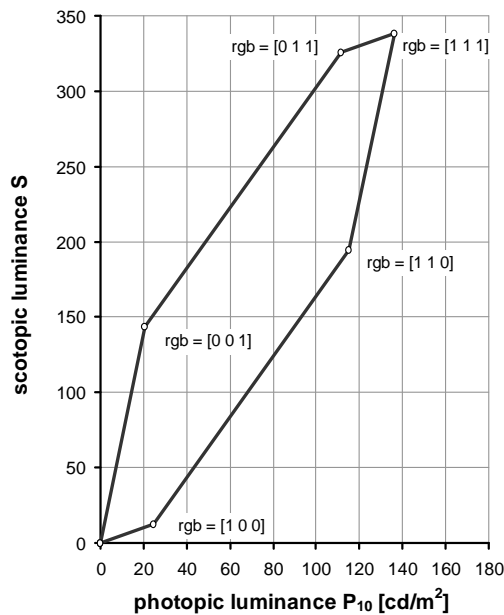
Figure 66: Monitor gamut in S-P space: The black lined area is the addressable luminance space of the Iiyama monitor without filters.

The gamma curves of all three phosphors and the white level were measured with a UDT S 370 (United Detector Technologies) photometer operated with a PCI-GPIB card from National Instruments. The monitor showed a gray background and a disc in the middle of the screen with varying RGB values. The photometer head was placed directly in front of the monitor screen to avoid stray light. For each of 256 steps of the digital-to-analog converter (DAC) the radiance was determined as the average of 3 repetitive measurements. Each of the four curves was measured 10 times. The order of the 256 steps was randomized. The averaged gamma curves of all measurements, shown in Figure 67 for the three phosphors were used to create a look-up-table for RGB DAC values to generate linear output intensities. The table assigns to each of the 256 intensity values a new DAC value for each phosphor. The aim of the calibration is to linearize the relation between the output luminance and the 256 RGB steps used in the experimental scripts that get send to the graphics card and the DA-converter. The relative deviation from linearity is plotted in Figure 68. The deviation from linearity is very small at generally less than 1%; only at DAC values below 28 the linearity failure exceeds 2%. Therefore, when defining the adaptation levels for the experiments DAC values in the linear range were chosen.
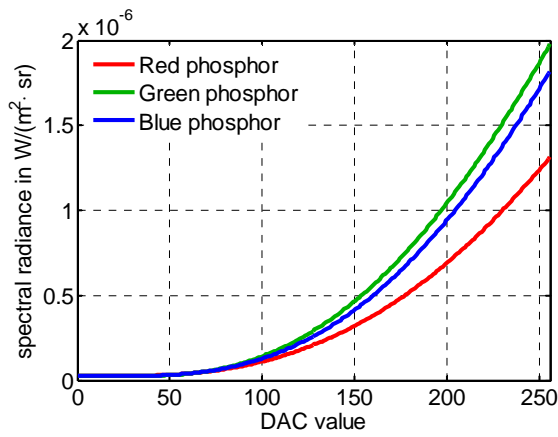
Figure 67: Gamma curves of the red, green, and blue phosphor, average of 10 measurements.
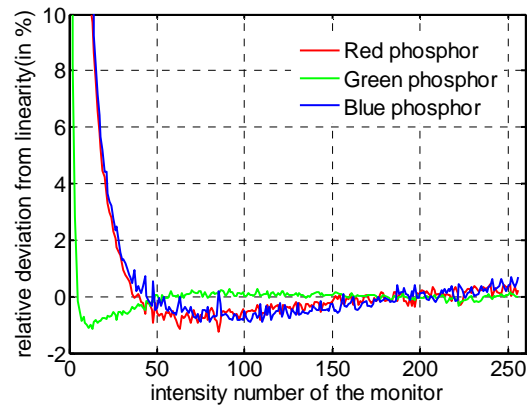
Figure 68: Relative deviation from linearity in % as a function of the DAC value of the monitor.

The deviation from linearity for each phosphor and wavelength is shown in Figure 69a-d.

a)

b)

c)

d)
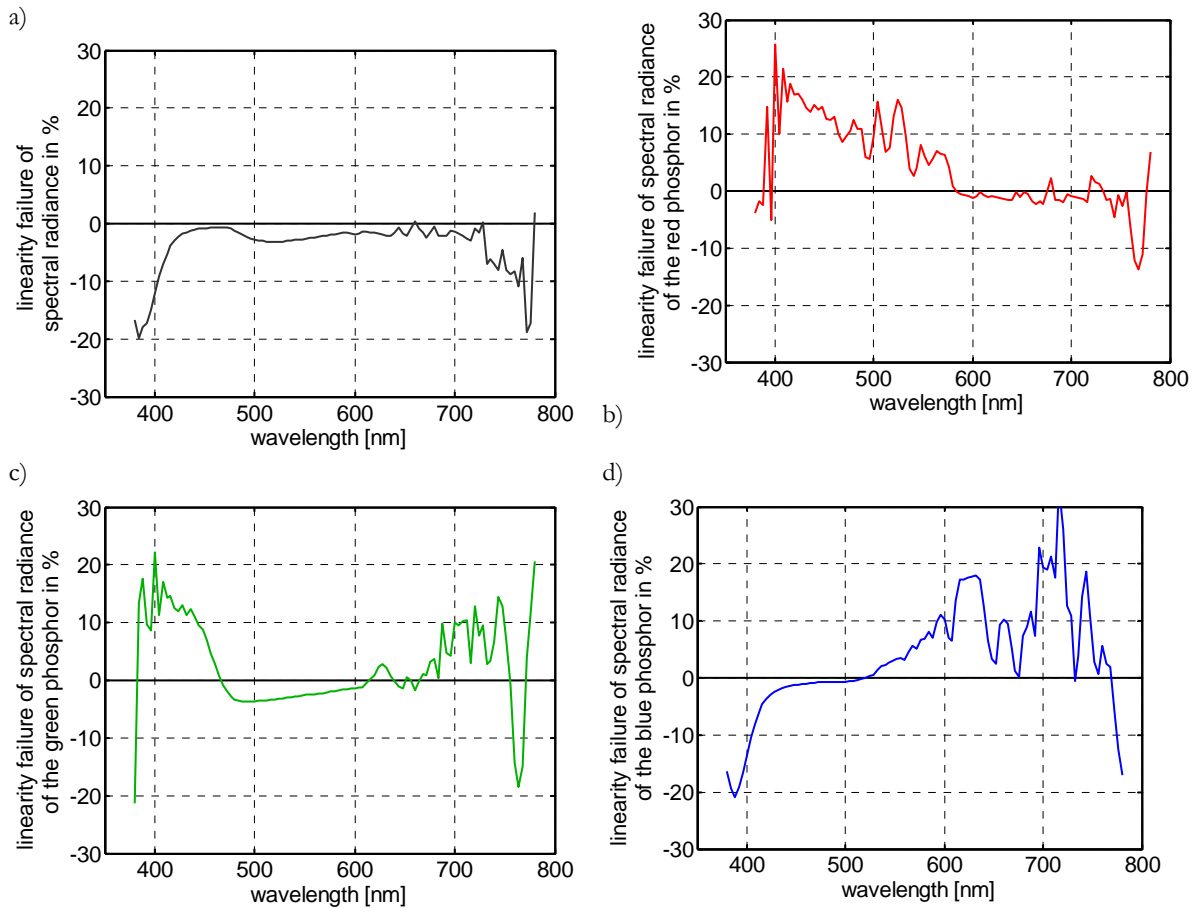
Figure 69: Linearity failure of spectral radiance for all phosphors in %. The spectral radiance of 100% intensity was compared with twice the spectral radiance of 50% of the maximum intensity for each wavelength. a) red, green, and blue phosphor together b) red phosphor c) green phosphor d) blue phosphor

Measurement of the spectral transmission of the filters

The low luminance levels in the minimum motion and minimally distinct border experiments were realized with several neutral density filters and their combinations. Table 11 gives an overview of all filters used and their densities. As reference light source to determine the spectral transmission of the neutral density filter sheets the light source of a slide projector was

used. To ensure a low noise level in the blue wavelength range by providing sufficient intensity there, while avoiding saturation of the detector by longer wavelengths, a blue filter was placed in front of the light source. For the spectral range above 640 nm a monochromator was used as light source. The filter-sheets were placed in between two polycarbonate sheets. The spectral transmissions of the polycarbonate sheets were measured separately for each filter. Each measurement was repeated 5 to 10 times with the PR-650 spectroradiometer. The resulting transmission curves are shown in Figure 70.

Filter optical density	% transmittance	f-stop reduction	Name of the filter
1.2	6.25%	4	F16
1.8	1.56%	2+4	F416
2.4	0.39%	2+4+2	F416F4
2.7	0.20%	2+4+3	F416F8
3.0	0.098%	2+4+4	F416F16
3.3	0.049%	4+4+3	F1616F8
3.6	0.024%	4+4+4	F1616F16
4.8	0.0015%	4+4+4+4	F16161616

Table 11: Optical density of the neutral density filters and their combinations
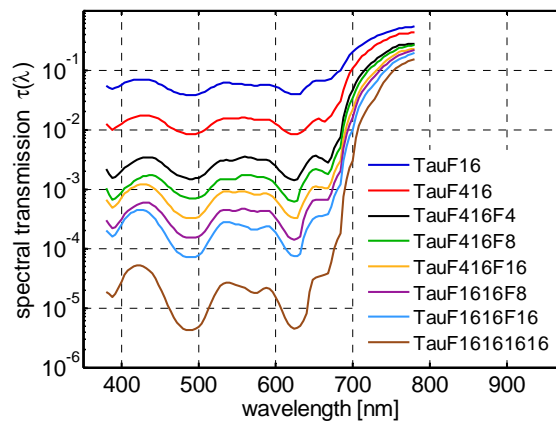
Figure 70: spectral transmission of the neutral density filters used for the minimum motion and MDB experiments

B Spectral data of the projector for the detection threshold experiment

For the detection threshold experiment in chapter 5 a Panasonic PT-AE 900 LCD projector with a resolution of 1280x720 and a 120 Watt UHP lamp was used. The spectra of the three color channels were measured with an OPTRONIC OL770 spectroradiometer with a resolution of 0.4 nm (Figure 71). The spectral transmission of the two neutral density filters used for the lower adaptation levels is shown in Figure 72.
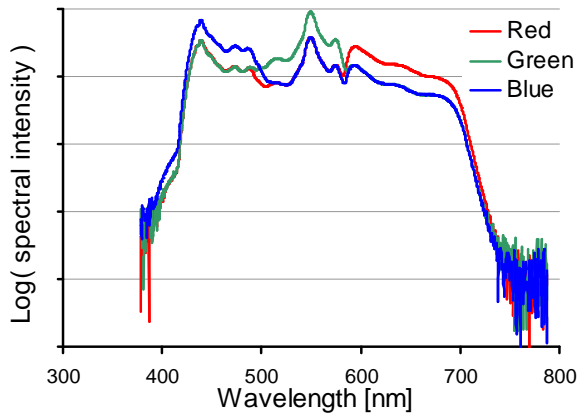
Figure 71: Spectra for the three color channels of the projector on a log scale.
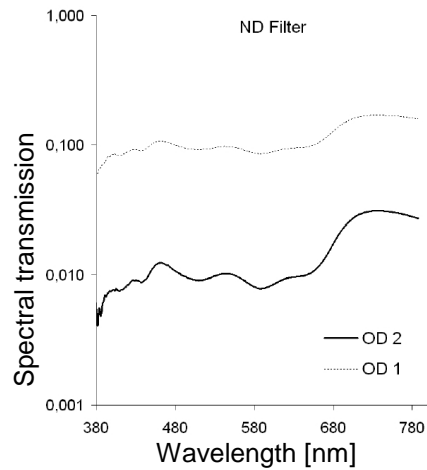
Figure 72: Spectral transmission of the neutral density filters used for the lower adaptation levels

Luminance measurements were done with the luminance camera LMK 98-3 color (TechnoTeam) with a 25 mm lens. The camera exhibits F_1-errors of $f_1 < 3\%$ for $V(\lambda)$, $f_1 < 6\%$ for $Z(\lambda)$, $f_1 < 4\%$ for $X(\lambda)$ and $f_1 < 6\%$ for $V'(\lambda)$. In addition a LMT Luminance meter L1009 with $f_1 = 1.7\%$ was used.

The non-uniformity of luminance across the screen was compensated by generating a luminance opponent background. The resulting uniformity of the background can be seen in Figure 73 which shows a luminance picture and a cross-section of the background.
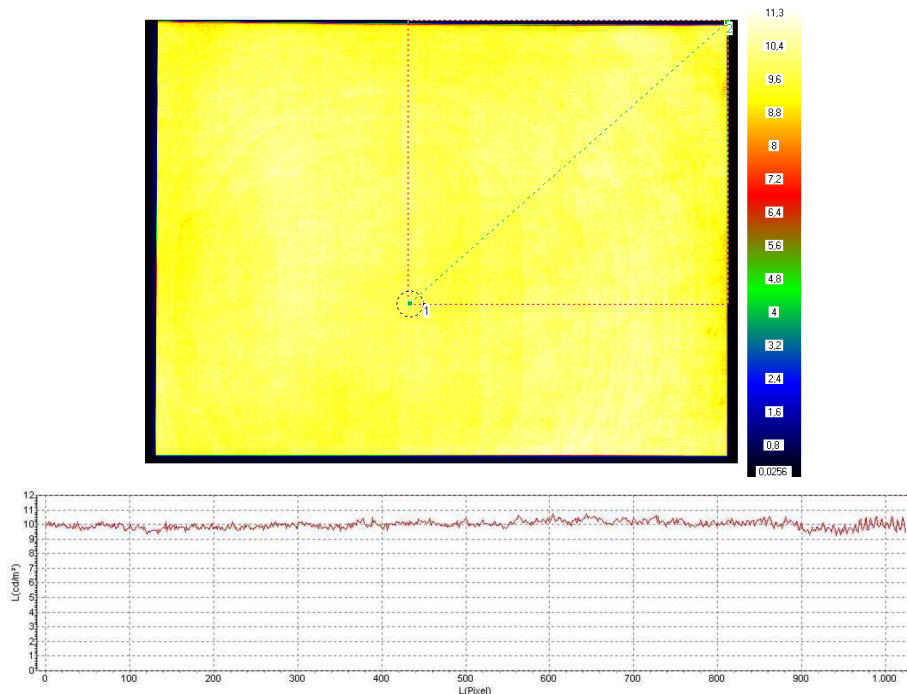
Figure 73: Luminance picture of the projection screen with a color scale, uniformity was reached by compensating for the hot spot of the projector. bottom: cross-section of the luminance picture

References

Abney W, Festing ER: Colour photometry. Philos. Trans. of the Royal Society, London, 177: 423-456 (1886)

Abney W: Researches in colour vision. London: Longmans, Green (1913)

Abramov I, Gordon J: Color vision in the peripheral retina. I. Spectral Sensitivity. J Opt Soc Am. 67(2): 195 (1977)

Adelson EH: Saturation and adaptation in the rod system. Vision Research 22: 1299-1312 (1982)

Aguilar M, Stiles WS: Saturation of the rod mechanism of the retina at high levels of stimulation. Optica Acta 1: 59–64 (1954)

Ahnelt P, Kolb H, Pflug R: Identification of a subtype of cone photoreceptor, likely to be blue sensitive, in the human retina. J. Comp. Neurol. 255: 18–34 (1987)

Akashi Y, Rea MS: Peripheral detection while driving under a mesopic light level. J. Illum. Eng. Soc. 31(1): 85–94 (2002)

Alpern M, Rushton WAH, Torii S: The attenuation of rod signals by backgrounds. Journal of Physiology 206: 209-227 (1970)

Anstis S, Cavanagh P: A minimum motion technique for judging equiluminance. In Colour Vision: Physiology and Psychophysics, J. D. Mollon and L. T. Sharpe, eds. (Academic, London, pp. 156-166 (1983)

Anstis S: Picturing peripheral acuity. Perception 27: 817-825 (1998)

Anstis S: The Purkinje rod-cone shift as a function of luminance and retinal eccentricity. Vision Research 42: 2485-2491 (2002)

Anstis SM: Phi movement as a subtraction process. Vision Research 10: 1411-1430 (1970)

Anstis SM: The perception of apparent movement. Philosophical Transactions of the Royal Society of London B 290: 153-168 (1980)

Asenja AB, Rim J, Oprian DD: Molecular determinants of human red/green color discrimination. Neuron 12(5) (1994)

Barlow HB, Fitzhugh R, Kuffler SW: Change of organization in the receptive fields of the cat's retina during dark adaptation. Journal of Physiology 137(3): 338-54 (1957)

Barlow HB: Increment Thresholds at low intensities considered as signal/noise discriminations. Journal of Physiology 136: 469-488 (1957)

Berman S, Clear R: Additivity constraints and visual task consideration in mesopic photometry. J. Illum. Eng. Soc. 30: 90-104 (2001)

Blackwell HR: Contrast Thresholds of the Human Eye. J Opt Soc Am. 36(11): 624-643 (1946)

Bone RA, Sparrock JMB: Comparison of macular pigment densities in the human eye. Vision Research 11: 1057-1064 (1971)

Bornstein MH, Marks LE: Photopic luminosity measured by the method of critical frequency. Vision Research 12: 2023-2034 (1972)

Bouman MA: Peripheral Contrast Thresholds of the Human Eye. J Opt Soc Am. 40(12): 825-832 (1950)

Boynton RM, Eskew RT, Olson CX: Blue cones contribute to border distinctness. Vision Research 25: 1349-1352 (1985)

Boynton RM, Greenspon TS.: The distinctness of borders formed between equally saturated, psychologically unique fields. Vision Research 12(3): 495-507 (1972)

Boynton RM, Kaiser PK: Vision: the additivity law made to work for heterochromatic photometry with bipartite fields. Science 161(839): 366-368 (1968)

Boynton RM, Whitten DN: Visual adaptation in monkey cones: recordings of late receptor potentials. Science 170: 1423-1426 (1970)

Boynton RM: Human Color Vision. New York, Holt, Rinehart and Winston (1979)

Boynton RM: Implications of the minimally distinct border. J Opt Soc Am. 63(9): 1037-1043 (1973)

Boynton, RM: Ten Years of Research with Minimally Distinct Border. In: J. C. Armington, J. Krauskopf and B.R. Wooten (Eds.), Visual psychophysics and physiology. Academic Press (1978)

Buck SL: Chapter 55 "Rod-Cone Interaction" in The visual neurosciences. edited by Chalupa LM, Werner JS, MIT Press (2003)

Carroll J, Neitz J, Neitz M: Estimates of L:M cone ratio from ERG flicker photometry and genetics. Journal of Vision 2: 531-542 (2002)

Cavanagh P, Anstis S: The contribution of color to motion in normal and color-deficient observers. Vision Research 31(12): 2109-2148 (1991)

Cavanagh P, Favreau OE: Color and luminance share a common motion pathway. Vision Research 25: 1595-1601 (1985)

Cavanagh P, MacLeod DIA, Anstis SM: Equiluminance: spatial and temporal factors and the contribution of blue-sensitive cones. J Opt Soc Am. A 4(8): 1428-1438 (1987)

Chaparro A, Stromeyer CF III, Huang EP, Kronauer RE, Eskew RT Jr: Colour is what the eye sees best. Nature 361: 348-350 (1993)

Chaparro A, Stromeyer CF III, Kronauer RE and Eskew Jr RT: Separable red-green and luminance detectors for small flashes. Vision Research 34(6): 751-762 (1994)

Chatterjee S, Callaway EM: S cone contributions to the magnocellular visual pathway in macaque monkey. Neuron 35(6): 1135-1146 (2002)

Chien SH, Teller DY, Palmer J: The transition from scotopic to photopic vision in 3-month-old infants and adults: an evaluation of the rod dominance hypothesis. Vision Research 40: 3853-3871 (2000)

CIE Commission Internationale de l'Eclairage Proceedings, 1924. Cambridge: Cambridge University Press (1926)

CIE Proceedings Vol. 1, Sec 4; Vol 3, p. 37, Bureau Central de la CIE, Paris (1951)

CIE Proceedings, Vienna Session, 1963, Vol. B, pp. 209-220 (Committee Report E-1.4.1), Bureau Central de la CIE, Paris (1964)

CIE Publication 17.4: International lighting vocabulary, 4th ed. (Joint publication IEC/CIE) (1987)

CIE Publication 18.2: The basis of physical photometry, 2nd ed., Technical Report, Commission Internationale de L'Eclairage (1983)

CIE-Publication 141: Testing of supplementary systems of photometry. Technical Report, Commission Internationale de L'Eclairage (2001)

CIE-Publication 165: CIE 10 Degree Photopic Photometric Observer. Technical Report, Commission Internationale de L'Eclairage (2005)

CIE-Publication 170-1: Fundamental chromaticity diagram with physiological axes – Part I, Technical Report, Commission Internationale de L'Eclairage (2006)

CIE-Publication 41: Light as a true visual quantity: Principles of measurement. Technical Report, Commission Internationale de L'Eclairage (1989) (reprint 1994)

CIE-Publication 81: History, special Problems & practical Solutions. Technical Report, Commission Internationale de L'Eclairage (1989)

CIE-Publication 86: CIE 1988 2° spectral luminous efficiency function for photopic vision, Technical Report, Commission Internationale de L'Eclairage (1990)

Clarke FJJ: A Study of Troxler's effect. Optica Acta 7: 219-236 (1960)

Coblentz WW, Emerson WB: Relative sensibility of the average eye to light of different color and some practical applications. U.S. Bureau of Standards Bulletin, 14, 167. (1918)

Comerford JP, Kaiser PK: Luminous-efficiency functions determined by heterochromatic brightness matching. J Opt Soc Am. 65: 466-468 (1975)

Conner JD, MacLeod DIA: Rod photoreceptors detect rapid flicker. Science 195: 689-699 (1977)

Conner JD: The temporal properties of rod vision. Journal of Physiology 332: 139-155 (1982)

Crawford BH: The scotopic visibility function, Proceedings of the Physical Society, Section B 62, 321-334 (1949)

Curcio CA, Allen KA, Sloan KR, Lerea CL, Hurley JB, Klock IB, Milam AH: Distribution and morphology of human cone photoreceptors stained with anti-blue opsin. J Comp Neurol. 312: 610–624 (1991)

Curcio CA, Sloan KR, Kalina RE, Hendrickson AE: Human photoreceptor topography. J Comp Neurol. 292(4): 497-523 (1990)

D'Zmura M, Lennie P: Shared pathways for rod and cone vision. Vision Research 26(8): 1273-1280 (1986)

Derrington AM, Badcock DR: The low level motion system has both chromatic and luminance input. Vision Resaerch 25(12): 1879-1884 (1985)

Drum B: Cone threshold vs. retinal eccentricity: changes with dark adaptation. Invest. Ophthalmol. Vis Sci. 19(4): 432-435 (1980a)

Drum B: Relation of brightness to threshold for light-adapted and dark-adapted rods and cones: effects of retinal eccentricity and target size. Perception 9: 633-650 (1980b)

Drum B: Short-wavelength cones contribute to achromatic sensitivity. Vision Research 23(12): 1433-1439 (1983)

Eisner A, MacLeod DIA: Blue-sensitive cones do not contribute to luminance. J Opt Soc Am. 70(1): 121-123 (1980)

Eisner A, MacLeod DIA: Flicker photometric study of chromatic adaptation: Selective suppression of cone inputs by colored backgrounds. J Opt Soc Am. 71(6): 705-718 (1981)

Eloholma M, Ketomäki J, Halonen L: Luminances and Visibility in Road Lighting – Conditions, Measurements and Analysis. Report 30 http://www.lightinglab.fi (2004)

Eloholma M, Viikari M, Halonen L, Walkey H, Goodman T, Alferdinck J, Freiding A, Bodrogi P, Várady G: Mesopic Models – from brightness matching to visual performance in night-time driving: A review. Lighting Research & Technology 37(2) (2005)

Elzinga CH, de Weert CMM: Spectral sensitivity functions derived from brightness matching: implication of intensity invariance for color-vision models. J Opt Soc Am. 3(8) (1986)

Fechner GT: Elemente der Psychophysik. Leipzig: Breitkopf und Hirtel (1860)

Field GD, Chichilnisky EJ: Information processing in the primate retina: Circuitry and Coding. Annu. Rev. Neurosci. 30: 1-30 (2007)

Frauenhofer J: On the refractive and dispersive power of different species of glass, in reference to the improvement of achromatic telescopes, with an account of the lines or streaks which cross the spectrum. Edinburgh Philosophical Journal 10: 26-40 (1824)

Freiding A, Eloholma M, Ketomäki J, Halonen L, Walkey H, Goodman T, Alferdinck J, Vàrady G, Bodrogi P: Mesopic visual efficiency I: detection threshold measurements. Lighting Research and Technology 39: 319-334 (2007)

Frome FS, Buck SL, Boynton RM: Visibility of borders: separate and combined effects of color differences, luminance contrast, and luminance level. J Opt Soc Am. 71(2): 145-150 (1981)

Gibson KS, Tyndall EPT: Visibility of radiant energy. Scientific Papers of the Bureau of Standards, 19, 131-191 (1923)

Giulianini F, Eskew RT Jr: Chromatic masking in the (L/L, M/M) plane of cone-contrast space reveals only two detection mechanisms. Vision Research 38: 3913-3926 (1998)

Golz J, MacLeod DIA: Colorimetry for CRT displays. J Opt Soc Am. A 20(5): 769-781 (2003)

Goodman T, Forbes A, Walkey H, Eloholma M, Halonen L, Alferdinck J, Freiding A, Bodrogi P, Varady G, Szalmas A: Mesopic visual efficiency IV: a model with relevance to nighttime driving and other applications. Lighting Research and Technology 39: 365-392 (2007)

Gouras P: Identification of cone mechanisms in monkey ganglion cells. J Physiology 199(3): 533-547 (1968)

Grassmann HG: Zur Theorie der Farbmischung. Annalen der Physik und Chemie, Leipzig, 89, 69-84 (1853)

Gregory RL, Harris JP: Real and apparent movement nulled. Nature 307: 729-730 (1984)

Guth SL, Donley NJ, Marrocco RT: On luminance additivity and related topics. Vision Research, 9: 537-575 (1969)

Guth SL: The effect of wavelength on visual perceptual latency. Vision Research 4: 567-578 (1964)

Hallett PE: Rod increment thresholds on steady and flashed backgrounds. Journal of Physiology 202(2): 355-377 (1969)

Hartge J: Untersuchungen zur spektralen Hellempfindlichkeit des menschlichen Auges bei kleinen Lichtquellen, Dissertation, TU-Darmstadt (1991)

Hayhoe MM, MacLeod DIA, Bruch TA: Rod-cone independence in dark adaptation. Vision Research 16: 591-600 (1976)

He Y, Bierman A, Rea MS: A system of mesopic photometry. Lighting Research and Technology 30(4): 175-181 (1998)

He Y, Rea M, Bierman A, Bullough J: Evaluationg light source efficacy under mesopic conditions using reaction times. Journal of the Illuminating Engineering Society 26: 125-138 (1997)

Hering E: Zur Lehre vom Lichtsinne, Carl Gerold's Sohn, Wien (1878)

Hess RF, Waugh SJ, Nordby K: Rod temporal Channels. Vision Research 36(4): 613-619 (1996)

Hough EA: The spectral sensitivity functions for parafoveal vision. Vision Research 8(11): 1423-1430 (1968)

Hyde, EP, Forsythe WE, Cady FE: The visibility of radiation. Astrophysics Journal 48: 65-83 (1918)

Ikeda M, Ikeda J, Ayama M: Specifications of individual variations in luminous efficiency for brightness. Color Research & Application 17: 31-44 (1992)

Ikeda M, Yaguchi H, Yoshimatsu K, Ohmi M: Luminous-efficiency functions for point sources. J Opt Soc Am. 72(1): 68-73 (1982)

Ikeda M. Shimozono H: Mesopic luminous-efficiency functions. J Opt Soc Am. 71 (3): 280-284 (1981)

Ikeda M: Linearity law reexamined for flicker photometry by the summation-index method. J Opt Soc Am. 73: 1055-1061 (1983)

Ingling CR Jr, Drum BA: Retinal receptive fields: correlations between psychophysics and electrophysiology. Vision Research 13: 1151-1163 (1973)

Ingling CR Jr, Tsou BH-B: Spectral sensitivity for flicker and acuity criteria. J Opt Soc Am A 5(8): 1374-1378 (1988)

Ingling CR Jr, Tsou, BH-P, Gast TJ, Burns SA., Emerick JO, Riesenberg L: The achromatic channel. I. The nonlinearity of minimum-border and flicker matches. Vision Research 18: 379-390 (1978)

ISO 23539:2005(E)/CIE S 010/E:2004: Joint ISO/CIE Standard: Photometry - The CIE System of Physical Photometry (2004)

Ives HE: Studies in the photometry of lights of different colours. I. Spectral luminosity curves obtained by the equality of the brightness photometer and the flicker photometer under similar conditions. Philosophical Mag. 24: 149-188 (1912)

Ives HE: Studies in the photometry of lights of different colours. V. The spectral luminosity curve of the average eye. Philosophical Magazine Series 6(24): 853-863 (1919)

Jamar JHT, Kwakman LFTz, Koenderink JJ: The sensitivity of the peripheral visual system to amplitude-modulation and frequency-modulation of sine-wave patterns. Vision Research 24 (3) (1984)

Judd DB: Report of the U.S. Secretariat Commission on Colorimetry and Artificial Daylight, CZE Proc. Z, part 7, p. 11 (Stockholm). Paris, Bureau Central CIE, 57, rue Cuvier (1951) Data reproduced by G. Wyszecki and W. S. Stiles(1967). Color Science, p. 436, Wiley, New York

Kaiser P.K., Greenspon, T.S.: Brightness Difference and its Relation to the Distinctness of a border. J Opt Soc Am. 61(7): 962-966 (1971)

Kaiser PK, Boynton RM: Role of the blue mechanism in wavelength discrimination. Vision Research 25: 523-529 (1985)

Kaiser PK, Herzberg PA, Boynton RM: Chromatic border distinctness and its relation to saturation. Vision Research 11(9): 953-968 (1971)

Kaiser PK, Lee BB, Martin PR, Valberg A: The physiological basis of the minimally distinct border demonstrated in the ganglion cells of the macaque retina. Journal of Physiology 422: 153-83 (1990)

Kaiser PK, Vimal RLP, Cowan WB, Hibino H: Nulling of apparent motion as a method for assessing sensation luminance: An additivity test. Color Research & Application 14(4): 187-191 (1989)

Kaiser PK, Wyszecki G: Additivity failures in heterochromatic brightness matching. Color Research & Application 3(4): 177-182 (1978)

Kaiser PK: Minimally distinct border as a preferred psychophysical criterion in visual heterochromatic photometry. J Opt Soc Am. 61(7): 966-971 (1971)

Kaiser PK: Sensation Luminance: A new name to distinguish CIE Luminance from Luminance dependent on an individual's spectral sensitivity. Vision Research 28(3): 455-456 (1988)

Kelly DH: Retinal inhomogeneity. I. Spatiotemporal contrast sensitivity. J Opt Soc Am. A 1(1): 107-113 (1984)

Kelly DH: Visual responses to time-dependent stimuli: I. Amplitude sensitivity measurements. J Opt Soc Am. 51: 422-429 (1961)

Kelly, DH: Stabilised spatio-tempral threshold surface for chromatic gratings. Supplement to Investig. Ophthalm. 22: 78 (1982)

Ketomäki J: Effects of Lighting parameters on contrast threshold in the mesopic and photopic luminance range. HUT Finland (2006)

King-Smith PE, Carden D: Luminance and opponent color contributions to visual detection and adaptation and to temporal and spatial integration. J Opt Soc Am. 66: 709-717 (1976)

Kinney JAS: Comparison of scotopic, mesopic, and photopic spectral sensitivity curves. J Opt Soc Am. 48: 185-90 (1985)

Kinney JAS: Effect of field size and position on mesopic spectral sensitivity. J Opt Soc Am. 54: 671-677 (1964)

Kishto BN, Saunders R: Variation of the visual threshold with retinal location. II. The fovea. Vision Research, 10: 762-767 (1970)

Kishto BN: Variation of the visual threshold with retinal location. Part I. The central 20° of the visual field. Vision Research 10: 745-767 (1970)

Kokoschka S, Adrian WK: Influence of field size on the spectral sensitivity of the eye in the photopic and mesopic range. Am J Optom Physiol Opt. 62(2): 119-126 (1985)

Kokoschka S: Advantages of Four component System and its application to Photometer. Proceedings of 1994 Annual Conference and 94' Intl. Symposium of the Illuminating Engineering Institute Japan p. 55-62 (2004)

Kokoschka S: Ein konsistentes System zur photometrischen Strahlungsbewertung im gesamten Adaptationsbereich. Proceedings of the CIE 18th Session CIE 36, 1975, p. 217-225 (1975)

Kokoschka S: Photometrie niedriger Leuchtdichten durch äquivalente Leuchtdichte des 10°- Feldes. Licht-Forschung 2(1): 1-13 (1980)

Kokoschka S: Untersuchungen zur mesopischen Strahlungsbewertung. Die Farbe (1972)

König A, Brodhun E: Gesammelte Abhandlungen zur Physiologischen Optik, pp. 116-143. Leipzig: J. A. Barth. (1903)

Kraft JM, Werner JS: Spectral efficiency across the life span: flicker photometry and brightness matching. J Opt Soc Am. A 11(4): 1213-1221 (1994)

Kremers J, Meierkord S: Rod-cone-interaction in deuteranopic observers: models and dynamics. Vision Research 39: 3372-3385 (1999)

Krizaj D: Mesopic state: cellular mechanisms involved in pre- and post-synaptic mixing of rod and cone signals. Microsc Res Tech. 50(5): 347-359 (2000)

Kuyk TK: Spectral sensitivity of the peripheral retina to large and small stimuli. Vision Research 22: 1293-1297 (1982)

Le Grand Y: Light, Colour and Vision, John Wiley and Sons, Inc., New York, (1957)

Lee BB, Martin PR, Valberg A: The physiological basis of heterochromatic flicker photometry demonstrated in the ganglion cells of the macaque retina. Journal of Physiology 404: 323-347 (1988)

Lee J, Stromeyer CF III: Contribution of human short-wave cones to luminance and motion detection. Journal of Physiology 413: 563-593 (1989)

Lennie P, Pokorny J, Smith VC: Luminance. J Opt Soc Am. A 10: 1283-1293 (1993)

Lewis A: Visual performance as a function of spectral power distribution of light sources at luminances used for general outdoor lighting. Journal of the Illuminating Engineering Society 28(1): 37-42 (1999)

Lindsey DT, Teller DY: Influence of variations in edge blur on minimally distinct border judgments: a theoretical and empirical investigation. J Opt Soc Am A. 6(3): 446-458 (1989)

Lit A, Young R, Shaffer M: Simple time reaction as a function of luminance for various wavelengths. Percept. Psychophys. 10: 397-399 (1971)

MacLeod DIA, Stockman A: Duplicity, phase lags and destructive interference in mesopic and scotopic flicker perception. In Night Vision, eds. Johnson CA and Leibowitz H, Washington: National Academy Press (1987)

MacLeod DIA: Psychophysical Studies of Signals from Rods and Cones. Doctoral thesis, King's College, University of Cambridge (1974)

MacLeod DIA: Rods Cancel Cones in Flicker. Nature 235(5334): 173-174 (1972)

Makous W, Boothe R: Cones block signals from rods. Vision Research 14(4): 285-294 (1974)

Marks LE, Bornstein MH: Spectral sensitivity of the modulation sensitive mechanism of vision. Vision Research 14: 665-669 (1974)

Merbs SL, Nathans J: Absorbtion spectra of human cone pigments. Nature 256(6368) (1992)

Mullen KT, Kingdom FA: Differential distributions of red-green and blue-yellow cone opponency across the visual field. Visual Neuroscience 19: 109-118 (2002)

Naka KI, Rushton WAH: S-potentials from luminosity units in the retina of fish (Cyprinidae) Journal of Physiology 185: 587-599 (1966)

Nakano Y, Ikeda M, Kaiser PK: Contributions of the opponent mechanisms to brightness and nonlinear models. Vision Research 28(7): 799-810 (1988)

Nakano Y, Ikeda M: A model for the brightness perception at mesopic levels (in Japanese). KOUGAKU 15: 295-302 (1986)

Norman RA, Werblin FS: Control of retinal sensitivity. I. Light and dark adaptation of vertebrate rods and cones. J. gen. Physiol. 63: 37-61 (1974)

Nutting PG: The visibility of radiation. Transaction of the Illuminating Engineering Society 9: 633-642 (1914)

Orreveteläinen P: Models for spectral luminous efficiency in peripheral vision at mesopic and low photopic luminance levels. Dissertation, Helsinki University of Technology (2005)

Palmer DA: A system of mesopic photometry. Nature 209: 276-281 (1966)

Palmer DA: Standard observer for large-field photometry at any level. J Opt Soc Am. 58(9): 1296-1299 (1968)

Palmer DA: The definition of a standard observer for mesopic photometry. Vision Research 7: 619-628 (1967)

Palmer DA: Visibility curves by direct comparison in a 10 degree field at 1000 Td. J Opt Soc Am. 2(4):578 (1985)

Pease PL, Adams AJ, Nuccio E: Optical density of human macular pigment. Vision Research 27: 705-710 (1987)

Pollack JD: Reaction time to different wavelengths at various luminances. Percept. Psychophys. 3: 17-24 (1968)

Polyak SL: The Retina. University of Chicago Press, Chicago (1941)

Purkinje JE: Beobachtungen und Versuche zur Physiologie der Sinne. Zweites Bändchen, G. Reiner, Berlin (1825)

Putnam NM, Hofer HJ, Doble N, Chen L, Carroll J, Williams DR: The locus of fixation and the foveal cone mosaic, Journal of Vision 5 (2005)

Ramachandran VS, Gregory RL: Does colour provide an input to human motion processing? Nature 275: 55-56 (1978)

Rea MS, Bullough JD, Freyssinier JP, Bierman A: A proposed unified system of photometry. Lighting Research and Technology 36(2): 85-111 (2004)

Rinalducci EJ, Higgins KE: An investigation of the effective intensity of flashing lights. Clearinghouse, AD 728 587, Springfield, Va (1971)

Ripamonti C, Woo WL, Crowther E, Stockman A: The S-cone contribution to luminance depends on the M- and L-cone adaptation levels: silent surrounds? Journal of Vision 9(3/10): 1-16 (2008)

Roorda A, Williams DR: The arrangement of the three cone classes in the living human eye. Nature 397: 520-522 (1999)

Sagawa K, Takeichi K: Spectral luminous efficiency functions for a ten-degree field in the mesopic range. Journal of Light and Visual Environment 7: 37-44 (1983)

Sagawa K, Takeichi K: Spectral luminous efficiency functions in the mesopic range. J Opt Soc Am. A. 3(1): 71-75 (1986)

Sagawa K, Takeichi K: System of mesopic photometry for evaluating lights in terms of comparative brightness relationships. J Opt Soc Am. A 9: 1240-1246 (1992)

Sagawa K: Toward a CIE supplementary system of photometry: brightness at any level including mesopic vision. Ophthalmic and Physiological Optics. 26: 240 (2006)

Sharpe LT, Fach C C, Stockman A: The spectral properties of the two rod pathways. Vision Research 33(18): 2705-2720 (1993)

Sharpe LT, Fach C, Nordby K, Stockman A: The Incremental Threshold of the Rod Visual System and Weber's Law. Science 244(4902): 354-356 (1989)

Sharpe LT, Fach C, Stockman A: The field adaptation of the human rod visual system. Journal of Physiology 445: 319-343 (1992)

Sharpe LT, Stockman A, Jägle H, Knau H, Klausen G, Reitner A, Nathans J: Red, green, and red-green hybrid pigments in the human retina: correlations between deduced protein sequences and psychophysically measured spectral sensitivities. Journal of Neuroscience 18(23) (1998)

Sharpe LT, Stockman A, MacLeod DIA: Rod flicker perception: Scotopic duality, phase lags and destructive interference. Vision Research 29: 1539-1559 (1989)

Sharpe LT, Stockman A: Rod pathways: Importance of seeing nothing. Trends in Neuroscience 22(11) (1999)

Sivak M, Flannagan MJ, Schoettle B, Adachi G: Driving with HID headlamps: A review of research findings. 2003 SAE World Congress, Warrendale, PA: Society of Automotive Engineers (2003)

Snowden RJ, Hess RF, Waugh SJ: The processing of temporal modulation at different levels of retinal illuminance. Vision Research 35(6): 775-789 (1995)

Sperling HG, Lewis WG: Some comparisons between foveal spectral sensitivity data obtained at high brightness and absolute threshold. J Opt Soc Am. 49(10): 983-989 (1959)

Stabell U, Stabell B: Variation in density of macular pigmentation and in short-wave cone sensitivity with eccentricity. J Opt Soc Am. 70: 706-711 (1980)

Stiles WS, Burch JM: Interim report to the Commission Internationale de 'Eclairage Zurich, 1955, on the National Physical Laboratory's investigation of colour matching, Opt. Acta 2: 168-181 (1955)

Stiles WS, Burch JM: NPL colour-matching investigation: Final report. Optica Acta, 6: 1-26 (1959)

Stockman A, MacLeod DIA, DePriest DD: An inverted S-cone input to the luminance channel: evidence for two processes in S-cone flicker detection. Investigative Ophthalmology and Visual Science (suppl.), 28, 92 (1987)

Stockman A, MacLeod DIA, Johnson NE: Spectral sensitivities of the human cones. J Opt Soc Am. A 10(12): 2491-2521 (1993)

Stockman A, Sharpe LT, Zrenner E, Nordby K: Slow and fast pathways in the human rod visual system: ERG and psychophysics. J Opt Soc Am. A 8: 1657-1665 (1991)

Stockman A, Sharpe LT: Into the twilight zone: Complexities of mesopic vision and luminous efficiency. Ophthal. Physiol. Opt. 26(3) (2006)

Stockman A, Sharpe LT: The spectral sensitivities of the middle- and long-wavelength-sensitive cones derived from measurements in observers of known genotype. Vision Research 40: 1711-1737 (2000)

Stromeyer CF III, Kronauer RE, Ryu A, Chaparro A, Eskew RT Jr: Contribution of human long-wave and middle-wave cones to motion detection. Journal of Physiology 485(1): 221-243 (1995)

Stromeyer CF III, Cole GR, Kronauer RE: Chromatic suppression of cone inputs to the luminance flicker mechanism. Vision Research 27(7) (1987)

Sun H, Smithson HE, Zaidi Q, Lee BB: Specificity of Cone Inputs to Macaque Retinal Ganglion Cells. Journal of Neurophysiology 95: 837-849 (2006)

Szalmas A, Bodrogi P, Sik-Lanyi C: Characterizing luminous efficiency functions for a simulated mesopic night driving task based on reaction times. Ophthal. Physiol. Opt. 26: 281-287 (2006)

Tansley BW, Boynton RM: A line, not a space, represents visual distinctness of borders formed by different colors. Science 191(4230): 954-957 (1976)

Tansley BW, Boynton RM: Chromatic border perception: the role of red- and green-sensitive cones. Vision Research 18: 683-697 (1978)

Tansley BW, Valberg A: Chromatic border distinctness: not an index of hue or saturation differences. J Opt Soc Am. 69(1): 113-118 (1979)

Thornton JE, Pugh Jr EN: Red/green opponency at detection threshold. Science 219: 191-193 (1983)

Trezona PW: A system of mesopic photometry Color Research & Application 16: 202-216 (1991)

Trezona PW: A system of photometry designed to avoid assumptions. Proceedings 21st Session Venice, CIE Publ. No. 71: 30-33 (1987)

Trezona PW: Guidelines for testing systems of mesopic photometry. Color Research & Application 17: 418-420 (1992)

Trezona PW: Luminance level conversions to assist lighting engineers to use fundamental visual data. Lighting Research & Technology 15(2): 83-88 (1983)

Trezona PW: The tetrachromatic color match as a colorimetric technique. Vision Research 13(1): 9 (1973)

Troy JB, Bohnsack DL, Diller LC: Spatial properties of the cat X-cell receptive field as a function of mean light level. Visual Neuroscience 16(6): 1089-1104 (1999)

Valberg A, Tansley BW: Tritanopic purity-difference function to describe the properties of minimally distinct borders. J Opt Soc Am. 67(10): 1330-1336 (1977)

Van Derlofske J, Bullough JD, Watkinson J: Spectral Effects of LED forward lighting. A transportation Lighting Alliance Report (2005)

Van Derlofske J, Bullough JD: Spectral Effects of High-Intensity Discharge Automotive Forward Lighting on Visual Performance. 2003 SAE World Congress, Warrendale, PA: Society of Automotive Engineers (2003)

Van Derlofske J, Dyer D, Bullough JD: Visual benefits of blue coated lamps for automotive forward lighting. 2003 SAE World Congress, Warrendale, PA: Society of Automotive Engineers (2003)

Várady G, Bodrogi P: Mesopic spectral sensitivity functions based on visibility and recognition contrast thresholds. Ophthal. Physiol. Opt. 26: 246-253 (2006)

Viénot F: Retinal distributions of the macular pigment and the cone effective optical density from colour matches of real observers. Color Research & Application 26: 264-268 (2001)

Von Helmholtz H: Handbuch der Physiologischen Optik. 2nd Edition, Verlag von Leopold Voss (1896)

Vos JJ: Colorimetric and photometric properties of a 2° fundamental observer. Color Research & Application 3: 125-128 (1978)

Vos JJ: On the merits of model making in understanding color-vision phenomena, Color Research & Application 7(2): 69-77 (1982)

Wagner G, Boynton RM: Comparison of four methods of heterochromatic photometry. J Opt Soc Am. 62(12): 1508-1515 (1972)

Wald G: Human vision and the spectrum. Science 101: 653-658 (1945)

Walkey H, Orreveteläinen P, Barbur J, Halonen L, Goodman T, Alferdinck J, Freiding A, Szalma A: Mesopic visual efficiency II: reaction time experiments. Lighting Res. Technol. 39: 335–354 (2007)

Walkey HC, Barbur JL, Harlow JA, Hurden A, Moorhead IR, Taylor JAF: Effective contrast of colored stimuli in the mesopic range: a metric for perceived contrast based on achromatic luminance contrast. J Opt Soc Am. 22(1):17 (2005)

Walkey HC, Harlow JA, Barbur JL: Characterising mesopic spectral sensitivity from reaction times. Vision Research 46: 4232-4243 (2006)

Weale, RA: The foveal and para-central spectral sensitivities in man. Journal of Physiology 114: 435-446 (1951)

Weber EH: Die Lehre vom Tastsinn und Gemeingefühle. Braunschweig, Germany Vieweg (1851)

Webster MA, MacLeod DIA: Factors underlying individual differences in the color matches of normal observers. J Opt Soc Am. A 5: 1722-1735 (1988)

White TW, Collins SB, Rinalducci EJ: The Broca-Sulza Effect under scotopic viewing conditions. Vision Research 16: 1436 (1976)

Williams DR, MacLeod DIA, Hayhoe MM: Punctate senstivitiy of the blue-sensitive mechanism. Vision Research 21: 1357-1375 (1981)

Wooten BR, Fuld K, Spillmann L: Photopic spectral sensitivity of the peripheral retina. J Opt Soc Am. 65: 334-342 (1975)

Wyszecki G & Stiles WS: Color Science: concepts and methods, quantitative data and formulae. (2nd ed.) New York: Wiley (1982)

Related Publications

Raphael S, MacLeod DIA: Mesopic luminance defined by minimum motion. European Conference on Visual Perception, Aug 2009, Regensburg, Germany (2009)

Raphael S, MacLeod DIA: Minimally distinct borders in mesopic vision. OSA Vision Fall Meeting 2008, Oct 2008, Rochester, NY, USA (2008)

Raphael S, Seyring C, Wernicke A, Völker S: Luminance as a criterion for the evaluation of discomfort and disability glare of headlamps. 7th International Symposium on Automotive Lighting, ISAL Proceedings, pp. 427-433, Darmstadt, Germany, Utz Verlag, (2007)

Raphael S, Leibenger M: Models of Mesopic Photometry applied to the contrast threshold of peripheral and foveal objects. Proceedings of the 26th Session of the CIE, pp. D1/38 - D1/41, July 2007, Beijing, China (2007)

Raphael S, Leibenger M, Tophinke M, Radtke B: Mesopische Photometrie basierend auf ortsaufgelöster Leuchtdichtemesstechnik. Licht 2006, 17. Lichttechnische Gemeinschaftstagung, Sept 2006, Bern, Switzerland (2006)

Raphael S: Ideas for a mesopic photometric model based on spatially resolved luminance measurements. Lux et Color Vespremiensis, Oct 2005, Vesprem, Hungary (2005)